Anion Basicity and Ionicity of Protic Ionic Liquids

by

Mohammad Hasani

A Dissertation Presented in Partial Fulfillment
of the Requirements for the Degree
Doctor of Philosophy

Approved June 2016 by the
Graduate Supervisory Committee:

Chair: C. Austen Angell
Jeffery Yarger
Ian Gould

ARIZONA STATE UNIVERSITY

August 2016

ABSTRACT

The field of Ionic Liquid (IL) research has received considerable attention during the past decade. Unique physicochemical properties of these low melting salts have made them very promising for applications in many areas of science and technology such as electrolyte research, green chemistry and electrodeposition. One of the most important parameters dictating their physicochemical behavior is the basicity of their anion. Using four sets of Protic Ionic Liquids (PILs) and spectroscopic characterization of them, a qualitative order for anion basicity of ILs is obtained.

Protic Ionic Liquids are made by proton transfer form a Brønsted acid to a base. The extent of this transfer is determined by the free energy change of the proton transfer process. For the cases with large enough free energy change during the process, the result is a fully ionic material whereas if the proton transfer is not complete, a mixture of ions, neutral molecules and aggregates is resulted. NMR and IR spectroscopies along with electrochemical and mechanical characterization of four sets of PILs are used to study the degree of ionicity.

DEDICATION

To My Family

ACKNOWLEDGMENTS

First and foremost, I would like to express my deep respect and gratitude to my advisor Reagent's Professor C. Austen Angell not only for giving me the opportunity to work in his laboratory but for his continues support all throughout the years.

I would also like to thank my dissertation committee members Professor Jeffrey Yarger and President's Professor Ian Gould for their help and support. I am glad I had the opportunity to meet them.

My coworkers in the lab, Dr. Zuofeng Zhao and Iolanda Klein, are acknowledged here for welcoming me in the group and for what they taught me of experimental techniques. I learned from them and will remember the setting up of new equipment, lab inspections, sink clogs, leaks and all the ups and downs we went through during these years.

I am grateful to thank Dr. Stephen Davidowski and Dr. Brian Cherry for helping me with the NMR experiments and for teaching me what they knew without reservation. Dr. Brian Cherry is credited for keeping the NMR laboratory a place on which function one can count.

I thank Dr. Jennifer Green for her understanding and support. I also thank Waunita Parrill, Martha McDowell, David Nutt and Gregory Memberto for their help and support during the years.

TABLE OF CONTENTS

Page

CHAPTER Page

LIST OF TABLES

LIST OF FIGURES

Figure Page

1 Introduction to Ionic Liquids

Ionic liquids (ILs) are material solely made of ions with melting points below 100 ^{o}C. They can be considered a subclass of molten salts. They are known for more than 100 years but have received considerable attention recently. The number of publications on ILs has gone up very fast and they have been the subject of a number of extensive and excellent reviews and books. Their application as material for energy generation and storage is reviewed by MacFarlane.[1] The use of weakly coordinating anions to make them and the analysis of the thermodynamics of their phase behavior is reviewed by Krossing.[2] Structure-property relationships and applications of a subclass of them is the subject of another extensive review by Drummond.[3,4] Gas solubilities in ionic liquids is reviewed in a recent review by Chen et al.[5] The old case of halometallate ionic liquids is revisited in a recent review by Estager et al.[6] Their energy applications, history and physicochemical properties are reviewed by Angell.[7–11] Their application as media for self-assembly of amphiphiles is also reviewed by Drummond.[12]

They show unique properties that make them very attractive for fundamental studies and for a wide range of applications.[13,14] They are considered green solvents as media for organic reactions because of their low vapor pressure, low flammability and high thermal stability.[15] They also have good solvating properties which can be tuned. Their solvent properties can be tailored to suite specific reactions. They are also attractive as high stability electrolyte material for their interesting electrochemical properties because of their high intrinsic ion conductivity. Their wide electrochemical stability window is another factor making them great candidates as electrolytes in electrochemical applications. When it comes to the usage of electrochemical devices, safety is a highly

important factor, even more important that performance. Ionic liquids with their low vapor pressure and low flammability offer safer electrolytes than the ones based on organic solvents. One other of their unique properties is their proton conduction at high temperatures. Aqueous proton conductor electrolytes cannot be used at temperatures above 100 ^{o}C because water will evaporate. Much help is expected from ionic liquids with the ability to transfer protons in the area of electrolytes for fuel cells.

They are in some aspect very similar to common high melting molten salts with small ions such as NaCl but they normally have larger size ions. Having bulky ions is a way to bring the melting point down.[16] Another way is to have the charge delocalized over more than one atom. When the charge is spread over a large area the electrostatic interaction comes down. Low internal symmetry also helps to bring the melting point down.[17]

It is contrary to one's elementary chemical knowledge that a salt should have a low melting point, a requirement for having an ionic liquid by definition. It is expected that the stabilization of the ionic lattice structure gained by uniform surrounding of ions of one charge by ions of the opposite charge will result in large enthalpies of fusion as in the case of simple salts. This lattice energy is known as Madelung energy and can reasonably be assumed to be mostly due to coulombic interaction between the oppositely charges ions. The coulomb force is inversely proportional to the distance between the two charges so it is expected to be lower for the bigger, non-symmetrical ions of ionic liquids causing a smaller lattice energy.

$$E_C = q_1 q_2 / 4\pi\varepsilon r$$

Even though the enthalpy of fusions of an ionic liquid is typically smaller than that of a simple salt, it is not the only factor effective on its lower melting point. The entropy of fusion for the larger ions of an ionic liquid is significantly larger than that of a simple salt and that has a lowering effect of the melting point according to the equation below:

$$T_m = \frac{\Delta H_f}{\Delta S_f}$$

The thermodynamics of the other phase-transition of ionic liquids is also interesting. Negligible vapor pressures of ionic liquids are a consequence of the Madelung energy of the qausi-lattice in their liquid phase. Enthalpies of vaporization of ionic liquids are much bigger than those for dipolar molecular liquids and show the work needed to overcome this Madelung energy to extract an ion pair from the liquid.

Another point worth making is the fact that considering the cohesive energy of ionic liquids, resulting from the coulombic interactions and also van der Waals forces, and their liquids states at ambient temperature, requires a melting point close to their glass transition temperature T_g. This explains their tendency to supercool and their super-Arrhenius transport properties near and below room temperature.

1.1 Classes of Ionic Liquids

There are a large number of ionic liquids designed and made. They can be classified base on different criteria but the classification below is widely accepted.[10] The two major classes of ionic liquids are aprotic ionic liquids (APILs) and protic ionic liquids (PILs). Solvate ionic liquids are a rather recent development in the area and because of their importance they are given a separate category.

1.1.1 Aprotic Ionic Liquids

The majority of ionic liquids belong to this class. They are normally made up of an organic cation and an inorganic weakly coordinating anion. Important examples are alkyl pyridinium and dialkylimidazolium cations which are the ones used in the study of chloroaluminate ionic liquids.[18,19] The efforts were aimed at electrodeposition of aluminum form these melts, the first phase diagram of an aluminum chloride plus organic cation halide system was presented there showing the existence of compositions giving stable ionic liquids at low temperatures.

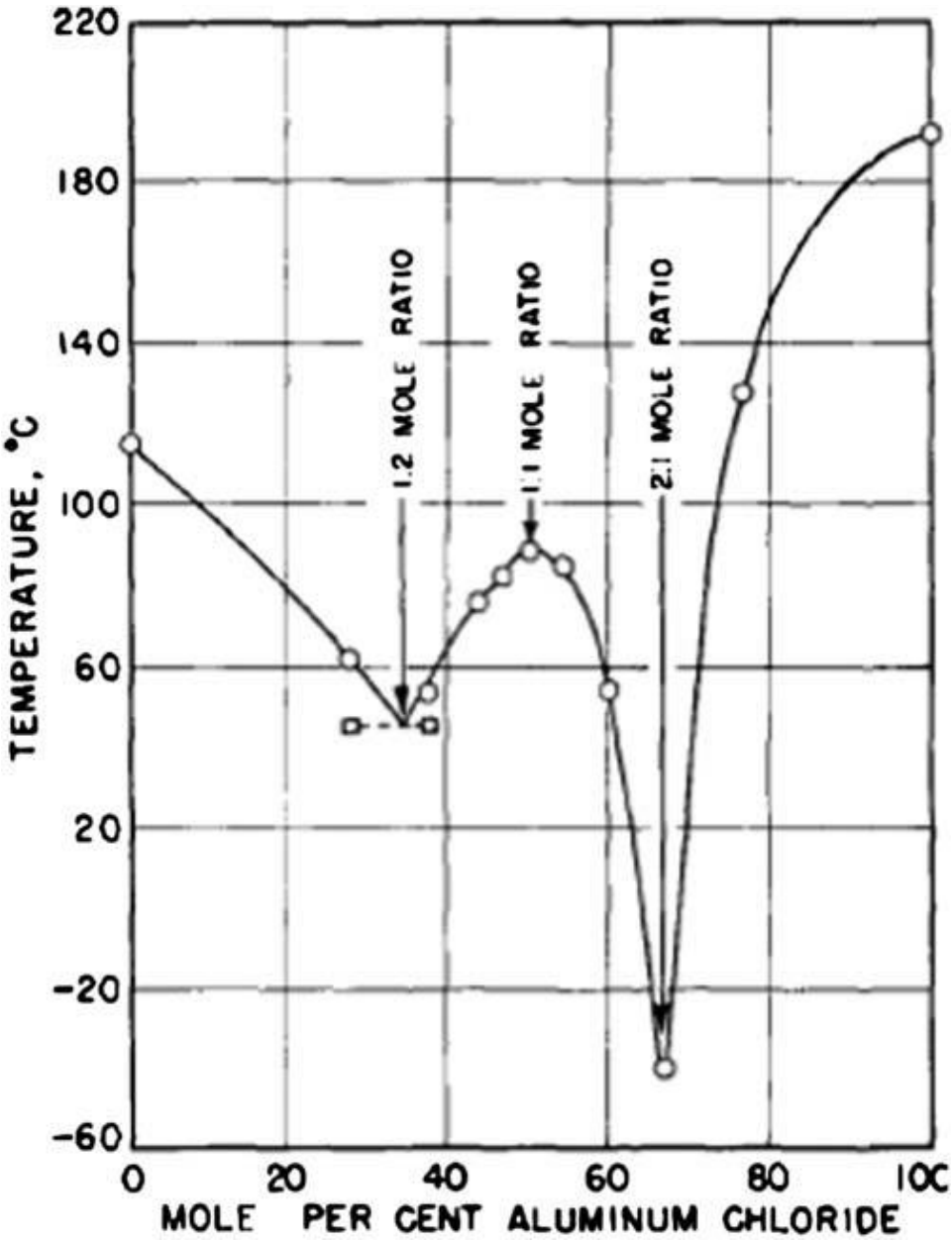

Figure 1-1- Phase diagram of the system ethylpyridinium bromide + AlCl3 (Adapted from Ref.[10] with permission of The Royal Society of Chemistry)

The use of tetraalkylammonium cations like dialkylpyrrolidinium is more recent. The popular anions can be usual conjugate bases of strong oxidic acids such as nitrate, perchlorate and hydrogensulfate or more recently fluorinate anions such as trifluoromethanesulfonate (triflate, OTf), bis-trifluoromethanesulfonylimide (NTf_2),

tetrafluoroborate (BF_4) and hexafluorophosphate (PF_6). The fluorinated anions have unpolarizable fluorine atoms therefor lower van der Waals interactions which leads to lower viscosities and higher conductivities.

1.1.2 Solvate Ionic Liquids

These are a rather new class of ionic liquids. Salts with multivalent cations normally have higher melting points and are hard to have them in the liquid state at low temperatures.

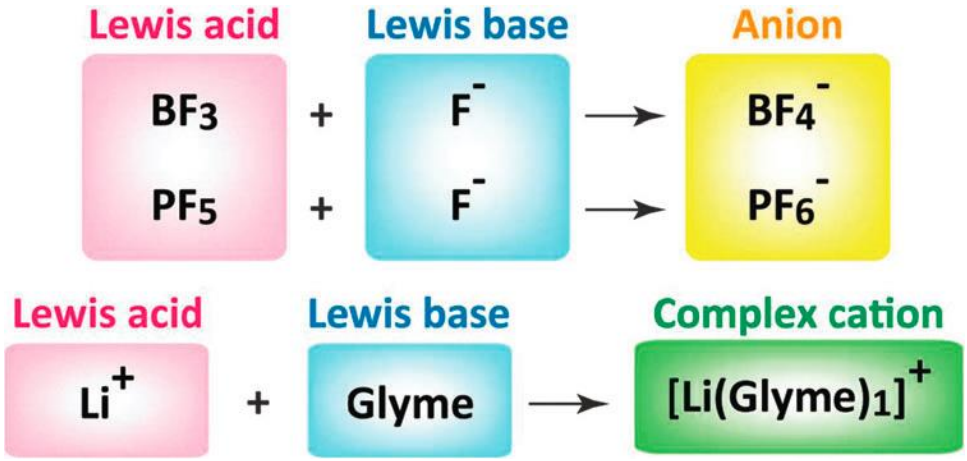

Figure 1-2- Concept of complex cations in solvate ionic liquids (Adapted from Ref.[20] with permission of The Royal Society of Chemistry)

The solvate ionic liquids include examples of multivalent ions in the liquid state. Molten salt hydrates, such as $Ca(NO_3)_2.4H_2O$, are first recognized examples of this category, with melting points below room temperature. The most popular example is the glyme solvate ionic liquids described recently by Watanabe in which the Li cation is solvated by 4 oxygens of the alkoxy groups of tetraglyme. It has been shown to have desirable electrochemical properties for electrolyte of batteries.

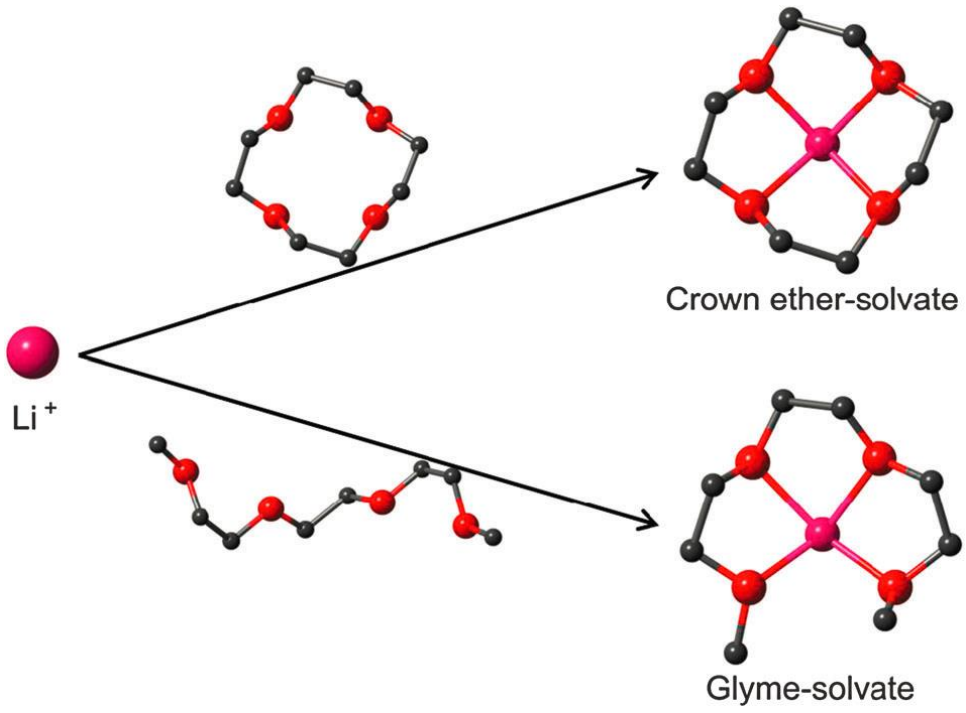

Figure 1-3- Crown ether- and glyme-based [Li(ligand)1]+ solvate models. (Adapted from Ref.[20] with permission of The Royal Society of Chemistry)

1.1.3 Protic Ionic Liquids

Protic ionic liquids are made by proton transfer from a Brønsted acid to a Brønsted base. They are an important subclass of ionic liquids and are the focus of this thesis. They have hydrogen bond donor and acceptor cites which can build up hydrogen-bonded network. The first reported ionic liquid is of this class. In 1888 Gabriel reported ethanolammonium nitrate with a melting point of 52-55 ^{o}C.[4] It is considered an ionic liquid, and a protic one, by the definition but it is not a room-temperature ionic liquid. Ethylammonium nitrate (EAN) which was deliberately made by Paul Walden and reported in 1914 has a melting point of 12 ^{o}C and is the first true room-temperature ionic liquids reported.[21] It has been the focus of a great number of studies because of its fame

and because of its water-like properties like having the same number of hydrogen bond donor and acceptor sites.

1.2 Protic Ionic Liquids and Ionicity

To get a fully ionic liquid, a complete proton transfer should occur from the acid to the base. In this ideal situation the species are fully charged and there is no aggregation or ion paring. In reality, often times it so happens that the proton transfer is not complete and the mixture of the acid and the base is not fully ionic because neutral acid and base species are present and sometimes aggregates or ion pairs. It is important in the characterization of PILs to have a way of assessing the extent of this proton transfer. There is not a "standard" way of measuring ionicity. The most widely used way of assessment is by using the Walden plot analysis of the conductivity and viscosity data.[22,23] This is a plot of the logarithm of equivalent conductivity versus logarithm of fluidity as is used for ionicity study of ILs as shown in the Figure 1-4.

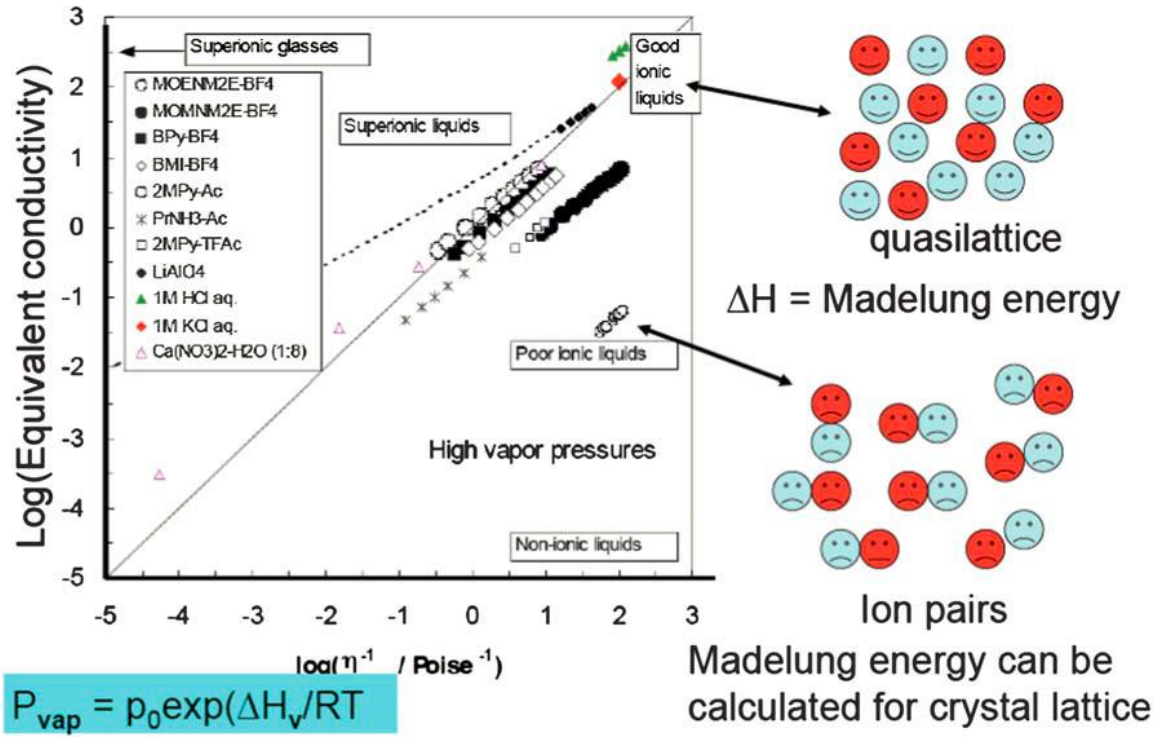

Figure 1-4- Walden plot showing the classification of ionic liquids into superionic, "good" and "poor" (subionic) and the relation between low equivalent conductivity and low ionicity (ion pairing). (Adapted from Ref.[10] with permission of The Royal Society of Chemistry)

The majority of PILs are not good ILs by this definition. It is not obvious what the reason for their deviation from the ideal behavior is. It can be incomplete proton transfer, it can be aggregation and ion pairing or formation of complex ionic species. There is a question to be answered here and that is "how ionic does a liquid need to be to be called an ionic liquid?". In other words, how much neutral species is tolerated if a liquid is to be called an ionic liquid. It is a more important question when dealing with PILs. One answer provided to this question by MacFarlane and Seddon states "Thus, as a guideline in respect to protic ionic liquids, we propose that less than 1% of the neutral species should be present if the ionic liquid is to be considered a 'pure ionic liquid'. In other words the degree of proton transfer should be >99%."[24] Other techniques have also been

employed to probe the ionicity of PILs, including NMR spectroscopy[25,26] and IR spectroscopy[27]. These techniques usually give qualitative measures of ionicity and the extent of the proton transfer.

The aqueous pKa values of the acid and the base has been used as an estimate to predict the proton transfer energetic of the PIL formation. It is suggested that a pKa difference of >8 units is needed to achieve high ionicities.[22]

$$\Delta pK_a = pK_a(BH^+) - pK_a(AH)$$

Other researchers suggest bigger numbers, more like 14 units of pKa.[28] It is suggested that there is a correlation between the excess boiling point, ΔT_b and ΔpKa. The boiling point of good PILs are considerably higher than the average boiling points of the acid and the base.[22] The existence of this relationship suggests that there indeed is a relevance for aqueous pKa in the ionic liquid medium, even though considering the fact that measurement by this technique is limited to the ionic liquids whose boiling point can be measured before decomposition.

Tokuda et al. reported on an extensive study on ionicity of aprotic ionic liquids using electrochemical impedance spectroscopy (EIS) to measure conductivities and comparing it to the conductivity obtained from Nernst-Einstein equations using the diffusion coefficients measured from Pulse Field Gradient (PFG) NMR method.

$$\Lambda_{NE} = \frac{N_A e^2}{kT}(D^+ + D^-)$$

The ratio $\Lambda_{exp}/\Lambda_{NE}$ is the ratio of the equivalent conductivity measure from EIS experiment which is a result of migration of the ions in an electric field and the conductivity result from the self-diffusion of the species calculated from Nernst-Einstein

equation. The degree of aggregation in both APILs and PILs can be estimated from this ratio.[29]

1.3 Proton Free Energy Level Diagram

One of the most important physicochemical characteristics of PILs is their proton activity, especially when they are considered as electrolytes for fuel-cell applications. It is determined by the acidity/basicity of the acid/base that is used to make them. The proton activity is approximately an average of its activity when on the acid and when on the base as the cation. When there is not direct proton activity measurement data available, this approximation can be used to estimate it. The proton activity on the acid and the base can be estimated from aqueous data or theoretical measurements. A Gurney type diagram for free energy of the proton transfer is proposed by Angell et al.[30] and even though it lacks a common solvent and a common reference state it is proved to be very useful and convenient when studying PILs.[31] A recent version of the diagram is presented in Figure 1-5.

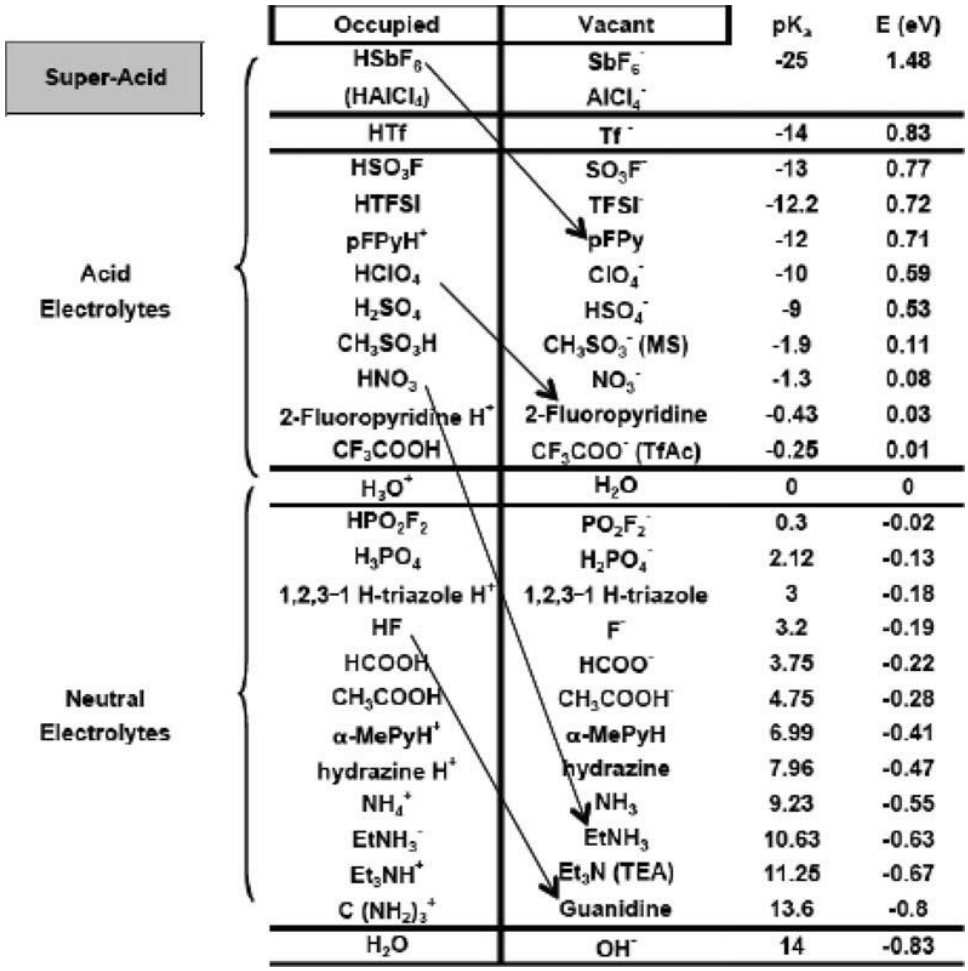

Figure 1-5- Gurney free energy level diagram for acid/base pairs, showing superacid, acid and neutral electrolyte formation possibilities. (Adapted from Ref.[10] with permission of The Royal Society of Chemistry)

1.4 Acidity of Protic Ionic Liquids

Brønsted acidity is one of the most important properties of PILs and is of interest when PILs are used as solvents to carry out acid catalyzed chemical reactions. Hammet[32] acidity functions have been measured in ionic liquids using Hammet UV-Vis dyes to measure the ratio of the protonated to unprotonated forms of the indicator.[33,34] Kamlet-Taft parameter of hydrogen bond acidity is also a measure of the acidity of ILs.[35,36] These are methods of acidity measurement which are based on using a spectroscopic probe that

is sensitive to acidity of the medium. UV dyes like phenol red,[37] 4-nitroaniline[38] and Reichardt's dye[39] are reported. 4-nitroaniline was used[38] to measure acidity level of propionate, acetate and formate ILs. It was observed that the order of acidity is propionate>acetate>formate which is opposite of the order observed in water. This was explained to be a result of the cation stabilization toward conjugate anion of the acid.[38] The issue of the acidity in ionic liquids has been addressed in multiple contributions using different electrochemical and spectroscopic methods. Most of these methods are based on spectroscopic characterization of a probe, dissolved in ILs at low concentrations, whose response is found to be correlated to the acidity of the medium. Hammett bases[40] and other UV-Vis probes[41] along with NMR probes to measure Guttmann donor and acceptor numbers (DN and AN)[42,43] have been suggested as means of acidity measurements in ILs. The main disadvantage of this approach is the disproportionate effect of impurities consequent on the low concentration of the probe. Using a higher concentration of the probe is possible in some cases as it is neatly done and reported for mesityl oxide.[44] One important limitation, especially for the super acidic range, is the loss of sensitivity of the probe outside the range H_0 = -1 to -9. The high concentration of the probe can also be argued to change the properties of the original liquid. In the case of Guttmann DN measured by ^{23}Na NMR, the broadness of sodium lines is another source of error. There is also a subtle point here worth making that the basicity of anions towards sodium ion is not necessarily the same as their basicity towards proton. This is in addition to the fact that the cation has a non-innocent effect on ^{23}Na chemical shift since it competes with the sodium ion for the anion and the result of this competition affects the chemical shift.

Another approach is to use an electrochemical or spectroscopic property of the ionic liquid itself as a measure of its acidity. It was realized in the author's lab that proton activity obtained from electrochemical properties of PILs can be used as a measure of their acidity.[45] Open Circuit Potential (OCP) in the presence of H_2 and the results of potentiometric and calorimetric titrations of PILs have been recently reported to be a mark of their acid strength.[46–48] Proton chemical shift of ILs cation have also been reported as indicative of the anions basicities.[43,49,50] The main advantage of the methods of this sort is that they rely on a property of the system itself and not on that of an external probe. Even though less sensitive to impurities compared to the former approach, because the measurement is directly on the proton, they are still sensitive to protic impurities such as water which is almost always present. In the work presented here, we try to keep the advantages of this approach but to use ^{15}N and ^{13}C chemical shifts, both separately and in concert. These are shown to be less sensitive to the presence of protic impurities, namely water.

Using any of the above mentioned methods, it is evident that there is strong correlation between the acidity and catalytic activity of the PILs. When the same base is used with a set of acids, the acidity depends on the basicity of the conjugate anion of the acid.[51,52]

1.5 Anion Basicity of Ionic Liquids

Anion basicity is an important parameter determining the properties of ionic liquids, yet there is not an easy way to quantify it. Anion basicity is defined under the Lewis definition of acids and bases and by testimony of the recent literature, it is impossible to have a single scale of Lewis basicity.[53,54] The impossibility comes from the

fact that in contrast to Brønsted acidity/basicity which is defined based on equilibria involving a single reference species, the proton, there does not exist a single Lewis acid toward which the basicity of all Lewis bases is defined. So there potentially are as many Lewis basicity scales as there are Lewis acid. As an example, when the Lewis basicity (basicity, from now on) of halide ions in aqueous solutions is studied, the order of basicity is reversed when the Lewis acid is changed from Hg^{+} to Fe^{3+}.[55] The impossibility does not prevent us from finding family dependent trends. There can be selected a few number of Lewis acids which can represent the rest of them and make scales for each to be consulted when quantification toward a similar Lewis acid is desired. This way, the basicity is not defined by a number but by a [1xn] matrix, in which "n" is the number of Lewis acid/base scales. Please refer to reference[54] for an excellent discussion and more information.

Basicity is a thermodynamic value related to the free energy change of an association process. A closely related value which is the heat of the same process at constant pressure, enthalpy, is affinity. These values are obtained from experimental and/or theoretical studies, such as gas-phase mass spectroscopic experiments, calorimetry experiments and ab initio calculations. There are also a number of spectroscopic scales for basicity which are based on the quantification of the equilibrium amounts of species or a spectroscopic response of a probe entity in the medium; the discussion of which is outside the scope of this piece.

It is then not surprising that the question of anion basicity in ionic liquids is one still under study. The most popular measure of anion basicity with the community is hydrogen bond basicity, β, parameter in Kamlet-Taft equation devised to explain the

polarity of solvents. The matter is discussed in more detail with reference to recent literature in chapter 2 of this thesis.

1.6 Works Cited

(1) MacFarlane, D. R.; Forsyth, M.; Howlett, P. C.; Kar, M.; Passerini, S.; Pringle, J. M.; Ohno, H.; Watanabe, M.; Yan, F.; Zheng, W.; Zhang, S.; Zhang, J. *Nat. Rev. Mater.* **2016**, 15005.

(2) Rupp, A. B. A.; Krossing, I. *Acc. Chem. Res.* **2015**, *48* (1), 2537–2546.

(3) Greaves, T. L.; Drummond, C. J. *Chem. Rev.* **2015**, *115*, 11379–11448.

(4) Greaves, T. L.; Drummond, C. J. *Chem. Rev.* **2008**, *108*, 206–237.

(5) Lei, Z.; Dai, C.; Chen, B. *Chem. Rev.* **2014**, *114* (2), 1289–1326.

(6) Estager, J.; Holbrey, J. D.; Swadźba-Kwaśny, M. *Chem. Soc. Rev.* **2014**, *43* (3), 847–886.

(7) Angell, C. A. *ECS Trans.* **2014**, *64* (4), 9–20.

(8) MacFarlane, D. R.; Tachikawa, N.; Forsyth, M.; Pringle, J. M.; Howlett, P. C.; Elliott, G. D.; Davis, J. H.; Watanabe, M.; Simon, P.; Angell, C. A. *Energy Environ. Sci.* **2014**, *7* (1), 232–250.

(9) Angell, C. A. *Molten Salts Ion. Liq. Never Twain?* **2012**, 1–24.

(10) Angell, C. A.; Ansari, Y.; Zhao, Z. *Faraday Discuss.* **2012**, *154* (1), 9.

(11) Angell, C. A.; Byrne, N.; Belieres, J. P. *Acc. Chem. Res.* **2007**, *40*, 1228–1236.

(12) Greaves, T. L.; Drummond, C. J. *Chem. Soc. Rev.* **2008**, *37* (8), 1709–1726.

(13) Endres, F. *Phys. Chem. Chem. Phys.* **2010**, *12*, 1648.

(14) Patel, D. D.; Lee, J. M. *Chem. Rec.* **2012**, *12* (3), 329–355.

(15) Earle, M. J.; Seddon, K. R. *Pure Appl. Chem.* **2000**, *72* (7), 1391–1398.

(16) Preiss, U.; Verevkin, S. P.; Koslowski, T.; Krossing, I. *Chem. - A Eur. J.* **2011**, *17* (23), 6508–6517.

(17) Slattery, J. M.; Daguenet, C.; Dyson, P. J.; Schubert, T. J. S.; Krossing, I. *Angew. Chemie - Int. Ed.* **2007**, *46* (28), 5384–5388.

(18) Xu, X.; Hussey, C. L. **1993**, *140* (3), 618–626.

(19) Wilkes, J. S. *Green Chem.* **2002**, *4*, 73–80.

(20) Mandai, T.; Yoshida, K.; Ueno, K.; Dokko, K.; Watanabe, M. *Phys. Chem. Chem. Phys.* **2014**, *16* (19), 8761–8772.

(21) Walden, P. *Bull. Acad. Imp. Sci.* **1914**, *8*, 405–422.

(22) Yoshizawa, M.; Xu, W.; Angell, C. A. *J. Am. Chem. Soc.* **2003**, *125* (8), 15411–15419.

(23) Xu, W.; Cooper, E. I.; Angell, C. A. *J. Phys. Chem. B* **2003**, *107*, 6170–6178.

(24) MacFarlene, D. R.; Seddon, K. R. *Aust. J. Chem.* **2007**, *60*, 3–5.

(25) MacFarlane, D. R.; Pringle, J. M.; Johansson, K. M.; Forsyth, S. A.; Forsyth, M. *Chem. Commun. (Camb).* **2006**, 1905–1917.

(26) Davidowski, S. K.; Thompson, F.; Huang, W.; Hasani, M.; Amin, S. A.; Angell, C. A.; Yarger, J. L. *J. Phys. Chem. B* **2016**, *120* (18), 4279–4285.

(27) Nuthakki, B.; Greaves, T. L.; Krodkiewska, I.; Weerawardena, A.; Burgar, M. I.; Mulder, R. J.; Drummond, C. J. *Aust. J. Chem.* **2007**, *60*, 21–28.

(28) Miran, M. S.; Kinoshita, H.; Yasud, T. *Phys. Chem. Chem. Phys.* **2012**, *14*, 5178.

(29) Tokuda, H.; Tsuzuki, S.; Susan, M. A. B. H.; Hayamizu, K.; Watanabe, M. *J. Phys. Chem. B* **2006**, *110*, 19593–19600.

(30) Angell, C. A.; Byrne, N.; Belieres, J. P. *Acc. Chem. Res.* **2007**, *40* (11), 1228–1236.

(31) Belieres, J.-P.; Angell, C. A. *J. Phys. Chem. B* **2007**, *111*, 4926–4937.

(32) Gillespie, R. J.; Peel, T. E. *J. Am. Chem. Soc.* **1973**, *95* (16), 5173–5178.

(33) Robert, T.; Magna, L.; Olivier-Bourbigou, H.; Gilbert, B. *J. Electrochem. Soc.* **2009**, *156*, F115.

(34) Johnson, K. E.; Pagni, R. M.; Bartmess, J. *Monatshefte fur Chemie* **2007**, *138*, 1077–1101.

(35) Kamlet, M. J.; Abboud, J. L.; Taft, R. W. *J. Am. Chem. Soc.* **1977**, *99* (18), 6027–6038.

(36) Kurnia, K. A.; Lima, F.; Claudio, A. F.; Coutinho, J. A. P.; Freire, M. G. *Phys. Chem. Chem. Phys.* **2015**, *17* (29), 18980–18990.

(37) Macfarlane, D. R.; Vijayaraghavan, R.; Ha, H. N.; Izgorodin, A.; Weaver, K. D.; Elliott, G. D. *Chem. Commun. (Camb).* **2010**, *46*, 7703–7705.

(38) Shukla, S. K.; Kumar, A. *J. Phys. Chem. B* **2013**, *117*, 2456–2465.

(39) Adam, C.; Bravo, M. V.; Mancini, P. M. E. *Tetrahedron Lett.* **2014**, *55* (1), 148–150.

(40) Thomazeau, C.; Olivier-Bourbigou, H.; Magna, L.; Luts, S.; Gilbert, B. *J. Am. Chem. Soc.* **2003**, *125* (18), 5264–5265.

(41) Bartosik, J.; Mudring, A. V. *Phys. Chem. Chem. Phys.* **2010**, *12*, 1648.

(42) Schmeisser, M.; Illner, P.; Puchta, R.; Zahl, A.; Van Eldik, R. *Chem. - A Eur. J.* **2012**, *18*, 10969–10982.

(43) McCune, J. A.; He, P.; Petkovic, M.; Coleman, F.; Estager, J.; Holbrey, J. D.; Seddon, K. R.; Swadźba-Kwaśny, M. *Phys. Chem. Chem. Phys.* **2014**, *16*, 23233–23243.

(44) Gräsvik, J.; Hallett, J. P.; To, T. Q.; Welton, T. *Chem. Commun. (Camb).* **2014**, *50*, 7258–7261.

(45) Tang, L.; Zeller, R.; Angell, C. A.; Friesen, C. *J. Phys. Chem. C* **2009**, *113*, 12586–12593.

(46) Miran, M. S.; Yasuda, T.; Susan, M. A. B. H.; Dokko, K.; Watanabe, M. *RSC Adv.* **2013**, *3* (13), 4141–4144.

(47) Kanzaki, R.; Doi, H.; Song, X.; Hara, S.; Ishiguro, S. I.; Umebayashi, Y. *J. Phys. Chem. B* **2012**, *116*, 14146–14152.

(48) Hashimoto, K.; Fujii, K.; Shibayama, M. *J. Mol. Liq.* **2013**, *188*, 143–147.

(49) Miran, M. S.; Kinoshita, H.; Yasuda, T.; Susan, M. A. B. H.; Watanabe, M. *Phys. Chem. Chem. Phys.* **2012**, *14*, 5178.

(50) Davidowski, S. K.; Thompson, F.; Huang, W.; Hasani, M.; Amin, S.; Yarger, J. L.; Angell, C. A. *J. Phys. Chem. B, Submitt.*

(51) Angell, C. A.; Shuppert, J. W. *J. Phys. Chem.* **1980**, *84*, 538–542.

(52) Johansson, K. M.; Izgorodina, E. I.; Forsyth, M.; MacFarlane, D. R.; Seddon, K. R. *Phys. Chem. Chem. Phys.* **2008**, *10*, 2972–2978.

(53) Laurence, C.; Graton, J.; Gal, J. F. *J. Chem. Educ.* **2011**, *88* (12), 1651–1657.

(54) Laurence, C.; Gal, J. F. *Lewis Basicity and Affinity Scales; Data and Measurement*; John Wiey & Sons: Chichester, U.K., 2010.

(55) Ahrland, S.; Chatt, J.; Davies, N. R. *Quart. Rev.* **1958**, *12*, 265–276.

2 On the Use of a Protic Ionic Liquid with a Novel Cation to Study Anion Basicity

The need for reliable means of ordering and quantifying the Lewis basicity of anions is discussed and the currently available methods are reviewed. Concluding that there is need for a simple impurity-insensitive tool, we have sought, and here describe, a new method using NMR spectroscopy of a weak base, a substituted urea, 1,3-Dimethyl-2-imidazolidinone (DMI), as it is protonated by Brønsted acids of different strengths and characters. In all cases studied the product of protonation is a liquid (hence a Protic Ionic Liquid). NMR detects changes in the electronic structure of the base upon interaction with the proton donors. As the proton donating ability, i.e. acidity, increases, there is a smooth but distinct transition from a hydrogen bonded system (with no net proton transfer) to full ionicity. The liquid state of the samples and high concentration of nitrogen atoms, despite the very low natural abundance of its preferred NMR active isotope (^{15}N), make possible the acquisition of ^{15}N spectra in a relatively short time. These ^{15}N, along with ^{13}C, chemical shifts of the carbonyl atom, and their relative responses to protonation of the carbonyl oxygen, can be used as a means, sensitive to anion basicity and relatively insensitive to impurities, to sort anions in order of increasing hydrogen bond basicity. The order is found to be as follows: $SbF_6^- < BF_4^- < NTf_2^- > ClO_4^- > FSO_3^- < TfO^- < HSO_4^- < Cl^- < MsO^-$.

2.1 Introduction

Protic ionic liquids (PILs) are made by proton transfer from a Bronsted acid to a base[1–3] and are the subject of increasing attention as solvents for new industrial processes as well as material for fundamental structural studies.[4,5] They can conveniently be made in one step by direct reaction between the acid and the base and in some cases can be purified by distillation.[6] These make them favorable for large scale production and attractive for industrial use.[7]

One of the most important factors determining the properties of an ionic liquid (IL) is the basicity of its anion. The effect of the anion on the physicochemical properties of ILs has been the subject of a great number of studies.[8–13] Their basicities can to some extent be inferred from the equilibrium constant of their corresponding acids' dissociation at low concentrations in water[2,14] (pKa values) but the accuracy of such deduction is limited by solvent (medium) and concentration effects.[15–17] The problem is more serious for the most common, least basic ones because of the controversy that already exists over the acidity (acidity function,[15,18] H_0 values) of superacids,[19] despite insightful studies suggesting acidity/basicity scales.[20–22] Most recent is the development of an absolute pH scale based on the gas phase standard state of the proton,[23] which has already found application in mixed-solvent liquid chromatography.[24] We make further reference to this in the discussion section. Other thermodynamic measures of the property, both from experiments and calculations, have been reported and include gas phase proton affinities/basicities[25,26], heats of reactions from calorimetry,[27,28] proton activity from its reduction potential[29–32] and partition coefficients between two phases from chromatography.[24,33] Anion basicity is also factored in equations to describe the

polarity[34,35] of solvents in general and ionic liquids in particular.[36,37] Kamlet-Taft multi-parameter equation is a well-known example.[38,39]

A number of qualitative and quantitative spectroscopic scales are also reported which are mostly based on UV-Vis[40–45], IR[46,47] and NMR[14,48–55] spectroscopies. Most of these methods are based on spectroscopic characterization of a probe, dissolved in ILs at low concentrations, whose response is found to be correlated to the acidity/basicity of the medium. The main disadvantage of this approach is the disproportionate effect of impurities consequent on the low concentration of the probe. In the case of Guttmann DN measured by ^{23}Na NMR, the broadness of sodium lines is another source of error. There is also a subtle point here worth making that the basicity of anions towards sodium ion is not necessarily the same as their basicity towards proton. This is in addition to the fact that the cation has a non-innocent effect on ^{23}Na chemical shift since it competes with the sodium ion for the anion and the result of this competition affects the chemical shift.

Proton chemical shifts of IL cations have been reported as indicative of their anions basicity.[49,52,56] The advantage of the methods of this sort is that they rely on a property of the system itself and not on that of an external probe. Even though less sensitive to impurities compared to the former approach, because the measurement is directly on the proton, they are still sensitive to protic impurities such as water which is almost always present. In the work presented here, we try to keep the advantages of this approach but to use ^{15}N and ^{13}C chemical shifts, both separately and in concert. These are shown to be less sensitive to the presence of protic impurities, namely water.

Figure 2-1. Protonation of DMI at its oxygen atom, developing a partial positive charge on nitrogen atoms and changing the C-O and C-N bond orders.

A weak base, 1,3-Dimethyl-2-imidazolidinone (DMI), is selected to obtain liquid mixtures with a wide range of Bronsted acids used in this study. DMI, which to the best of our knowledge has not been used to make PILs before, shows larger changes in the ^{15}N and ^{13}C chemical shifts upon interaction with acids, compared to aliphatic amines for example, and the presence of the amide bond also makes it suitable and conveniently responsive for vibrational spectroscopic characterization. It is known that amides interact with electrophiles,[57] specifically proton,[58–60] through their oxygen atom (Figure 2-1), putting a positive charge on the nitrogen atom and giving C-N bond more, and C-O bond less, of a double-bond character. This change in the electronic structure of the base is what causes the change in the directly involved ^{15}N and ^{13}C nuclei chemical shifts, and also the disappearance of the C=O stretching band upon protonation (explained further below). The change in the ^{15}N and ^{13}C chemical shifts of DMI are carefully monitored in its mixtures with two acids, sulfuric acid (H_2SO_4) and methanesulfonic acid (HOMs), over the full range of compositions and then measured at composition 1:1 (i.e. for DMI-based PILs) using different acids of different character and strength. It will be presented in the results section how this systematic change can give a qualitative order of the basicity of IL anions. It is also shown that infrared (IR) spectroscopy can show the partial protonation suggested by using Walden plots.[2]

In summary, this contribution addresses the subject of anion basicity and ionicity of protic ionic liquids by briefly acknowledging the existing methods and then offering a new tool for assessment of the basicity of the anions used to make ILs with a certain novel cation of specific electronic structure, suitable for NMR and vibrational spectroscopic characterization. A qualitative order of basicity is presented for the weakly coordinating anions which for the most part agrees with the results of other studies but suggests values for the strength of some important cases different from those seen before.

2.2 Experimental and Results

Materials. 1,3-Dimethyl-2-imidazolidinone (DMI, >99.5%) was obtained from Sigma-Aldrich and stored over activated molecular sieves in a glove box. Acetic acid (HOAc, >99%), acetic anhydride (Ac_2O, >99%), dichloroacetic acid ($HOAcCl_2$, >99%), phosphoric acid (H_3PO_4, >99.9%), trifluoroacetic acid (TFA, >99%), trifluoroacetic anhydride (TFA_2O, >99%) methanesulfonic acid (HOMs, >99.5%), sulfuric acid (H_2SO_4, >99.99%), fluorosulfuric acid (FSO_3H, triple-distilled), fluoroantimonic acid ($HSbF_6$, triple distilled) and 3Å molecular sieves were obtained from Sigma-Aldrich. Acid anhydrides were used to control the water content of the corresponding acids. Trifluoromethanesulfonic acid (triflic acid, HOTf, 98+%), hydrogenbistrifluoromethanesulfonylimide ($HNTf_2$, 95%) and tetrafluoroboric acid (HBF_4, 48% w/w aqueous solution) were obtained from Afla-Aesar and used as received.

Synthesis of PILs. All glassware were thoroughly dried in a vacuum oven prior to use. The PIL samples were made by directly mixing equimolar amounts of the base and the acids under an inert atmosphere at lowered temperatures (0 ^oC using an ice-bath for acids weaker than sulfuric acid and -78 ^oC using an acetone/dry ice bath for the stronger ones). No further preparation was performed on the samples except for the case of tetrafluoroborate salt which was dried under vacuum at 80 ^oC for 16 hours. When possible, to ensure the correct stoichiometry between the acid and the base, careful integration of ^1H NMR peaks was used.

Water content control. The water content of the liquid starting material and of the resulting mixtures was measured using a Karl Fischer titrator, Mettler Toledo DL32X. Aquastar® CombiCoulomat Fritless, from EMD, was used as the electrolyte. Plastic

syringes were filled with around 200 μL of the samples in the glovebox, wrapped with parafilm and their water contents measured immediately after being taken out of the box.

A standard Karl-Fischer titration method was used to measure the water content of the PILs. None of the samples interfere with the bipotentiometric detection of the end point. The sample sizes, the measured water content and the ppm values of the water content are listed in the table below (Table 2-1).

Table 2-1- Water content KF measurement data for the PIL samples.

Sample Name	Sample Mass (g)	Water Content (µg)	Water Content (ppm)
DMI	0.2659	9.1	34
DMI-H_2O	-	-	--
DMI-HOAc	0.3658	12.5	34
DMI-$HOAcCl_2$	0.374	15	40
DMI-HTFA	0.2554	6.4	25
DMI-H_3PO_4	0.3614	21	58
DMI-HOMs	0.318	33	104
DMI-HCl	0.289	6.8	24
DMI-H_2SO_4	0.3344	28	84
DMI-HOTf	0.2965	31.4	106
DMI-FSO_3H	0.2441	13.3	54
DMI-$HClO_4$	0.3276	15	46
DMI-$HNTf_2$	0.386	26.1	68
DMI-HBF_4	0.2248	22	98
DMI-$HSbF_6$	0.3015	20.6	68

The chemical shift change data resulted from addition of water to DMI-HOTf is presented in Table 2-2.

Table 2-2- The effect of added water on chemical shifts of different nuclei

Added Water μL	**δ ^{1}H** ppm	**%Δ δ ^{1}H**	**δ ^{15}N** ppm	**%Δ δ ^{15}N**	**δ ^{13}C** ppm	**%Δδ ^{13}C**
0	12.48	0	-298.45	0	159.63	0
5	12.29	-2.375	-298.64	-1.1875	159.77	2
10	12.1	-4.75	-298.8	-2.1875	159.86	3.28571
15	11.86	-7.75	-298.9	-2.8125	159.98	5
20	11.64	-10.5	-299.02	-3.5625	160.08	6.42857
30	11.24	-15.5	-299.23	-4.875	160.25	8.85714
40	10.91	-19.625	-299.45	-6.25	160.41	11.14286
60	10.38	-26.25	-299.82	-8.5625	160.68	15

The normalized values are obtained by dividing the amount of the chemical shift change (Δδ) by the range over which the chemical shift changes (8, 16 and 7 ppm for H, N and C nuclei, respectively).

For example, adding 10 μL of water causes a change of 0.2 ppm in both ^{1}H and ^{15}N chemical shifts but because ^{15}N chemical shift range (16 ppm) is twice that of ^{1}H (8 ppm), the error caused by this change is half. It can be seen that the effect of water is less on ^{13}C than ^{1}H and the least on ^{15}N chemical shifts; i.e. the farther the nucleus is from the site of protonation the less sensitive it is to the protic impurity.

NMR spectroscopy. The samples were transferred to 5 mm NMR tubes in a glove box and flame-sealed. All spectra were collected on a 400 MHz Varian VNMRS spectrometer equipped with a Varian 5 mm double resonance ^{1}H – X broad band probe operating at 40.499 MHz resonant frequency. All ^{1}H spectra were collected using a recycle delay of 10 seconds, 8 scans and a 45^{o} ^{1}H pulse with a duration of 10.60 μs. ^{1}H and ^{13}C chemical shifts were externally referenced to the TMS peak of a mixture of 1% TMS in $CDCl_3$ shortly before the spectra were collected. The magnetic field was shimmed manually for each sample to minimize magnetic field inhomogeneities. ^{15}N spectra were collected using a recycle delay of 1-3 seconds averaging 512-1024 transients and a 60^{o} pulse with a duration of 19.40 μs. All ^{15}N chemical shifts were indirectly referenced to methyl nitrite by setting the resonance for benzamide to -277.8 ppm shortly before the spectra were collected.

Infrared spectroscopy. IR spectra were recorded on a NICOLET 380 FT-IR spectrometer in the 500-4000 cm^{-1} range using a diamond ATR element. A drop of the sample was directly placed on the ATR element before collecting the spectrum.

Conductivity measurements. Ionic conductivity of the ILs was measured using a home-made dip cell with two platinum discs. The cell constant was determined with a solution of 0.1 M KCl at 25 ^{o}C. The complex impedance spectra were taken using a potentiostat (PAR VMP2) in the frequency range between 10 MHz and 0.01 Hz and the Nyquist plot of impedance data was used to obtain the conductance. Each measurement was made three times to ensure that the samples were thermally equilibrated. A constant temperature oven (Yamoto DKN402) was used for temperature control and the samples were kept at each temperature for an hour before the measurement is made.

The resistances of the samples were measured in a home-made dip cell with two platinum discs electrodes and a glass capillary to place a thermocouple. The thermocouple is used to precisely monitor the temperature of the sample in the vicinity of the measuring electrodes. Each resistance measurement was repeated 3 times to ensure the thermal equilibrium of the sample. The values in the tables below are the average of the three measurements. The ionic conductivity of the sample is related to the measured resistance through the equation below:

$$\sigma = \frac{l}{RA}$$

where the ratio l/A is the cell constant and is measured using standard aqueous solutions of KCl (0.01, 0.1 and 1 M). The dip cell used in obtaining the results below has a cell constant of 1.8 cm^{-1}. Tables 2-3 through 2-5 list the measured resistance and calculated conductivity data of the three samples, DMI-H_2SO_4, DMI-HOMs and DMI-HTFA, respectively. The Arrhenius plot of the logarithm of conductivity versus 1000/T is shown in Figure 2-2.

Table 2-3- Measured resistance and calculated conductivity data of DMI-H_2SO_4 at different temperatures.

Temperature °C	**1000/T** K^{-1}	**Resistance (R)** Ohm	**Conductivity (σ)** $S.cm^{-1}$	**log σ**/$S.cm^{-1}$
28.1	3.32116	1089	0.00165	-2.78176
38.7	3.20821	624	0.00288	-2.53991
58.9	3.01296	271	0.00664	-2.1777
79.1	2.8401	139	0.01295	-1.88774
98.8	2.68962	86	0.02093	-1.67923
118.2	2.55624	65	0.02769	-1.55764

Table 2-4- Measured resistance and calculated conductivity data of DMI-HOMs at different temperatures.

Temperature °C	**1000/T** K^{-1}	**Resistance (R)** Ohm	**Conductivity (σ)** $S.cm^{-1}$	**log σ**/$S.cm^{-1}$
27.3	3.33	580	0.0031	-2.50816
38.6	3.20924	426	0.00423	-2.37414
58.8	3.01386	248	0.00726	-2.13918
79.1	2.8401	160	0.01125	-1.94885
98.7	2.69034	114	0.01579	-1.80163
118.1	2.55689	88	0.02045	-1.68921

Table 2-5- Measured resistance and calculated conductivity data of DMI-HTFA at different temperatures.

Temperature °C	**1000/T** K^{-1}	**Resistance (R)** Ohm	**Conductivity (σ)** $S.cm^{-1}$	**log σ**/$S.cm^{-1}$
29.2	3.30907	798	0.00226	-2.64673
38	3.21543	683	0.00264	-2.57915
57.4	3.02663	517	0.00348	-2.45822
78.3	2.84657	403	0.00447	-2.35003
97.7	2.6976	331	0.00544	-2.26456
117.1	2.56345	280	0.00643	-2.19189

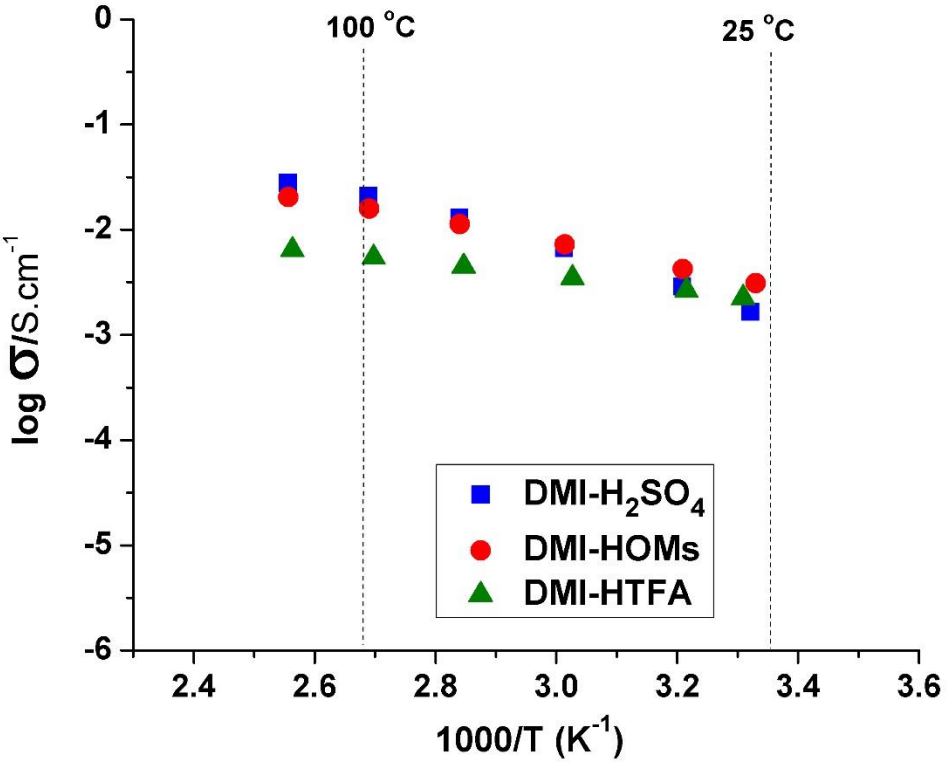

Figure 2-2- Ionic conductivity of the PIL samples as a function of temperature

Viscosity measurements. Kinematic viscosities were measured using a small sample U-tube CANNON kinematic viscometer. An aluminum block was used for temperature control within 0.2 ^{o}C.

Kinematic viscosity of the PIL samples were measured using small sample U-tube CANNON™ viscometers per standard test ASTM D 445 and ISO 3104. Size 450 U-tube with a kinematic viscosity range of 500 to 2500 cSt was used for DMI-H_2SO_4 whereas for DMI-HOMs and DMI-HTFA, size 150 with a kinematic viscosity range of 7 to 35 cSt was used. Each tube was calibrated at two temperatures (40 and 100 ^{o}C) and a calibration line was used to obtain the kinematic viscosity constant (in mm^2/s^2) at different temperatures.

Dynamic (absolute) viscosity values ($\boldsymbol{\eta}$ in cP) were calculated by multiplying the constant by the measured flow time in the capillary and the density. Each measurement was carried out three times and the average recorded. Considering the importance of the temperature control in viscosity measurements, an aluminum block was used to control the temperature within 0.2 ^{o}C during the measurements.

Fluidity ($\boldsymbol{\eta}^{-1}$ in cP^{-1}) of the liquids is the reciprocal of their dynamic (absolute) viscosities and is reported in reciprocal centipoise.

Table 2-6- Viscosity data for DMI-H_2SO_4 at different temperatures

Temp. °C	**Constant** mm^2/s^2	**Time** s	**Viscosity(η)** cP	**1000/T** K^{-1}	**log η**/cP	**Fluidity (η^{-1})** cP^{-1}
26.5	2.33158	146	477.93567	3.3389	2.67937	0.00209
25.1	2.33288	158	517.50781	3.35458	2.71392	0.00193
28.1	2.33008	133	435.101	3.32116	2.63859	0.0023
38.7	2.32019	73	237.80121	3.20821	2.37621	0.00421
48.9	2.31068	45	145.98853	3.10655	2.16432	0.00685
58.9	2.30135	30	96.93271	3.01296	1.98647	0.01032
68.6	2.2923	21	67.58606	2.9274	1.82986	0.0148
79.1	2.2825	14	44.86481	2.8401	1.65191	0.02229
86.3	2.27578	11.5	36.74478	2.78319	1.5652	0.02721
98.8	2.26412	8.1	25.74847	2.68962	1.41075	0.03884

Table 2-7- Viscosity data for DMI-HOMs at different temperatures

Temp. °C	**Constant** mm^2/s^2	**Time** s	**Viscosity(η)** cP	**1000/T** K^{-1}	**log η**/cP	**Fluidity (η^{-1})** cP^{-1}
26.6	0.03811	630	30.87904	3.33778	1.48966	0.03238
27.3	0.03811	600	29.40483	3.33	1.46842	0.03401
26.6	0.03811	630	1.286	30.87904	3.33778	1.48966
38.6	0.03803	409	1.286	20.00269	3.20924	1.30109
58.8	0.03789	222	1.286	10.81684	3.01386	1.0341
79	0.03775	136	1.286	6.6018	2.84091	0.81966
98.7	0.03761	100	1.286	4.83653	2.69034	0.68453
118.1	0.03747	75	1.286	3.6143	2.55689	0.55802

Table 2-8- Viscosity data for DMI-HTFA at different temperatures

Temp. °C	**Constant** mm^2/s^2	**Time** s	**Viscosity(η)** cP	**1000/T** K^{-1}	**log η**/cP	**Fluidity (η^{-1})** cP^{-1}
26.5	0.03811	61	3.48748	3.3389	0.54251	0.28674
29.2	0.0381	59	3.37146	3.30907	0.52782	0.29661
39.6	0.03802	50	2.85171	3.19898	0.45511	0.35067
58	0.03789	38	2.15996	3.02115	0.33445	0.46297
78.3	0.03775	29	1.64221	2.84657	0.21543	0.60894
98	0.03761	24	1.3541	2.69542	0.13165	0.7385
117.1	0.03748	20.5	1.15252	2.56345	0.06165	0.86766

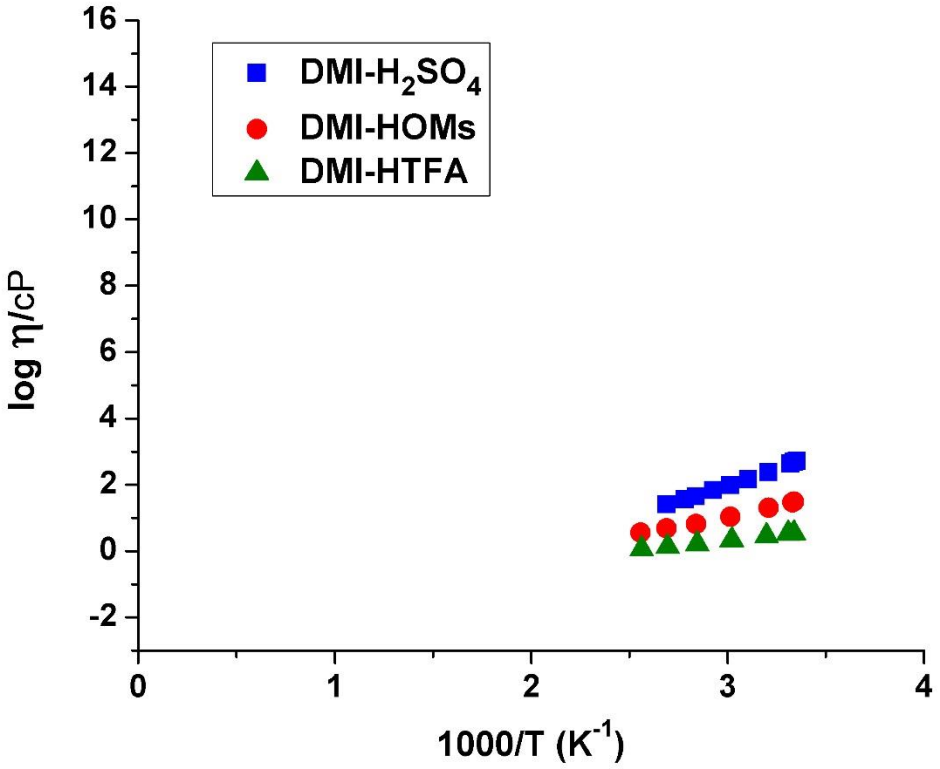

Figure 2-3- Dynamic viscosity of the PIL samples as a function of temperature

Walden plot analysis of the conductivity and viscosity data. To illustrate the conductivity-viscosity relationship of the PILs, a Walden plot representation of the data is employed. The analysis is based on the classical Walden rule which states that the product of the limiting equivalent conductivity ($\boldsymbol{\Lambda}$) and the viscosity ($\boldsymbol{\eta}$) of the medium in which the ions move is constant for infinitely dilute electrolyte solutions:

$$\Lambda\eta = Constant$$

In the absence of any ion-ion and specific ion-solvent interactions where ion mobilities are only governed by ion migration in the viscose medium, the ionic conductivity of the solution follows the Walden rule well and a slope of unity should be obtained for this "ideal" situation when logarithm of the equivalent conductivity is plotted against the logarithm of fluidity:

$$\log \Lambda = \log \eta^{-1} + \log \mathrm{C}$$

The equivalent conductivity used here is the ionic conductance of the fluid medium per volume per equivalent of charge present in that volume. In the case of pure ionic liquids, it can be calculated by dividing the product of ionic conductivity and molar mass of the PIL by its density. A fit of the viscosity data was used to obtain viscosity at the temperatures at which the conductivity data were recorded. The data are presented in tables 2-9 through 2-11. Figure 2-10 represents the Walden plots of the three PILs of this study plus EAN and EAFm for comparison.

Table 2-9- Equivalent conductivity fluidity relationship for DMI-H2SO4 at different temperatures.

Temp. °C	**Cond. (σ)** S cm^{-1}	**Fluid. (η^{-1})** cP^{-1}	**Equiv. Cond. (Λ)** S cm^2 mol^{-1}	**log Λ/** S cm^2 mol^{-1}	**log η^{-1}/**P^{-1}
28.1	0.00165	0.0023	0.24942	-0.60308	-0.63859
38.7	0.00288	0.00421	0.43534	-0.36117	-0.37621
58.9	0.00664	0.01032	1.00371	0.00161	0.01353
79.1	0.01295	0.02229	1.95753	0.29171	0.34809
98.8	0.02093	0.03884	3.1638	0.50021	0.58925

Table 2-10- Equivalent conductivity fluidity relationship for DMI-HOMs at different temperatures.

Temp. °C	**Cond. (σ)** S cm^{-1}	**Fluid. (η^{-1})** cP^{-1}	**Equiv. Cond. (Λ)** S cm^2 mol^{-1}	**log Λ/** S cm^2 mol^{-1}	**log η^{-1}/**P^{-1}
27.3	0.0031	0.034	0.46912	-0.32872	0.53148
38.6	0.00423	0.04999	0.63871	-0.1947	0.69891
58.8	0.00726	0.09245	1.09714	0.04026	0.9659
79.1	0.01125	0.15147	1.70056	0.23059	1.18034
98.7	0.01579	0.20676	2.38675	0.37781	1.31547
118.1	0.02045	0.27668	3.09193	0.49023	1.44198

Table 2-11- Equivalent conductivity fluidity relationship for DMI-HTFA at different temperatures.

Temp. ^{o}C	**Cond. (σ)** S cm^{-1}	**Fluid. (η^{-1})** cP^{-1}	**Equiv. Cond. (Λ)** S cm^2 mol^{-1}	**log Λ/** S cm^2 mol^{-1}	**log η^{-1}/**P^{-1}
29.2	0.00226	0.29661	0.34096	-0.46729	1.47218
38	0.00264	0.35067	0.39837	-0.39971	1.47218
57.4	0.00348	0.46297	0.52629	-0.27878	1.47218
78.3	0.00447	0.60894	0.67516	-0.17059	1.47218
97.7	0.00544	0.7385	0.82202	-0.08512	1.47218
117.1	0.00643	0.86766	0.97175	-0.01245	1.47218

DFT calculations. The structure of the neutral Brønsted acids, their conjugate anions, the neutral base and its conjugate cation were optimized. These optimized structures were used to make the input for optimization of the adducts. The respective coordinates, vibrational frequencies and energy levels are listed in the tables included in Appendix A. All the 3N-6 normal modes of the three adducts, DMI-$HAlBr_4$, DMI-$HAlCl_4$ and DMI-HBF_4, are listed in tables 2-12 to 2-14 below. The lack of any imaginary vibrations (those with negative frequency values) indicates a minimum in energy in the optimization process is reached. Tables 2-15 and 2-16 summarize the calculated thermochemical data for the acids and the adducts. The proton affinity results are used in a subsequent chapter as a descriptor of anion basicity and is suggested to be a better measure than pKa values. The calculated vibrational frequency of the OH bond in the adducts is also listed in Table 2-16 which can serve as an indication of the hydrogen bond interaction.

Table 2-12- DMI-$HAlBr_4$ Vibration Frequencies of Normal Modes

Normal Mode	Frequency cm^{-1}	Normal Mode	Frequency cm^{-1}
1	10.9563	**34**	1095.865
2	35.7122	**35**	1109.392
3	45.2117	**36**	1152.833
4	46.8997	**37**	1168.238
5	62.7627	**38**	1239.905
6	72.3324	**39**	1240.627
7	83.1738	**40**	1247.567
8	96.9397	**41**	1272.05
9	104.4383	**42**	1303.301
10	108.1616	**43**	1316.121
11	110.435	**44**	1349.264
12	134.1327	**45**	1417.553
13	138.143	**46**	1454.642
14	152.9149	**47**	1462.531
15	168.1229	**48**	1483.339
16	198.6259	**49**	1494.148
17	213.419	**50**	1504.467
18	259.409	**51**	1513.839
19	286.261	**52**	1516.714
20	335.0452	**53**	1532.596
21	349.942	**54**	1647.752
22	388.4909	**55**	1660.67
23	434.823	**56**	3026.542
24	494.0693	**57**	3036.776
25	576.3692	**58**	3036.945
26	651.2333	**59**	3046.43
27	674.5157	**60**	3074.333
28	707.4897	**61**	3085.057
29	751.65	**62**	3097.015
30	860.7492	**63**	3101.574
31	974.0745	**64**	3102.853
32	980.6293	**65**	3155.534
33	1056.029	**66**	3156.978

Table 2-13- DMI-$HAlCl_4$ Vibration Frequencies of Normal Modes

Normal Mode	Frequency cm^{-1}	Normal Mode	Frequency cm^{-1}
1	25.0473	**34**	1096.63
2	53.997	**35**	1110.524
3	62.6357	**36**	1153.313
4	67.6912	**37**	1169.269
5	78.8333	**38**	1239.926
6	107.8028	**39**	1241.756
7	115.4352	**40**	1250.284
8	119.6339	**41**	1272.924
9	142.6437	**42**	1304.145
10	148.3314	**43**	1328.368
11	150.806	**44**	1356.541
12	168.8521	**45**	1417.561
13	170.8608	**46**	1455.515
14	181.7444	**47**	1461.747
15	205.9979	**48**	1485.647
16	227.0037	**49**	1495.137
17	267.6095	**50**	1506.199
18	287.1988	**51**	1514.868
19	330.3125	**52**	1515.519
20	340.1358	**53**	1532.663
21	431.8292	**54**	1647.809
22	482.1453	**55**	1660.038
23	496.1286	**56**	3027.683
24	537.078	**57**	3035.283
25	578.2829	**58**	3036.962
26	672.5569	**59**	3048.102
27	696.0205	**60**	3063.377
28	710.2662	**61**	3087.287
29	754.5701	**62**	3097.81
30	863.0123	**63**	3103.393
31	976.2755	**64**	3110.077
32	981.1737	**65**	3155.479
33	1056.332	**66**	3159.855

Table 2-14- DMI-HBF_4 Vibrational Frequencies of Normal Modes

Normal Mode	Frequency cm^{-1}	Normal Mode	Frequency cm^{-1}
1	26.107	**34**	1113.206
2	46.4014	**35**	1153.61
3	59.1804	**36**	1165.294
4	70.6159	**37**	1186.799
5	90.8206	**38**	1238.799
6	120.8862	**39**	1241.944
7	131.4742	**40**	1260.508
8	150.1274	**41**	1277.521
9	154.8607	**42**	1307.48
10	201.7262	**43**	1338.061
11	231.788	**44**	1418.276
12	281.5656	**45**	1433.126
13	285.9661	**46**	1459.348
14	327.6237	**47**	1460.873
15	335.692	**48**	1491.025
16	384.7059	**49**	1495.874
17	481.3615	**50**	1505.469
18	489.7563	**51**	1507.87
19	501.5881	**52**	1516.337
20	509.6372	**53**	1534.71
21	582.2122	**54**	1642.002
22	672.4015	**55**	1654.224
23	698.1856	**56**	2667.678
24	727.2752	**57**	3030.113
25	756.6358	**58**	3030.874
26	861.7141	**59**	3035.468
27	865.1935	**60**	3038.474
28	912.6642	**61**	3079.834
29	978.2792	**62**	3094.062
30	983.0655	**63**	3096.9
31	1058.073	**64**	3107.645
32	1068.315	**65**	3152.56
33	1102.247	**66**	3153.902

Table 2-15- Calculated Gas-Phase Enthalpies of Acids and their Conjugate Anions

Acid	Enthalpy, Acid	Enthalpy, Anion	ΔH (H_{acid} - H_{anion})	Proton Affinity
	Hartree	Hartree	Hartree	kcal mol^{-1}
H_2O	-76.43786	-75.81813	-0.61973	388.88369
HOAc	-229.09991	-228.5581	-0.54182	339.99242
$HOAcCl_2$	-1148.35281	-1147.83815	-0.51465	322.94693
HTFA	-526.93718	-526.43054	-0.50664	317.91875
H_3PO_4	-644.27275	-643.75301	-0.51974	326.1359
HOMs	-664.41548	-663.90819	-0.5073	318.32976
HCl	-460.82769	-460.30137	-0.52632	330.26926
H_2SO_4	-700.35994	-699.86663	-0.4933	309.54974
HOTf	-962.24106	-961.76452	-0.47654	299.03091
FSO_3H	-724.39156	-723.91658	-0.47498	298.05137
$HClO_4$	-761.47494	-760.99553	-0.4794	300.82808
$HNTf_2$	-1828.13809	-1827.67141	-0.46669	292.84687
HBF_4	-425.13967	-424.67484	-0.46483	291.68285
$HAlCl_4$	-2084.17935	-2083.75851	-0.42083	264.0746
$HAlBr_4$	-10539.84762	-10539.42914	-0.41848	262.59746
$HAsF_6$	-2835.78748	-2835.35673	-0.43076	270.30194
HPF_6	-941.37709	-940.93079	-0.4463	280.05333

Table 2-16- Calculated Gas-Phase Enthalpies and Free Energies of DMI Adducts

Adduct	**Enthalpy** Hartree	**Free Energy** Hartree	**OH Vibration Freq.** cm^{-1}
H_2O	-457.70932	-457.76063	3609.15
HOAc	-610.37769	-610.43912	3416.24
$HOAcCl_2$	-1529.62976	-1529.69599	3188.83
HTFA	-908.21814	-908.28316	3095.75
HOMs	-1045.69745	-1045.75973	2863.71
HCl	-842.10245	-842.15016	2453.66
H_2SO_4	-1081.6447	-1081.70618	2737.19
HOTf	-1343.52916	-1343.59726	2513.52
FSO_3H	-1105.68367	-1105.74397	2518.97
$HClO_4$	-1142.76096	-1142.82099	2647.83
HBF_4	-806.43571	-806.49459	2667.68
$HAlCl_4$	-2465.49377	-2465.55992	3063.38
$HAlBr_4$	-10921.15859	-10921.23167	3074.33

2.3 Discussion

The results of the NMR chemical shift measurements of the IL samples are listed in Table 2-17. The proton chemical shifts are for the exchangeable proton and the carbon chemical shifts are for the carbonyl carbon. The transferred proton in the cases made with polyprotic acids, i.e. H_2O, H_3PO_4 and H_2SO_4, is in fast exchange with the other acidic proton(s) and the ^{1}H chemical shifts listed are for the weighted average. For this reason and also the effect of water impurity, explained in the introduction section, the attention is focused on ^{15}N and ^{13}C chemical shifts.

Table 2-17- Exchangeable proton ^{1}H, carbonyl ^{13}C and ^{15}N chemical shifts of DMI in its 1:1 mixtures with different acids. The ^{1}H and ^{13}C shifts are externally referenced to tetramethylsilane (TMS) at 0 ppm.The ^{15}N shifts are externally referenced to nitromethane.

	δ -^{1}H (ppm)	**δ-^{13}C (ppm)**	**δ -^{15}N (ppm)**
DMI (neat)	-	161.90	-309.76
DMI-H_2O	4.19	162.40	-308.12
DMI-HOAc	11.73	162.79	-307.59
DMI-$HOAcCl_2$	13.80	162.83	-306.32
DMI-TFA	15.31	163.10	-305.98
DMI-H_3PO4	15.52	162.84	-305.02
DMI-HOMs	15.58	162.50	-302.89
DMI-HCl	14.81	161.20	-300.58
DMI-H_2SO_4	13.05	160.89	-299.93
DMI-HOTf	12.47	159.82	-298.40
DMI-FSO_3H	12.20	159.6	-298.11
DMI-$HClO_4$	11.90	159.18	-297.78
DMI-$HNTf_2$	9.43	157.96	-297.56
DMI-HBF_4	8.00	156.42	-296.02
DMI-$HSbF_6$	7.73	156.05	-295.81

As suggested by the ^{15}N chemical shifts in Table 2-17 and as seen in Figure 2-4, there is a systematic increase in ^{15}N chemical shift with the increase in acid strength. The

acidity order suggested by ^{15}N chemical shift presented in Figure 2-4 is for the most part consistent with the pKa values for weaker acids and H_0 values for the stronger ones.

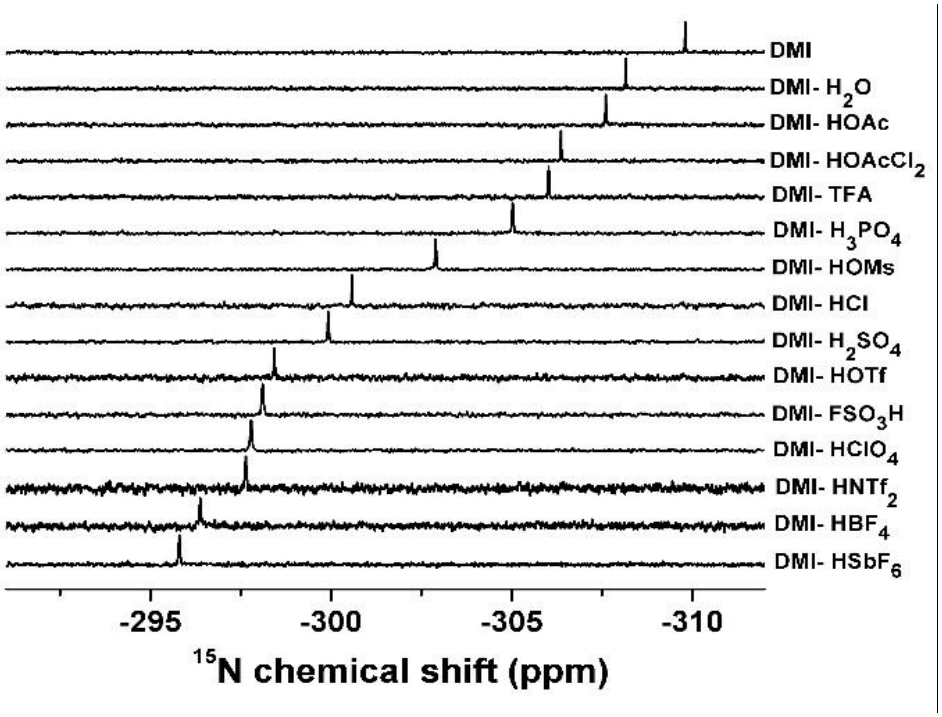

Figure 2-4- ^{15}N spectra of DMI in its 1:1 mixtures with proton donors. The downfield shift is attributed to the change in the electronic structure of DMI caused by protonation.

H_3PO_4 (with a pKa value of 2.12) is one exception causing a bigger downfield shift than trifluoroacetic acid (pKa = 0.52). It will be explained, later, that neither of the two acids is strong enough to effectively transfer a proton to DMI (pKa = 2) and the effect on the chemical shift is a result of change in the polarity of the medium, specifically hydrogen bonding. The superacid part of the order which is of more interest to us will be explained later in this section after considering some results of complimentary studies.

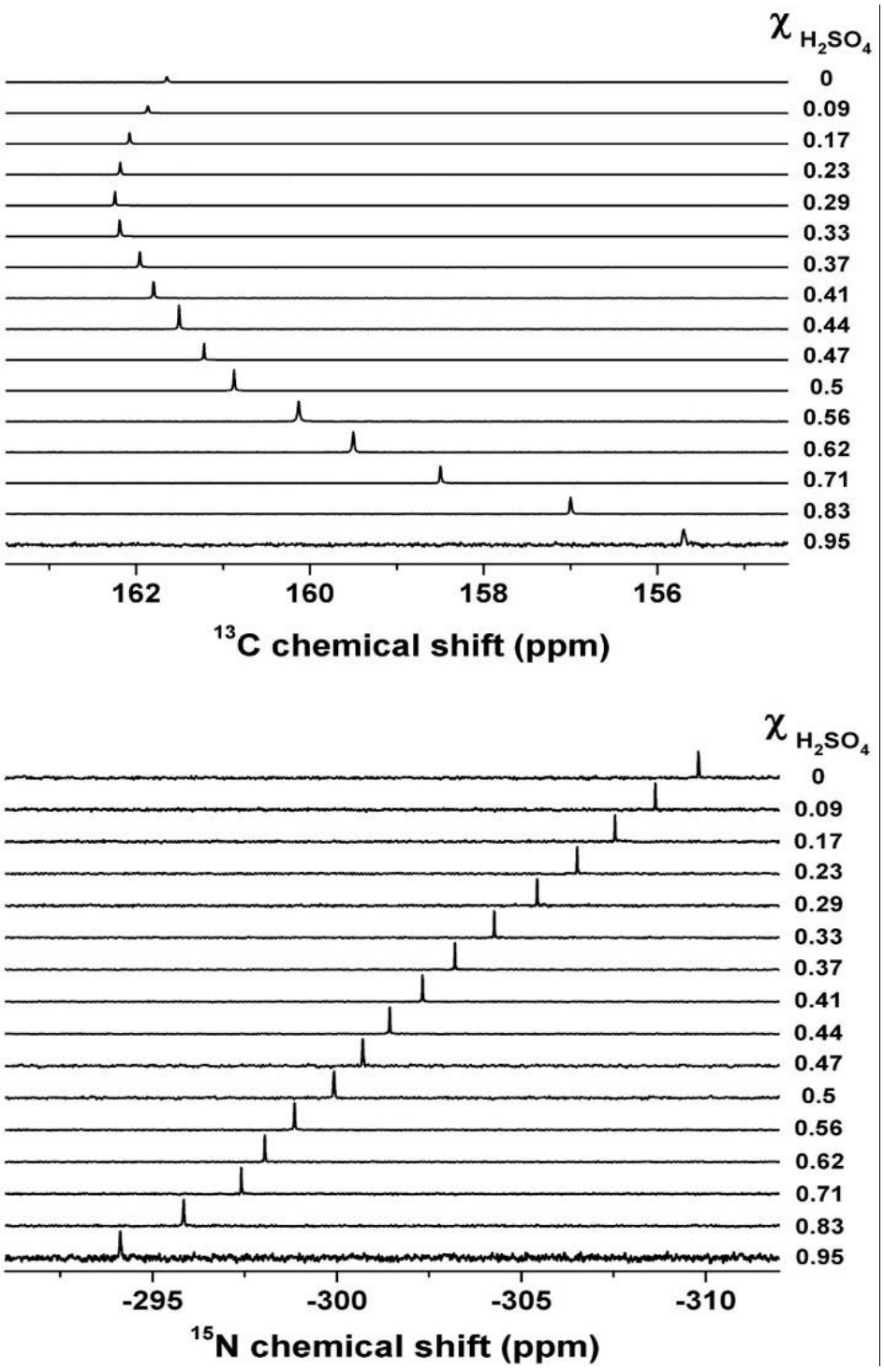

Figure 2-5- ^{13}C (top) and ^{15}N (bottom) spectra of DMI in media with varying acid strengths. Only the carbonyl region is shown in the ^{13}C spectra.

To study the effect of medium acidity on the nuclear magnetic resonance behavior of the DMI nuclei more carefully, the chemical shifts were examined as the base is titrated with two acids, H_2SO_4 and HOMs. The spectra are shown in Figure 2-5. When ^{13}C and ^{15}N chemical shifts are plotted against mole fraction of the acid, seen in Figure 2-6, the trends are clearer. ^{15}N chemical shift monotonically decreases as the mole fraction of the acid increases. It was expected from the results shown in Figure 2-4 that increasing acidity is correlated with decrease in ^{15}N chemical shift and supports the order suggested in Figure 2-4.

However, the ^{13}C chemical shift shows a more interesting trend. On adding the acid, it initially increases in both cases, until, after reaching a maximum, it sharply decreases. The maximum occurs at a lower acid concentration for the stronger acid, H_2SO_4, and marks the cross over to protonation regime from hydrogen bonding regime (Figure 2-6). At lower acidity, the hydrogen bonding and the change in the polarity of the medium result in an increase in ^{13}C chemical shift as the acidity increases. Beyond a certain mole fraction that depends on the acid used, increase in acid content causes effective protonation of the base which counters the increase in chemical shift and eventually becomes the only factor determining the ^{13}C chemical shift, causing a linear decrease with increase in acidity. The relationship between the ^{13}C chemical shift and mole fraction of the acid is evident from the linear fits and can be used to estimate the acidity of acids stronger than HOMs.

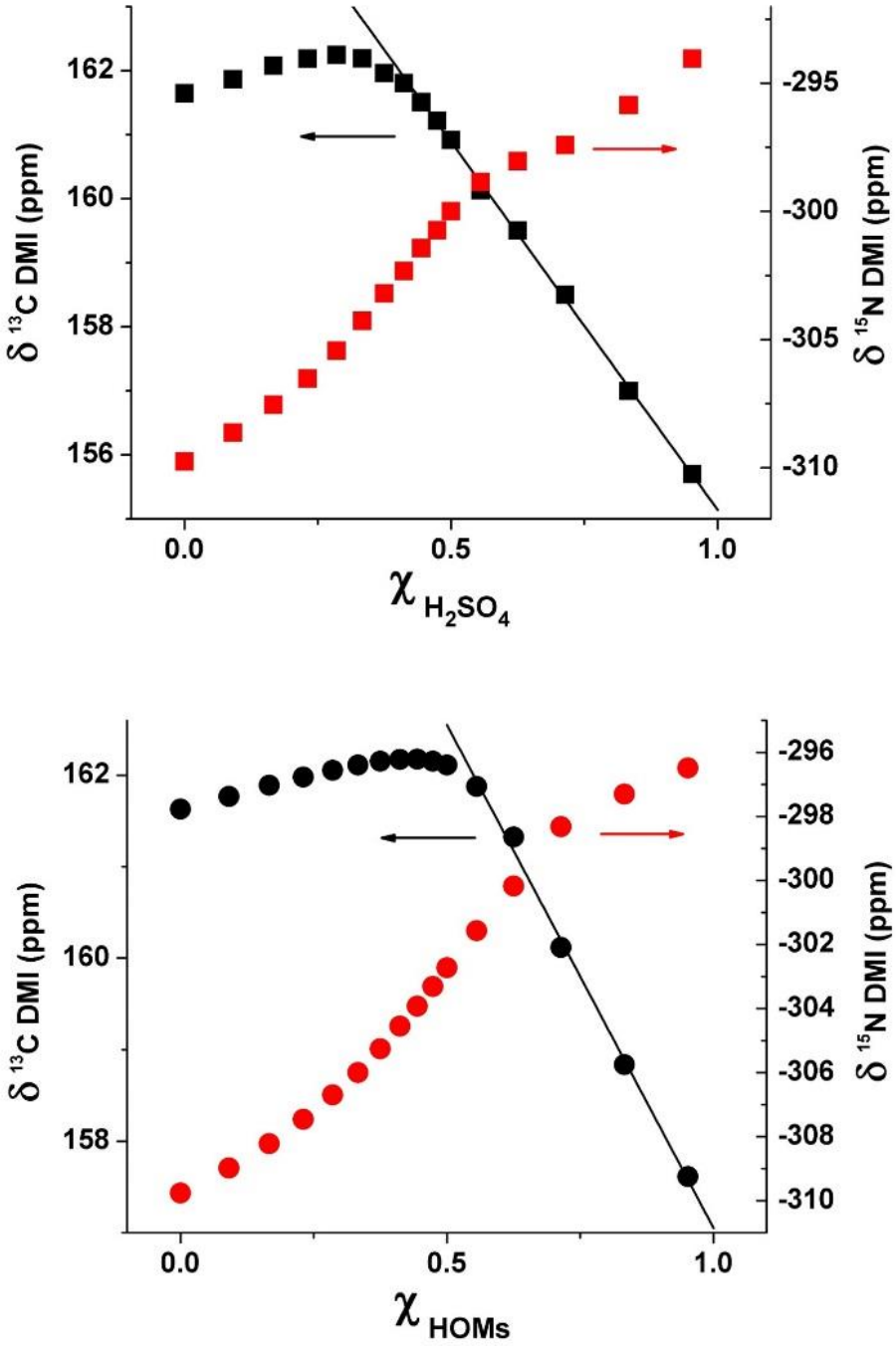

Figure 2-6- The ^{13}C and ^{15}N chemical shifts of DMI in its mixtures with H_2SO_4 (top) and HOMs (bottom) with different compositions. The linear part of the ^{13}C curve after the maximum shows the isolated effect of anion basicity. In this regime the proton is transferred to the base and the change in ^{13}C chemical shift is a result of the varying

extent of the proton interaction with the conjugate anion. The relationship between ^{13}C chemical shift and acidity is explained by the linear fits.

The relationship between acidity and mole fraction of the acids (for the regime where the dominant factor is the anion combination with free acid, $0.5 < \chi < 1$, to form hydrogen bonded di-anions and clusters $[A(HA)_x]^-$)[54,61] needs more explanation. This association of the free acid and the anion lowers the basicity of the counter-ion as explained by Polyakov et al..[62] It is shown in a recent communication[53] that H_0 values of a hydrogen sulfate ionic liquid's mixtures with H_2SO_4 changes linearly with mole ratio of the acid over almost the full range of compositions. The same behavior can be assumed for DMI hydrogen sulfate and methanesulfonate PILs so it can be concluded that ^{13}C chemical shift of DMI after protonation changes linearly with acidity. The similar slopes of the fitted lines (-11.5 for H_2SO_4 and -11.0 for HOMs), seen in Figure 2-7, show similar effect of anion combination with free acids on their basicities for the two cases.

Figure 2-7 shows the order we obtain for strong acids in the series and their relative strength based on DMI ^{13}C chemical shifts in their PILs. As shown in Figure 2-7, BF_4^- and SbF_6^- are significantly weaker bases than the rest of the anions in the series followed by NTf_2^- anion which is in turn separated from the group of other very weak bases by a considerable distance. $HNTf_2$ is reported to be a stronger acid than HOTf in the gas phase and in acetonitrile but weaker in glacial acetic acid.[63,64] Its acidity, along with those of other strong neutral Bronsted acids, in different media is tabulated and presented nicely in a more recent publication.[65] Being weaker bases than hydrogen sulfate, as suggested in Figure 2-7, makes the conjugate acids of NTf_2^- and OTf^- superacids even though it is reported that $HNTf_2$ cannot protonate water in a non-

coordinating solvent like CCl_4.[66] As far as concerns the relative strengths, it is clear from the results of ^{13}C chemical shifts that HOTf is considerably weaker than $HNTf_2$ and not quite as strong as FSO_3H which in turn is weaker than $HClO_4$. Perchloric acid which was studied at early stages of defining superacidity by Gillespie,[67,68] was only studied in concentrations up to %60 (presumably because it is explosive) but seems to be considerably more acidic than sulfuric acid based on their relative anion basicities. This order is in harmony with the Guttmann DN results on the anions of ILs.[51]

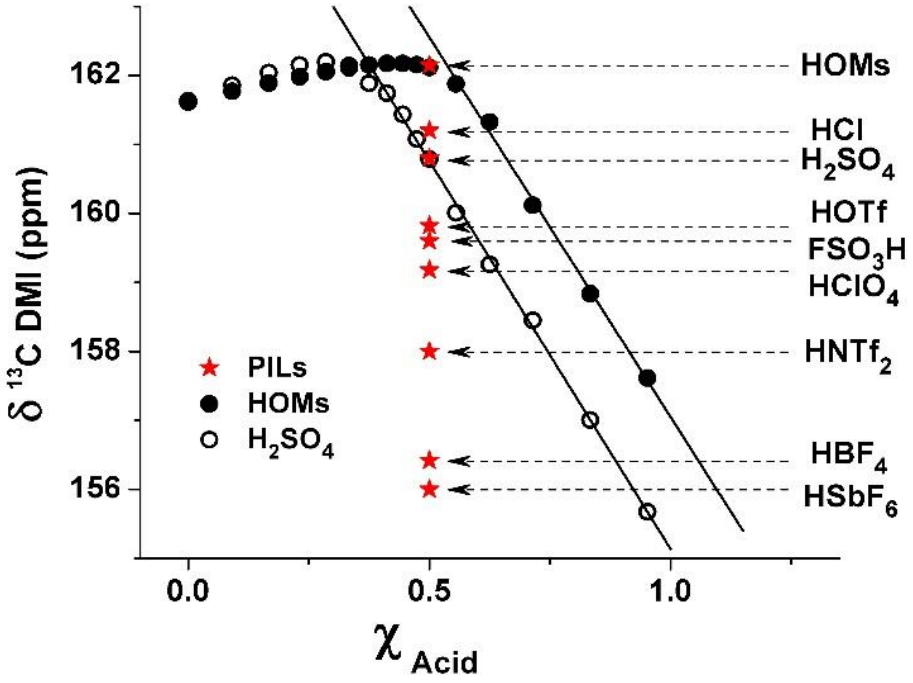

Figure 2-7- ^{13}C chemical shifts of DMI in its 1:1 mixtures with strong acids (red stars) as a measure of their anion basicities. In addition to the qualitative order presented in Figure 2-4 and Figure 2-8, the linear range of the change in ^{13}C chemical shift with acidity can be used to get a rough quantitative comparison between anion basicities of the strong acids themselves. The linear range is studied by using different mole fractions χ of two strong acids (H_2SO_4 and HOMs) and is found to include the chemical shifts obtained from all the strong acid PILs used in this study.

In an attempt to quantify acidities of these strong acids, the Hammet acidity function values (H_0 values) were calculated, based on the H_0 of the pure forms of H_2SO_4

(H_0= -12) and FSO_3H (H_0= -15.1).[55,68] The change of the ^{13}C Chemical shift (δ) is considered linear with acidity (H_0):

$$H_0 = a\delta + b$$

Where a and b are constants. We have $H_0(H_2SO_4)$ = -12 and δ (H_2SO_4) = 160.89 ppm

$$-12 = a(160.89) + b$$

Similarly, for FSO_3H we have $H_0(FSO_3H)$ = -15.1 and δ (FSO_3H) = 159.60 ppm

$$-15.1 = a(159.60) + b$$

Solving for a and b gives a=2.403 and b= -398.62 and we have:

$$H_0 = 2.403\delta - 398.62$$

The results are shown in Table 2-18.

It is noteworthy that the H_0 value obtained for triflic acid (H_0= -14.6) is exactly what Olah and coworkers[69] report for the pure form of the substance. However, it should be noted that the values used to get the above equation are for the pure acids (and hence a solvent acidity scale) and so the values in Table 2-18 are for the pure acids as well and are valid under the assumption that they behave the same in going from the X=0.5 to X=1; an assumption better held for the members of the sulfuric acid family.

Table 2-18- Hammet acidity function values

Acid	**δ -^{13}C (ppm)**	H_0
HOMs	162.5	-8.1
HCl	161.2	-11.2
H_2SO_4	160.89	-12
HOTf	159.82	-14.6
FSO_3H	159.6	-15.1

$HClO_4$	159.18	-16.1
$HNTf_2$	157.96	-19.0
HBF_4	156.42	-22.7
$HSbF_6$	156.05	-23.6

Hammet acidity functions are referenced to aqueous medium. We also recognize the possibility of using a gas phase reference state as suggested by Krossing and coworkers,[23] to quantify the acidities of these strong acids in ionic liquid media.

It is also possible to directly use Hammet dyes to measure the H_0 values of the PILs and also those of the hydrogen sulfate-sulfuric acid mixtures then relate the change in the ^{13}C chemical shift to H_0 values through composition, the same way as described by Welton for imidazolium based PILs.[53] It might be noted from Figure 2-7 that there is a possibility of using DMI as a ^{13}C NMR probe or as a prototype to design one since its response stays linear even in very acidic media (for example almost pure sulfuric acid, the last open circle to the right). This would be an advantage over other probes, such as mesityl oxide (non-linear outside H_0 = -1 to -9).[53]

Finally, both ^{15}N and ^{13}C chemical shifts of DMI in each of its mixtures with acids were considered together and plotted against each other to show the agreement between the acidity orders that each suggests (Figure 2-8). The ^{13}C chemical shifts are spread out along the horizontal axis by using ^{15}N chemical shifts so that all the PILs/mixtures can be seen in relation to each other. The ^{13}C chemical shift serves as another internal measure to show the outcome is an order agreed on by both ^{13}C and ^{15}N chemical shifts. We use color shading to depict different domains of behavior that are of interest.

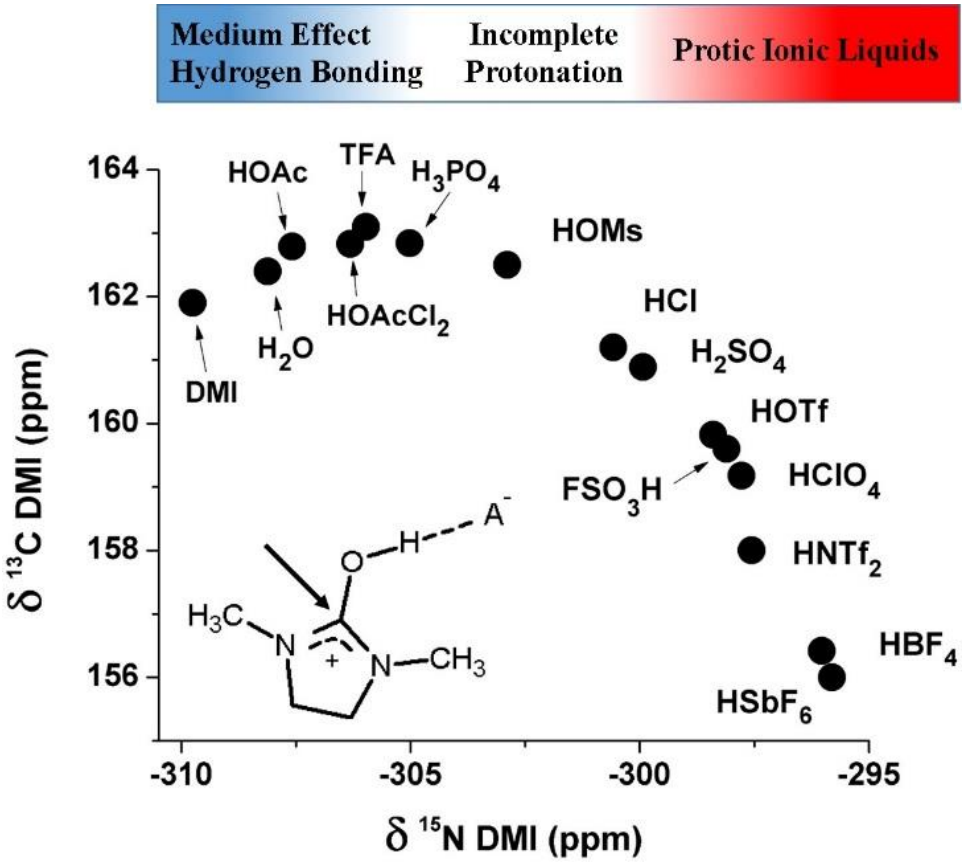

Figure 2-8- ^{13}C and ^{15}N chemical shifts of DMI in its 1:1 mixtures with acids considered simultaneously to give an order of the acid strength. The ^{13}C chemical shifts are of the marked atom in the inset structure.

As pointed out earlier, water is a common impurity in ionic liquids and its effects on any measurement should be taken into account. DMI-HOTf was picked to study the effect of water content on the chemical shifts. The original PIL contained 106 ppm of water to which was gradually added more water (up to 40,000 ppm, a mole ratio of 0.11) and mixed well. As expected, the addition of water caused a change in all three nuclei chemical shifts.

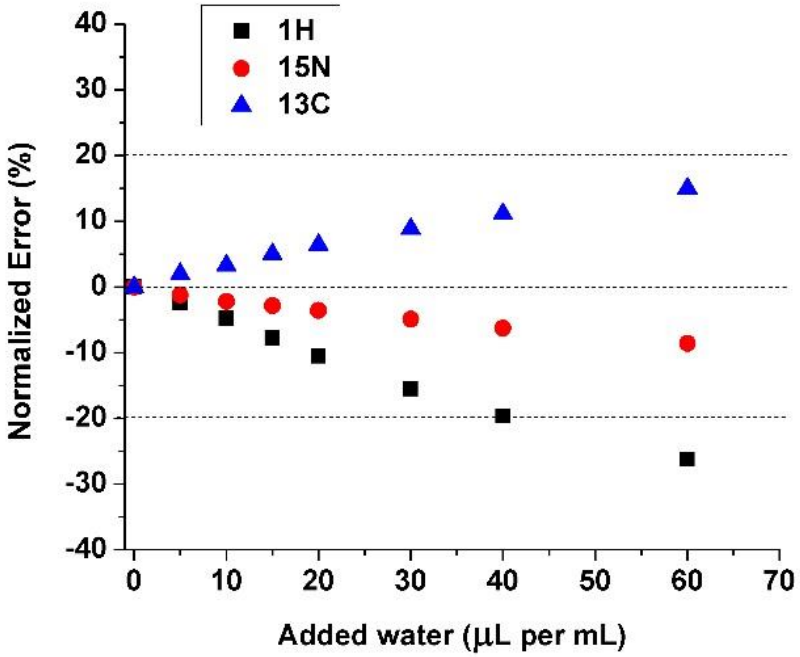

Figure 2-9- The effect of water content on ^{1}H, ^{13}C and ^{15}N Chemical shifts for DMI-HOTf (initial water content 106 ppm). The changes caused by addition of water is divided by the range over which each chemical shift changes to obtain normalized values.

To evaluate the significance of this change in each case, its ratio to the range over which the parameter changes for different samples was considered and plotted in Figure 2-9 against the added water. For example, adding 10 µL of water causes a change of 0.2 ppm in both ^{1}H and ^{15}N chemical shifts but because ^{15}N chemical shift range (16 ppm) is twice that of ^{1}H (8 ppm), the error caused by this change is half. It can be seen that the effect of water is less on ^{13}C than ^{1}H and the least on ^{15}N chemical shifts; i.e. the farther the nucleus is from the site of protonation the less sensitive it is to the protic impurity.

Ionic conductivities of the samples show the ionic nature of the DMI mixtures. A Walden plot analysis was made on a few selected samples to show the effect of the acid strength on the ionicity of the mix. Three cases are shown in Figure 2-10. H_2SO_4 is a

strong enough acid to effectively protonate all the DMI molecules and give a true ionic liquid. HOMs, as expected from the chemical shifts plots, can only incompletely protonate the base (even though there are more than three units of pKa difference between them) and this results in a lower conductivity than expected from its fluidity. The effect of incomplete protonation is more pronounced for the weaker HTFA which is some two orders of magnitude below the ideal line.

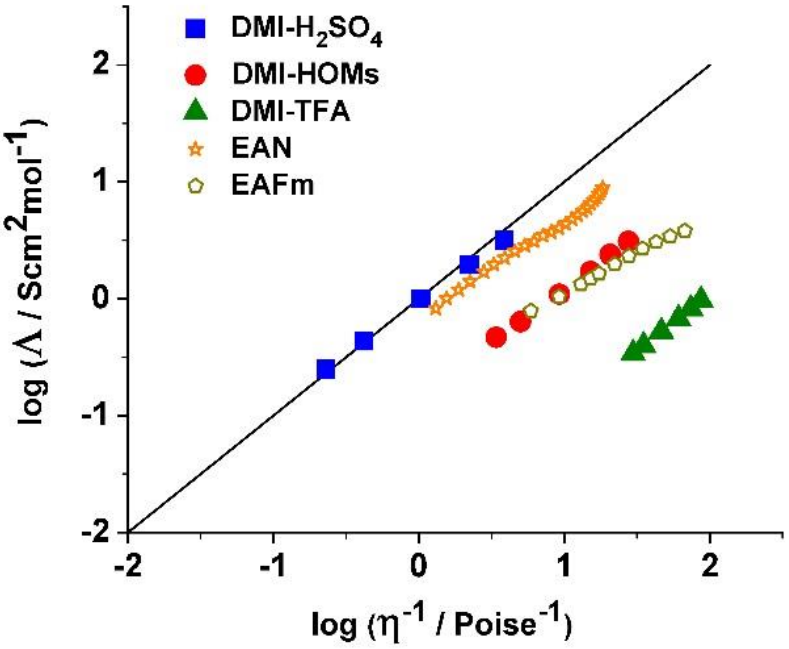

Figure 2-10- Walden plot for selected DMI mixtures with three acids of different strength. As expected, lower ionicities are obtained as the extent of protonation decreases with acid strength. The data points for ethylammonium nitrate (EAN or EA+HNO_3) and ethylammonium formate (EAFm or EA+HFm) are reproduced from an earlier work[70] and provided for comparison.

Vibrational spectroscopy also shows the incomplete protonation of DMI with HOMs suggested by the Walden plot (Figure 2-11). The presence of the carbonyl group in the structure of the base and the shorter time scale of IR spectroscopy compared to

proton exchange, allows for probing the extent of protonation. This was not possible using NMR spectroscopy because of its slow relaxation compared to proton exchange. It is shown in Figure 2-11 how the amide band is still present in DMI-HOMs mixture while it has completely disappeared in the case of H_2SO_4. To further confirm that the disappearance of the amide peak is solely due to protonation and is not dependent on the nature of the acid, it was monitored as DMI is titrated by H_2SO_4. The results shown in Figure 2-11 display the gradual disappearance of the carbonyl stretching band as the strong acid is added. The quantitative assessment of the extent of protonation using vibrational spectroscopy (IR and Raman) on DMI and similar cations is in progress and will be the subject of a separate publication.

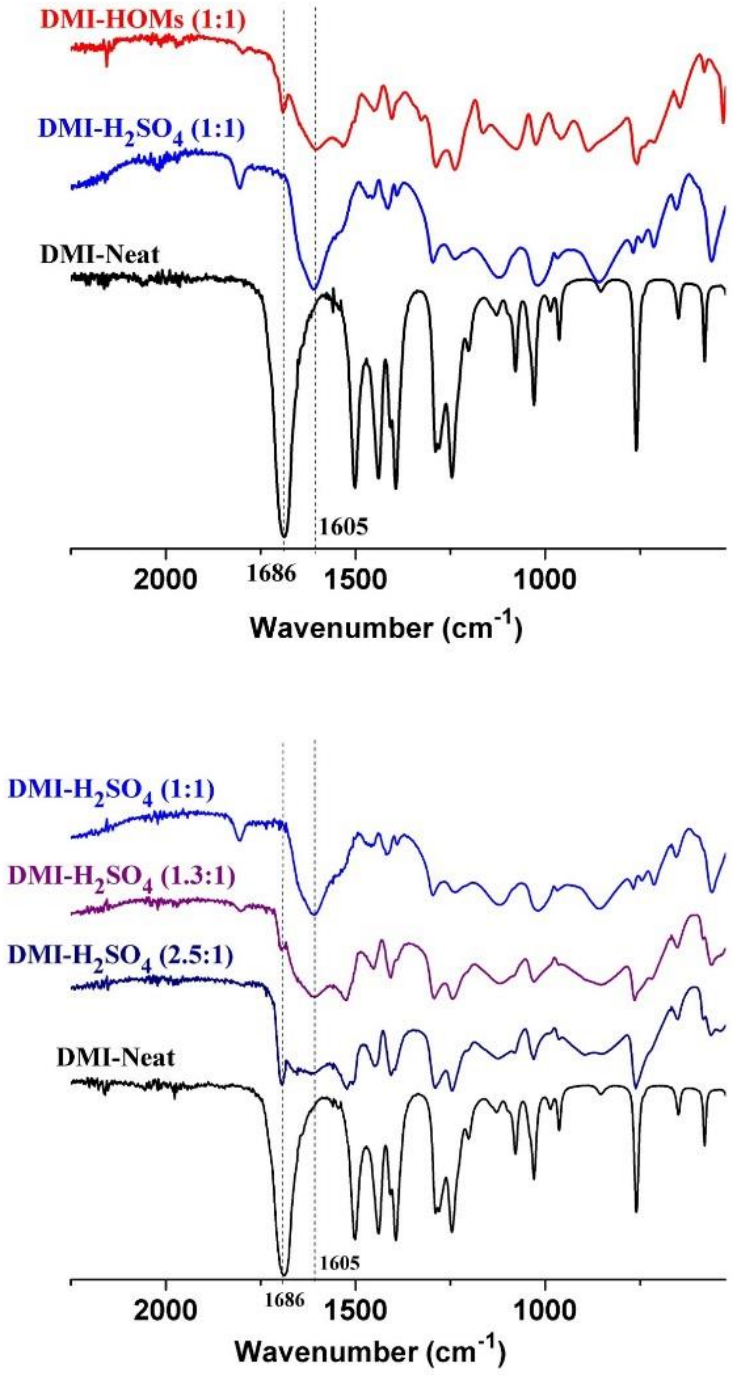

Figure 2-11- IR spectra of DMI in its selected 1:1 mixtures with two acids of different strength (top) and as titrated with H_2SO_4 (bottom). The amide band at 1686 cm^{-1} disappears as DMI is completely protonated. The presence of the band in the case of HOMs shows the incomplete protonation suggested by Walden plot.

Finally, it might be noticed that, among the weak base anions of common ionic liquid experience, the cases of $AlBr_4^-$ and $AlCl_4^-$ are missing from Figure 2-8. There is a good reason for this omission, related to the hydrolysis of these anions by DMI. Yet the resurgent importance of bromoaluminate,[55,71] chloroaluminate,[72] and chloroferrate[73] anions in fundamental studies of establishing abosolute pH scales and in ionic liquid battery chemistries, demands that some effort be made to include them in our overall acidity picture. To this end Density Functional Theory (DFT) calculations (B3LYP functional with the 6311G++(3d,3p) basis set) were carried out to obtain optimized structures of the chloroaluminate adduct at absolute zero. They suggest that $AlCl_4^-$ is a weaker base than BF_4^-, when judged by the N-H bond lengths shown in Figure 2-12. Indeed, at 1.00674 Å, it is nearly midway between that for the fluoroborate adduct (1.02908 Å) and that for free cation in vacuum (0.96615 Å). Yet it is still not as weakly basic as $AlBr_4^-$ (1.00218 Å) which is getting very close to the value for the free cation and suggests that the heptabromodialuminate ($Al_2Br_7^-$)might reach that lowest level.

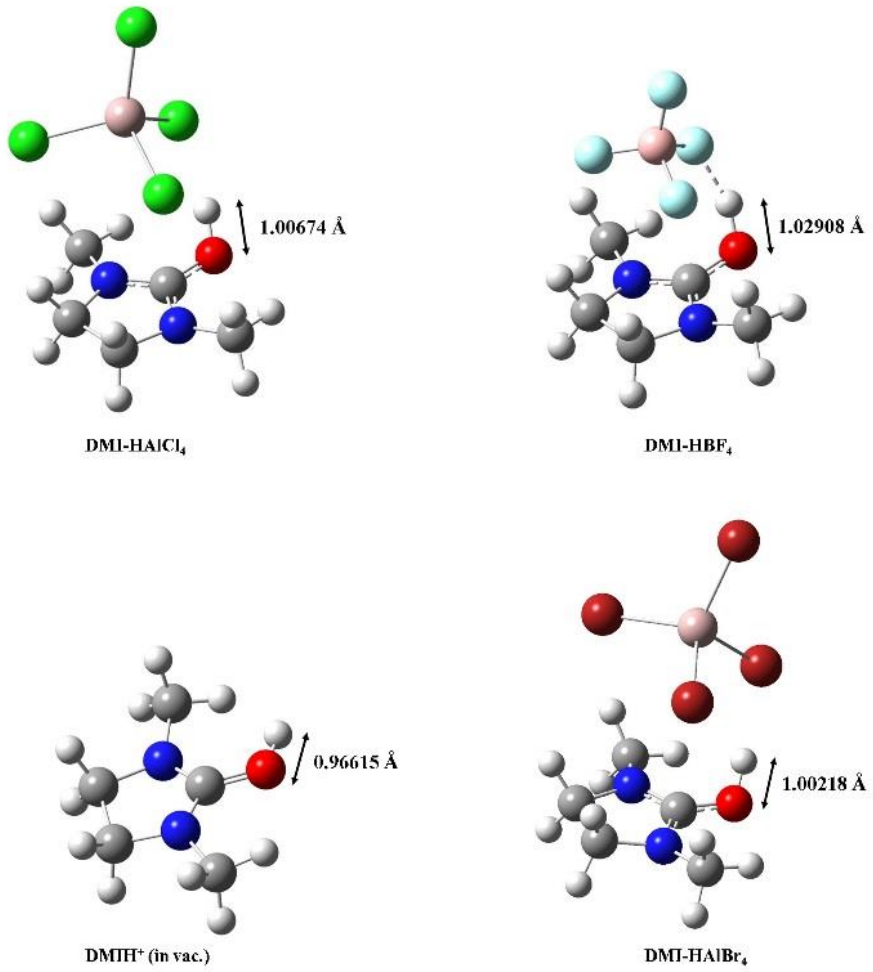

Figure 2-12- Optimized structures of $DMIHBF_4$ (top-right), $DMIHAlCl_4$ (top-left), $DMIHAlBr_4$ (bottom-right) and $DMIH^+$ in vacuum (bottom-left) obtained from DFT calculations shows shorter N-H bonds in the cases of the haloaluminate adducts. Note close approach of bromoaluminate to free cation value.

For confirmation of this remarkable result, we also made a separate experimental study utilizing the alternative single cation probe approach that has been developed here[74,75] and elsewhere[14] based on the chemical shift of protons transferred to a selected, and stronger, Brønsted base, for instance, diethyl methyl amine, DEMA, as featured in a companion study.[75] In Table 2-19 we list additional N-H chemical shifts in the liquid

states of PILs that we have obtained with the anions $AlCl_4^-$, SbF_6^-, AsF_6^- BF_4^- and HSO_4^-, the last four of which also establish the superacid order in Figure 2-8.

We see that the order of the last four is the same as it is in Figure 2-8, and that $AlCl_4^-$ is indicated as the weakest base of all. We will show elsewhere that the ^{13}C chemical shifts are in exact proportion to the N-H vibration frequencies for these anions reported by Reed and Stoyanov,[46] supporting the use of either experimental quantity for the purpose of classifying superacid strengths. We note that although $FeCl_4^-$ and $GaCl_4^-$ were included in the ref 42 tabulation, the more interesting case of $AlCl_4^-$ was not.

An older study of proton transfer to the intermediate strength bases, pyridine and 2-methylpyridine, from HCl, and HCl enhanced by $AlCl_3$ to give both $AlCl_4^-$ and $Al_2Cl_7^-$ anions, showed the $Al_2Cl_7^-$ anions to be even more weakly basic than $AlCl_4^-$, providing an electronic environment for the >NH proton that is close to that of a pyridinium cation in free space.[49] Such observations help in understanding not only the exceptional properties of chloroaluminate ionic liquids[72,76] (and their chloroferrate relatives)[73] but also the stabilization (at low temperatures) of toluenium cations in the presence of $AlCl_4^-$ and $Al_2Cl_7^-$ anions, in the classic work of Brown and Pearsall.[77]

Table 2-19- ^1H chemical shift of the acidic proton in PILs made from DEMA

	δ -^{1}H (ppm)
DEMA-$HAlCl_4$	5.62
DEMA-$HSbF_6$	5.70
DEMA-$HAsF_6$	5.73
DEMA-HBF_4	6.67
DEMA-H_2SO_4	8.85

For economic reasons, we have been unable to include in our study, the "strongest acid" identified by the Reed group, carborane acid.[78] We were also unable to include the very weakly coordinating anions of highly fluorinated aluminates $[Al(OR_f)_4]^-$ because of the decomposition of the anion by our oxygenic base.[79] Comparable acidity might be found in the protonated form of the giant bis-perfluoropinacolatoborate anion "LiBPFPB" (24 fluorines).[80]

2.4 Conclusions

A set of new protic ionic liquids with a novel cation has been made and the change in the cation's electronic structure caused by the interaction with different anions (conjugate bases of the acids used) has been probed by ^{13}C and ^{15}N NMR spectroscopy to obtain a basicity order for the anions. Walden plot analysis has been carried out for selected cases and reflects the incomplete protonation for mixtures made from HOMs and the weaker acids, an outcome consistent with the chemical shifts results and supported by IR spectroscopy. Our method is simple to apply. It will be interesting to use it to rank basicities of a number of anions of supposedly strong acids or unusual character, such as the $H_2(PO_3SO_3)^-$, $F(HF)_3^-$, $S_2O_7^{2-}$, $Re_2O_7^-$, and oxometallate cluster anions.

2.5 Works Cited:

(1) Walden, P. *Bull. Acad. Imp. Sci.* **1914**, *8*, 405–422.

(2) Yoshizawa, M.; Xu, W.; Angell, C. A. *J. Am. Chem. Soc.* **2003**, *125* (8), 15411–15419.

(3) Greaves, T. L.; Drummond, C. J. *Chem. Rev.* **2015**, *115*, 11379–11448.

(4) Ohno, H. *Electrochemical Aspects of Ionic Liquids*; Ohno, H., Ed.; Wiley and Sons: Hoboken, New Jersey, 2011.

(5) Wasserscheid, P.; Welton, T. *Ionic Liquids in Synthesis*, Second.; Wiley-VCH: Weinheim, 2008.

(6) Idris, A.; Vijayaraghavan, R.; Patti, A. F.; Macfarlane, D. R. *ACS Sustain. Chem. Eng.* **2014**, *2* (7), 1888–1894.

(7) Maase, M.; Massonne, K.; Halibritter, K. No Title. WO 2003062171, 2008.

(8) Wang, L.; Kefalidis, C. E.; Roisnel, T.; Sinbandhit, S.; Maron, L.; Sarazin, Y. **2015**, No. Ii.

(9) Fumino, K.; Fossog, V.; Stange, P.; Wittler, K.; Polet, W.; Hempelmann, R.; Ludwig, R. *ChemPhysChem* **2014**, *15*, 2604–2609.

(10) Engesser, T. A.; Lichtenthaler, M. R.; Schleep, M.; Krossing, I. *Chem. Soc. Rev.* **2016**.

(11) Dong, K.; Zhang, S.; Wang, J. *Chem. Commun.* **2016**.

(12) Weber, C. C.; Kunov-Kruse, A. J.; Rogers, R. D.; Myerson, A. S. *Chem. Commun. (Camb).* **2015**, *51* (20), 4294–4297.

(13) Kumar, A.; Rani, A.; Venkatesu, P. *New J. Chem.* **2015**, *39* (2), 938–952.

(14) Miran, M. S.; Kinoshita, H.; Yasuda, T.; Susan, M. A. B. H.; Watanabe, M. *Phys. Chem. Chem. Phys.* **2012**, *14*, 5178.

(15) Anslyn, E. V; Dougherty, D. A. *Modern Physical Organic Chemistry*; University Science Books: Sausalito, California, 2006.

(16) Johnson, K. E.; Pagni, R. M.; Bartmess, J. *Monatshefte fur Chemie* **2007**, *138*, 1077–1101.

(17) Mihichuk, L. M.; Driver, G. W.; Johnson, K. E. *ChemPhysChem* **2011**, *12*, 1622–1632.

(18) Cox, R. A. *Can. J. Chem.* **1983**, *61*, 2225–2243.

(19) Klumpp, D. A.; Yeung, K. Y.; Prakash, G. K. S.; Olah, G. A. *Superacid chemistry*; 1998.

(20) Laurence, C.; Gal, J. F. *Lewis Basicity and Affinity Scales; Data and Measurement*; John Wiey & Sons: Chichester, U.K., 2010.

(21) Kütt, A.; Rodima, T.; Saame, J.; Raamat, E.; Mäemets, V.; Kaljurand, I.; Koppel, I. A.; Garlyauskayte, R. Y.; Yagupolskii, Y. L.; Yagupolskii, L. M.; Bernhardt, E.; Willner, H.; Leito, I. *J. Org. Chem.* **2011**, *76* (2), 391–395.

(22) Himmel, D.; Goll, S. K.; Leito, I.; Krossing, I. *Angew. Chemie - Int. Ed.* **2010**, *49* (38), 6885–6888.

(23) Himmel, D.; Goll, S. K.; Scholz, F.; Radtke, V.; Leito, I.; Krossing, I. *ChemPhysChem* **2015**, *16* (7), 1428–1439.

(24) Suu, A.; Jalukse, L.; Liigand, J.; Kruve, A.; Himmel, D.; Krossing, I.; Rosés, M.; Leito, I. *Anal. Chem.* **2015**, *87* (5), 2623–2630.

(25) Koppel, I. A.; Burk, P.; Koppel, I.; Leito, I.; Sonoda, T.; Mishima, M. *J. Am. Chem. Soc.* **2000**, *122* (21), 5114–5124.

(26) Carlin, C.; Gordon, M. S. *J. Comput. Chem.* **2015**, *36* (9), 597–600.

(27) Olofsson, G.; Lindqvist, I.; Sunner, S. *Acta Chem. Scand.* **1963**, *17*, 259–265.

(28) Gutmann, V. *The Donor-Acceptor Approach to Molecular Interactions*; Plenum Press: New York, 1978.

(29) Tang, L.; Zeller, R.; Angell, C. A.; Friesen, C. *J. Phys. Chem. C* **2009**, *113*, 12586–12593.

(30) Kanzaki, R.; Doi, H.; Song, X.; Hara, S.; Ishiguro, S. I.; Umebayashi, Y. *J. Phys. Chem. B* **2012**, *116*, 14146–14152.

(31) Miran, M. S.; Yasuda, T.; Susan, M. A. B. H.; Dokko, K.; Watanabe, M. *RSC Adv.* **2013**, *3* (13), 4141–4144.

(32) Driver, G. W. *ChemPhysChem* **2015**, *16* (11), 2432–2439.

(33) Cho, C.-W.; Stolte, S.; Ranke, J.; Preiss, U.; Krossing, I.; Thoeming, J. *ChemPhysChem* **2014**, *15* (11), 2351–2358.

(34) Muller, P. *Pure Appl. Chem.* **1994**, *66* (5), 1077–1184.

(35) Reichardt, C. *Angew. Chemie Int. Ed. …* **1965**, *4* (1), 29.

(36) Reichardt, C. *Green Chem.* **2005**, *7* (5), 339–351.

(37) Stark, A. *Top. Curr. Chem.* **2009**, *209*, 41–81.

(38) Kamlet, M. J.; Taft, R. W. *J. Am. Chem. Soc.* **1975**, *98*, 377–383.

(39) Cláudio, A. F. M.; Swift, L.; Hallett, J. P.; Welton, T.; Coutinho, J. a P.; Freire, M. G. *Phys. Chem. Chem. Phys.* **2014**, *16* (14), 6593–6601.

(40) Lungwitz, R.; Spange, S. *New J. Chem.* **2008**, *32* (3), 392.

(41) Bartosik, J.; Mudring, A. V. *Phys. Chem. Chem. Phys.* **2010**, *12*, 1648.

(42) Holzweber, M.; Lungwitz, R.; Doerfler, D.; Spange, S.; Koel, M.; Hutter, H.; Linert, W. *Chem. - A Eur. J.* **2013**, *19*, 288–293.

(43) Schade, A.; Behme, N.; Spange, S. *Chem. - A Eur. J.* **2014**, *20* (8), 2232–2243.

(44) Thomazeau, C.; Olivier-Bourbigou, H.; Magna, L.; Luts, S.; Gilbert, B. *J. Am. Chem. Soc.* **2003**, *125* (18), 5264–5265.

(45) Robert, T.; Magna, L.; Olivier-Bourbigou, H.; Gilbert, B. *J. Electrochem. Soc.* **2009**, *156* (9), F115.

(46) Stoyanov, E. S.; Kim, K. C.; Reed, C. A. *J. Am. Chem. Soc.* **2006**, *128* (4), 8500–8508.

(47) Stoyanov, E. S.; Stoyanova, I. V.; Reed, C. A. *Chem. - A Eur. J.* **2008**, *14*, 7880–7891.

(48) Mayer, U.; Gutmann, V.; Gerger, W. *Monatshefte fur Chemie* **1975**, *106* (6), 1235–1257.

(49) Angell, C. A.; Shuppert, J. W. *J. Phys. Chem.* **1980**, *84*, 538–542.

(50) Farcasiu, D.; Ghenciu, A. *J. Am. Chem. Soc.* **1993**, *115* (23), 10901–10908.

(51) Schmeisser, M.; Illner, P.; Puchta, R.; Zahl, A.; Van Eldik, R. *Chem. - A Eur. J.* **2012**, *18*, 10969–10982.

(52) Lungwitz, R.; Spange, S. *Chemphyschem* **2012**, *13*, 1910–1916.

(53) Gräsvik, J.; Hallett, J. P.; To, T. Q.; Welton, T. *Chem. Commun. (Camb).* **2014**, *50*, 7258–7261.

(54) McCune, J. A.; He, P.; Petkovic, M.; Coleman, F.; Estager, J.; Holbrey, J. D.; Seddon, K. R.; Swadźba-Kwaśny, M. *Phys. Chem. Chem. Phys.* **2014**, *16*, 23233–23243.

(55) Scholz, F.; Himmel, D.; Eisele, L.; Unkrig, W.; Martens, A.; Schlüter, P.; Krossing, I. *Chem. - A Eur. J.* **2015**, *21* (20), 7489–7502.

(56) Bonhôte, P.; Dias, A.-P.; Armand, M.; Papageorgiou, N.; Kalyanasundaram, K.; Grätzel, M. *Inorg. Chem.* **1996**, *35* (5), 1168–1178.

(57) Ghandi, M.; Hasani, M.; Salahi, S. *Monatshefte fur Chemie* **2012**, *143* (3), 455–460.

(58) Gideon, B. Y. *J. Am. Chem. Soc.* **1960**, *82* (17), 4478–4483.

(59) Morgan, J.; Greenberg, A.; Liebman, J. F. *Struct. Chem.* **2012**, *23*, 197–199.

(60) Gillespie, R. J.; Birchall, T. *Can. J. Chem.* **1963**, *41* (6), 148–155.

(61) Johansson, K. M.; Izgorodina, E. I.; Forsyth, M.; MacFarlane, D. R.; Seddon, K. R. *Phys. Chem. Chem. Phys.* **2008**, *10*, 2972–2978.

(62) Polyakov, O. G.; Nolan, B. G.; Fauber, B. P.; Miller, S. M.; Anderson, O. P.; Strauss, S. H. *Inorg. Chem.* **2000**, *39* (8), 1735–1742.

(63) Foropoulos Jr, J.; DesMarteau, D. D. *Inorg. Chem.* **1984**, *12* (10), 3720–3723.

(64) Koppel, I. A.; Taft, R. W.; Zbu, A. S.; Hu, L.; Sung, K.; Desmarteau, D. D.; Yagupolskii, L. M.; Yagupolskii, Y. L.; Ignat, N. V; Kondratenko, V.; Volkonskii, Y.; Vlasov, V. M.; Notario, R.; Maria, P. *J. Am. Chem. Soc.* **1994**, *116* (2), 3047–3057.

(65) Raamat, E.; Kaupmees, K.; Ovsjannikov, G.; Trummal, A.; Kütt, A.; Saame, J.; Koppel, I.; Kaljurand, I.; Lipping, L.; Rodima, T.; Pihl, V.; Koppel, I. a.; Leito, I. *J. Phys. Org. Chem.* **2013**, *26*, 162–170.

(66) Stoyanov, E. S.; Kim, K. C.; Reed, C. A. *J. Phys. Chem. A* **2004**, *108* (42), 9310–9315.

(67) Gillespie, R. J.; Peel, T. E. *Adv. Phys. Org. Chem.* **1971**, *9*, 1–24.

(68) Gillespie, R. J.; Peel, T. E. *J. Am. Chem. Soc.* **1973**, *95* (2), 5173–5178.

(69) Olah, G. A.; Prakash, G. K. S.; Sommer, J. *Science (80-.).* **1979**, *206*, 13–20.

(70) Angell, C. A.; Ansari, Y.; Zhao, Z. *Faraday Discuss.* **2012**, *154* (1), 9.

(71) Himmel, D.; Goll, S. K.; Scholz, F.; Radtke, V.; Leito, I.; Krossing, I. *ChemPhysChem* **2015**, *16* (7), 1428–1439.

(72) Lin, M.-C.; Gong, M.; Lu, B.; Wu, Y.; Wang, D.-Y.; Guan, M.; Angell, M.; Chen, C.; Yang, J.; Hwang, B.-J.; Dai, H. *Nature* **2015**, *520*, 324–328.

(73) Xue, L.; Tucker, T. G.; Angell, C. A. *Adv. Energy Mater.* **2015**, *5* (12), 1500271.

(74) Byrne, N.; Angell, C. A. *Chem. Today* **2009**, *27* (1), 51–53.

(75) Davidowski, S. K.; Thompson, F.; Huang, W.; Hasani, M.; Amin, S. A.; Angell, C. A.; Yarger, J. L. *J. Phys. Chem. B* **2016**, *120* (18), 4279–4285.

(76) Mantz, R. A.; Trulove, P. C.; Carlin, R. T.; Theim, T. L.; Osteryoung, R. A. *Inorg. Chem.* **1997**, *36* (10), 1227–1232.

(77) Brown, H. C.; Pearsall, H. W. *J. Am. Chem. Soc.* **1952**, *74*, 191–195.

(78) Nava, M.; Stoyanova, I. V; Cummings, S.; Stoyanov, E. S.; Reed, C. A. *Angew. Chem. Int. Ed. Engl.* **2014**, *53* (4), 1131–1134.

(79) Rupp, A. B. A.; Krossing, I. *Acc. Chem. Res.* **2015**, *48* (1), 2537–2546.

(80) Xu, W.; Angell, C. A. *Electrochem. Solid-State Lett.* **1999**, *3* (8), 366.

3 NMR Characterization of Ionicity and Transport Properties for a Series of Tertiary Amine Based Protic Ionic Liquids

Protic Ionic liquids (PILs) are made by proton transfer from a Bronsted acid to a base and are of interest for their solvent and electrolyte properties such as high ionic conductivity. One way to describe their charge transport properties in an electric field is by the use of "ionicity" as a measure of the fraction of total possible number of ions which take part in ionic conduction. Lower ionicities are commonly observed in PILs, supposedly as a result of 1) incomplete proton transfer (low degree of ionization) and 2) the formation of ion pairs and/or larger aggregates. The presence of neutral species resulting from incomplete ionization makes the liquid a salt solution (and not an ionic liquid) while ion pair formation is observed in pure aprotic ionic liquids as well. Here, we show that the degree of ionization in two sets of pyridine-based PILs can be determined based on the ^{15}N chemical shift change caused by protonation. It is shown that some PIL cases with low ionicities, suggested by Walden plot analysis and Pulse Field Gradient-Stimulate Echo (PFG-STE) results, are indeed almost fully ionic and merit the name. 2-Methylpyridine and 2-fluoropyridine are selected for their similar structures and different basicities to make 1:1 mixtures with a set of Bronsted acids (covering a wide range of acidity). Gas-phase proton affinities (PAs) of the conjugate anions of the acids are used instead of aqueous pKa values as a measure of acid strength to rationalize the changes in ^{15}N chemical shifts.

3.1 Introduction

Ionic liquids (ILs)[1–5] are a class of compounds which are completely made of ions and have a liquidus temperature of 100 ^{o}C or lower. As promising electrolytes for electro-chemical devices,[6,7] much interest lies in the charge transport properties of their ions in the presence of an electric field.[8] It can be described by comparison of conductivity relaxation times and structural relaxation times using easily made conductivity and viscosity measurements. The behavior is "ideally" governed by Walden rule, with "ideal" behavior being that of dilute aqueous KCl solutions. The Walden analysis has been adopted by Angell [9,10] to characterize charge transport properties of ILs and to introduce "ionicity" based on the deviation from ideal behavior as a measure of "the effective fraction of ions available to participate in conduction" as framed later by MacFarlane.[11] The ratio of measured equivalent conductivity to that estimated from Nernts-Einstein equation based on Pulse Field Gradient-Stimulate Echo (PFG-STE) measured self-diffusion coefficients is also suggested by Watanabe to be a measure of ionicity.[12] The deviation from ideal behavior is attributed to ion-pairing and the formation of larger aggregates; and is seen even in ILs with weakly interacting ions.

Protic Ionic Liquids (PILs), as a subclass of ILs which are made by proton transfer, normally show lower ionicities than their aprotic counterparts. It can reasonably be understood considering the inherent hydrogen bond interaction between the anion and the transferred proton on the cation. Low ionicities of PILs can also be a result of the presence of neutral, unreacted acid/base molecules when the free energy of proton transfer is small (low degree of protonation). This free energy can be estimated from the difference between aqueous pKa values of the acid and the protonated base. It is

suggested that a difference of at least 10 pKa units,[10] or 14 as suggested by a different study,[13] is required for obtaining high ionicities. Even if the pKa values are considered inexact, because of solvent and concentration effects as explained elsewhere, {DMI paper} the criterion seems severe for a complete proton transfer; something expected achievable with a 4 unit difference as shown by MacFarlane.[14] It is unclear whether low ionicities are a result of the presence of unreacted neutral species or the effect of ion interactions. We report here that with the use of ^{15}N NMR spectroscopy the complete protonation can be marked to make clearer the presence of other contributing factors to low ionicities.

Two sets of PILs were synthesized using 2-methylpyridine (2mPy, pKa= 5.9) and 2-fluoropyridine (2FPy, pKa= -0.4) as bases together with a series of acids covering a wide range of acidities. The bases were chosen for their similar structures and different basicities. ^{15}N NMR spectroscopy is used based on the change in the chemical shift of the nucleus in the base upon protonation to determine the degree of protonation. Walden Plot analysis and PFG-STE results are used to characterize the charge transport properties of the liquids. We have shown recently,[15] in harmony with previous reports,[16] that the gas-phase Proton Affinity (PA) is a better measure of the property than aqueous pKa values; as evident in the proton chemical shift results presented below.

Figure 3-1 shows the agreement between the calculated and experimental PA values listed in Table 3-1.

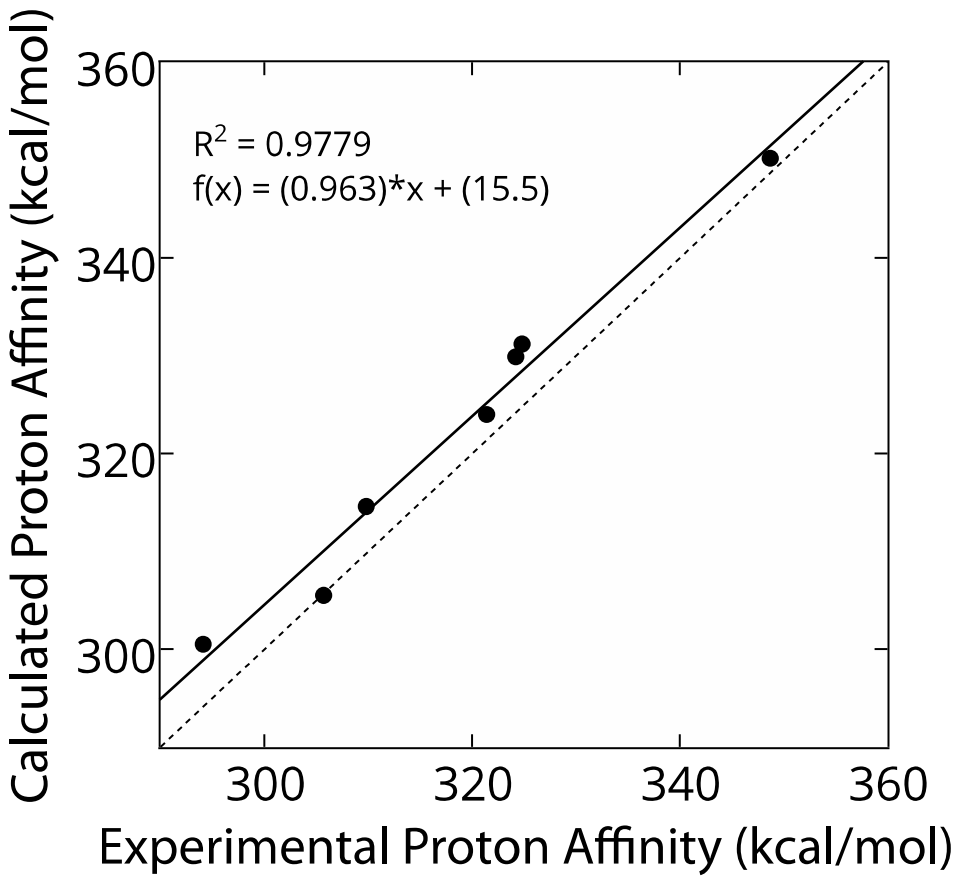

Figure 3-1- Gas phase proton affinity values obtained via electronic structure calculations carried out at the DFT-B3LYP level of theory with a basis set of 6-31G(d) compared to values obtained from the literature. The solid line is a fit of the data points, and the dotted line is along y=x. (Reprinted with permission from Ref.[15])

Table 3-1- Summary of proton affinity calculation results at various levels of theory and literature values. (Reprinted with permission from Ref.[15])

PIL	PA (kcal/mol) DFT(6-31G(d))	PA (kcal/mol) DFT(6-31G^{++}(2d,dp))	PA(kcal/mol) Experimental
DEMA-NTf_2	300.5	291.7	294
DEMA-OTf	305.5	298.0	305
DEMA-ClO_4	303.9	299.3	
DEMA-HSO_4	314.6	307.9	310
DEMA-MS	324.0	317.4	321
DEMA-NO_3	331.2	320.7	325
DEMA-BF_4	297.5	290.0	
DEMA-TFA	329.9	316.4	324
DEMA-Ac	350.2	338.4	349

It is shown that the proton chemical shift of the transferred proton to DEMA depends on the nature of the anion as seen in Figure 3-2.

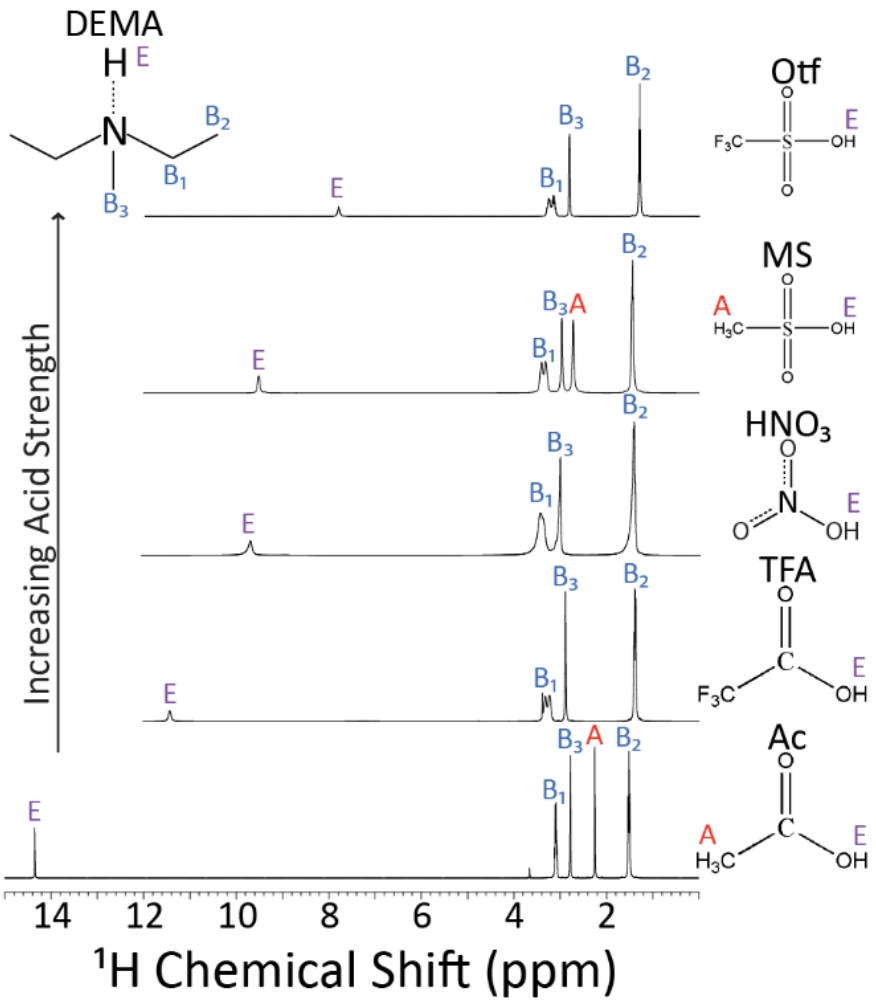

Figure 3-2- ^{1}H NMR spectra for DEMA based ionic liquids generated with various acids. The structure and abbreviation for each acid is shown to the right of the corresponding spectrum. The symbols A, B, and E correspond to protons associated with the acid, base, and exchangeable protons, respectively. (Reprinted with permission from Ref.[15])

The general trend observed in spectra of Figure 3-2 is that as the anion basicity decreases, the chemical shift of the transferred proton is shifted to lower ppm values. Depending on the strength of the interaction between the base and the exchangeable proton the chemical shift changes. The difference in chemical shift between the proton associated with an acid (c.10-12 ppm) and associated with the DEMA-H^{+} (3-4 ppm) is quite large.

A similar but slightly different trend is observed for the weaker bases of the series. For 2mPy and 2FPy mixtures, the chemical shift of the exchangeable proton is maximum in their adducts with HTFA and HOMs, respectively. We shall see later that the maximum corresponds to an abrupt change in ^{15}N chemical shift of the amine which marks the equivalent point of a titration curve. It may be noted that the maximum occurs with the weaker acid (HTFA) for the stronger base (2mPy), suggesting a balance between the free energy of the proton on the acid and the base (a set ΔpK_a, one might say) being required. A chemical shift maximum was not observed in the case of DEMA due to it being a stronger base (pK_a = 10.6) than both 2mPy (pK_a = 5.9) and 2FPy (pK_a = -0.4). We predict that if weaker acids, than HOAc, were included in the set of DEMA ionic liquids, a similar result would be observed. A similar trend to that of weaker bases is observed for a base of a different nature, 1,3-dimethyl-2-imidazolidinone (DMI), discussed in the previous chapter as manifested in Table 2-17. It is also in agreement with the results reported by Denisov et al. on the ^{1}H chemical shifts of a series of 1:1 mixtures of acids and pyridine to form ion pairs in the nonpolar solvent CD_2Cl_2.[17] A chemical shift maximum was observed here as well at 20.5 ppm for the exchangeable proton of dichloroacetic acid and pyridine (ΔpK_a=3.9). This chemical shift indicates the presence of a strong hydrogen bond between the acid and the base.

A way to quantify anion basicity, which does not rely on the solvation environment, is by determining their gas phase proton affinity using electronic structure calculations. Proton affinities were calculated by obtaining the ΔH of the protonation of the anions; this reaction scheme is shown in eq. 1:

$$A^-_{(g)} + H^+_{(g)} \rightarrow AH_{(g)} \qquad (1)$$

The lower the proton affinity of an anion, the stronger the associated acid. Similar gas phase ab initio calculation studies have been a focus of recent publications estimating the acidity of superacids.[18,19] A plot correlating the gas phase proton affinity for each anion and the chemical shift of the exchangeable proton upon reaction with the base DEMA is shown in Figure 3-3.

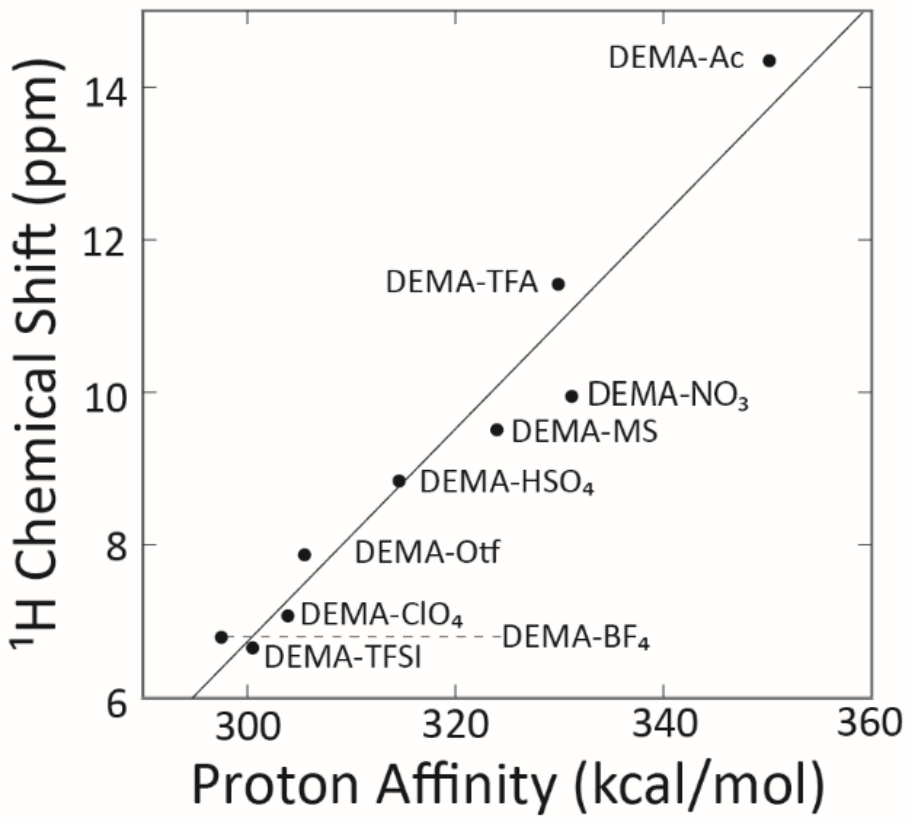

Figure 3-3- Chemical shift of the exchangeable proton for an array of DEMA based protic ionic liquids correlated with the proton affinity of the acid used to generate the PIL. The proton affinities in this plot were obtained by calculating the proton affinity of each acid using Gaussian09 to perform DFT-B3LYP with the basis set 6-31G (d). The equation for the trend line shown is δ=0.14*PA-35.11. (Reprinted with permission from Ref.[15])

A correlation between acid proton affinity and the chemical shift of exchangeable proton has also been observed in a set of PILs generated with a base of considerably different basicity, 1,3-dimethyl-2-imidazolidinone (DMI), see Figure 3-4.

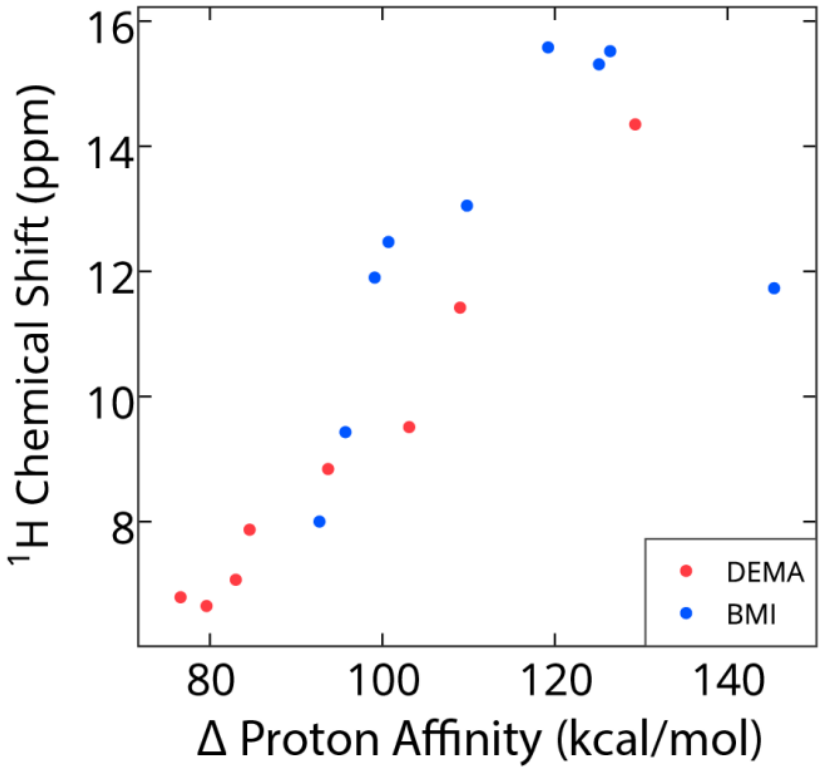

Figure 3-4- Plot exemplifying the relation of the exchangeable proton's chemical shift in protic ionic liquids (PILs) with the difference in the proton affinity of the acid and base (ΔPA) used to generate the PIL. The data are shown for 2 sets of PILs made with the bases diethylmethylamine (DEMA) and 1,3-Dimethyl-2-imidazolidinone (DMI). (Reprinted with permission from Ref.[15])

^{15}N NMR can be done on neat ionic liquids without isotope enrichment due to the high concentration of the nitrogen atoms. A series of ^{15}N NMR spectra are shown in Figure 3-5 without decoupling from ^{1}H to observe the J_{NH} coupling.

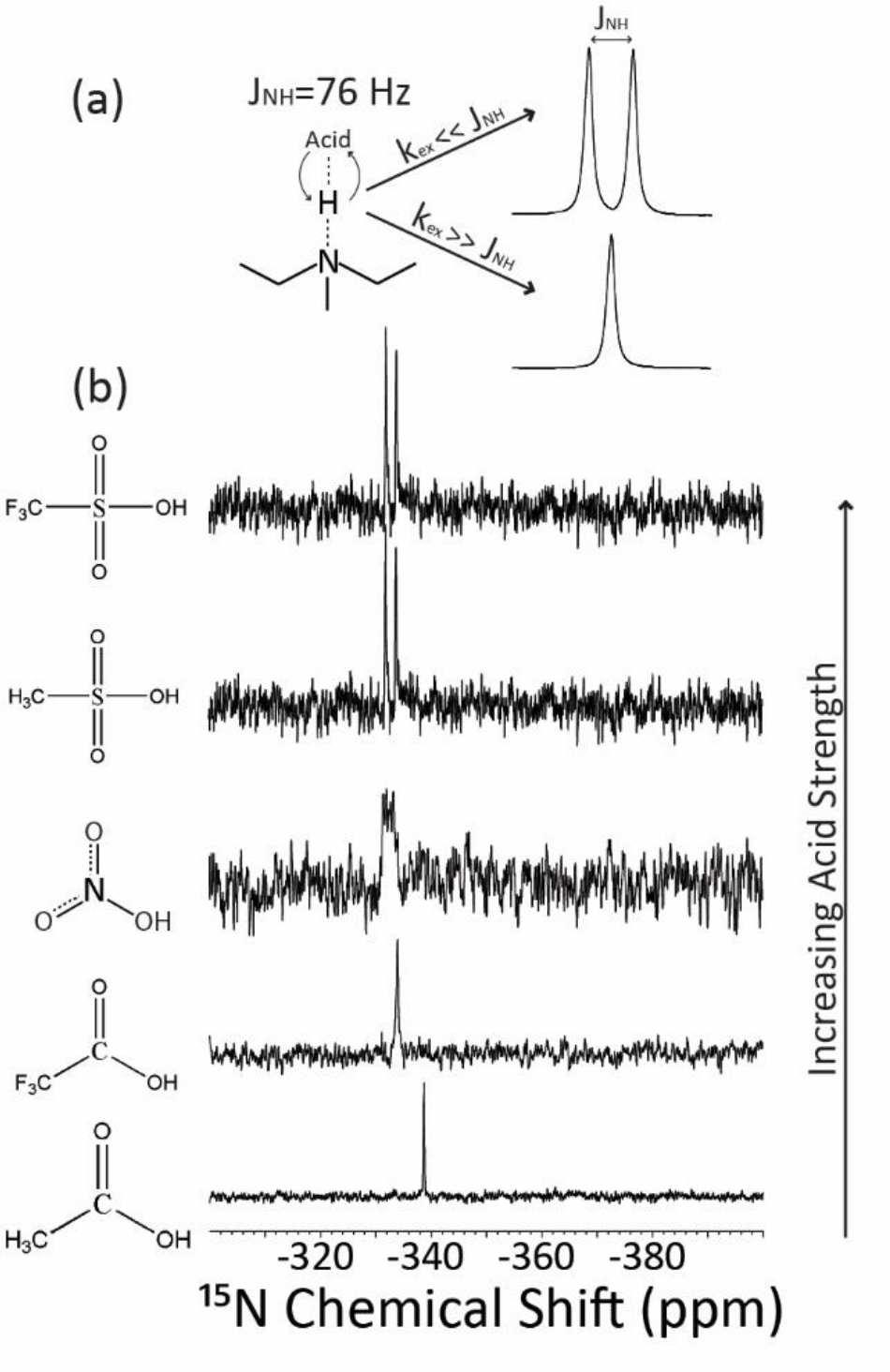

Figure 3-5- (a) The schematic representation of a DEMA based ionic liquid in exchange and an example splitting pattern for the case of fast and slow exchange. (b) ^{15}N NMR spectra for an array of DEMA based ionic liquids collected without ^{1}H decoupling to allow for the observation of J_{NH}. (Reprinted with permission from Ref.[15])

For acids stronger than nitric acid, the J_{NH} coupling (76 Hz) of the two nuclei on the cation is clearly observed. For weaker acids, a singlet is observed due to the faster exchange of the exchangeable proton than the timescale of the ^{15}N NMR measurement. A peak broadening is seen for the intermediate case (DEMA-NO_3) which is reminiscent of a temperature-induced coalescence.[20] The observation of the J_{NH} splitting in ionic liquids made with strong and super acids implies a slower proton exchange than the J_{NH} Observation time scale in these PILs.

The proton spectrum of DEMA-$AlCl_4$ showed an interesting splitting pattern, involving ^{1}H-^{1}H and ^{1}H-^{14}N J-coupling of the "exchangeable" ammonium proton, due to the very low basicity of the anion and its almost non-existence hydrogen bond interaction with the cation. The results are presented in Appendix B to avoid the interruption of the narrative of the chapter.

The PA values, obtained from Density Functional Theory (DFT) calculations, are what is used to rationalize the trend in chemical shift change. NMR spectroscopy in general[21] and ^{15}N NMR spectroscopy in specific have been used[22–28] in the study of ILs but the use in the degree of ionization in different PILs and explaining the charge transport properties is new.

3.2 Experimental and Results

Materials. 2-Methylpyridine (2mPy, >99.5%) and 2-fluoropyridine (2FPy, 99%) were purchased from Sigma-Aldrich, distilled over CaH2 and stored over activated molecular sieves in a glove box. The water contents were below the detection limit of Karl-Fischer titrator. Acetic acid (HOAc, >99%), acetic anhydride (Ac2O, >99%), dichloroacetic acid (HOAcCl2, >99%), trifluoroacetic acid (TFA, >99%), trifluoroacetic

anhydride (TFA2O, >99%) methanesulfonic acid (HOMs, >99.5%), methanesulfonic anhydride (Ms2O, 98%), sulfuric acid (H2SO4, >99.99%), hydrochloric acid (HCl, 37%) and 3Å molecular sieves were obtained from Sigma-Aldrich. Acid anhydrides were used to control the water content of the corresponding acids. Trifluoromethanesulfonic acid (triflic acid, HOTf, >98%), hydrogenbistrifluoromethanesulfonylimide (HNTf2, 95%) and Aluminum chloride (AlCl3, 99.7%) were obtained from Afla-Aesar and used as received.

Ionic liquid synthesis. Ionic liquids were synthesized following a procedure outlined before12 by directly mixing equimolar amounts of the base and the acid under an inert atmosphere at lowered temperatures (0 ^{o}C using an ice-bath for acids weaker than sulfuric acid and -78 ^{o}C using an acetone/dry ice bath for the stronger ones). Typically, the liquid acid was added drop-wise to the base, the exception is the case of NTf_2^- salts where the liquid bases where added to the solid acid. The tetrachloroaluminate ($AlCl_4^-$) salts were synthesized by controlled addition of the hydrochloride (HCl) salts of the base to equimolar amount of $AlCl_3$ in a glove box. When possible, to ensure the correct stoichiometry between the acid and the base, careful integration of ^{1}H NMR peaks was used.

NMR spectroscopy. All NMR studies were carried out on samples that were flame sealed in 5 mm NMR tubes to prevent air exposure. ^{1}H NMR spectra were collected using a 400 MHz Varian VNMRS spectrometer equipped with a Varian 5mm double resonance ^{1}H-X broadband probe. Data were collected using a recycle delay of 5-10 seconds, 8 scans and a 45^{o} ^{1}H pulse with a duration of 5.30 μs. The frequency of the spectrometer was not locked during data acquisition due to the lack of a deuterated

solvent. The magnetic field was shimmed manually for each sample to minimize magnetic field inhomogeneities. ^{1}H and ^{15}N chemical shifts for all PILs were found to have a negligible dependence on temperature in this range. All ^{1}H chemical shifts were externally referenced to the TMS peak of a mixture of 1% TMS in $CDCl_3$ shortly before the spectra were collected. ^{15}N NMR spectra of the ionic liquids were collected using a 400 MHz Varian VNMRS spectrometer equipped with a Varian 5 mm double resonance ^{1}H – X broad band probe operating at a 40.499 MHz resonant frequency. ^{15}N spectra were collected without ^{1}H decoupling to allow observation of J_{NH} coupling when present. Data were collected using a recycle delay of 2 seconds and averaging 256-1024 transients. All ^{15}N chemical shifts were indirectly referenced to methyl nitrite by setting the resonance for benzamide to -277.8 ppm shortly before the spectra were collected.

Diffusion coefficients were measured using a pulsed field gradient stimulated echo (PFG-STE) pulse sequence with bipolar gradient pulses.[29] Data were collected on an 800 MHz Varian VNMRS spectrometer equipped with a 5 mm Doty PFG probe operating at proton resonant frequency of 799.85 MHz, and a ^{19}F resonant frequency of 752.5 MHz Proton spectra were collected with a recycle delay of 5 seconds, 16 transients, a 90^{o} pulse with a duration of 16.5-18.0 μs, 20-40 ms diffusion delay (Δ), 0.5 ms gradient length (δ), and a maximum gradient strength (g) of approximately 1200 G/cm depending on the diffusivity of the ionic liquid. For the PILs synthesized with fluorinated acids, (TFA and OTf) ^{19}F PFG-NMR was used to measure the diffusivity of the anions. The ^{19}F spectra were collected with a recycle delay of 3 seconds, 16 transients, a 90^{o} pulse with a duration of 19.5 μs, 25 ms diffusion delay (Δ), 0.5 ms gradient length (δ), and a

maximum gradient strength (g) of approximately 1000 G/cm depending on the diffusivity of the ionic liquid. During each measurement the temperature was regulated at 25 °C.

Electronic structure calculations. Proton affinities of the anions of the acids used in this study were calculated using Gaussian09. For each anion, the PA value was calculated using the density functional theory (DFT) B3LYP functional with the 6-311G++ (3d,3p) basis set.[27] The structures of each acid and its conjugate base were geometry optimized prior to executing thermochemistry calculations. The proton affinities of the bases were also calculated in the same manner by optimizing the structures of each base and its protonated form. We have shown before[15] that the results obtained via electronic structure calculations are all within ±6 kcal/mol of literature values.

Conductivity and viscosity measurements. Ionic conductivities were determined from complex impedance data from a PAR VMP2 potentiostat (Princeton Applied Research) with a frequency range of 10 Hz to100 kHz. Ionic conductivity of the ILs was measured using a homemade dip cell with two platinum discs. The cell constant was determined with a solution of 0.1 M KCl at 25 °C. The cell constant was measured to be 1.06 cm^{-1} using a standard 0.1 M KCl solution. Temperature was controlled using Yamato Scientific DKN-402 programmable oven. Kinematic viscosities of the PIL samples were measured using small sample U-tube CANNON™ viscometers per standard test ASTM D 445 and ISO 3104. Either a size 450 U-tube with a kinematic viscosity range of 500 to 2500 cSt or a size 150 with a kinematic viscosity range of 7 to 35 cSt was used depending on the viscosity of the sample. Each tube was calibrated at two temperatures (40 and 100 °C) and a calibration line was used to obtain the kinematic

viscosity constant at different temperatures. Densities were measured using a 1.5 mL volumetric flask and a scale.

3.3 Results and Discussion

As the acid strength increases, the exchangeable proton is more associated with the nitrogen of the base, resulting in a shift of the ^{15}N resonance down field (higher ppm). This shift is consistent with previous studies which measured the ^{15}N chemical shift of amines as a function of the extent of protonation.[22,28]

For the substituted pyridines, a trend opposite to that of DEMA, and aliphatic amines, is observed. The ^{15}N chemical shifts of the pyridine bases change over 100 ppm upfield as it is protonated by successively stronger acids with a sudden change resembling the sigmoidal shape of an acid-base titration when the chemical shifts are plotted against the proton affinities of the acids used (Figures 3-6 and 3-7).

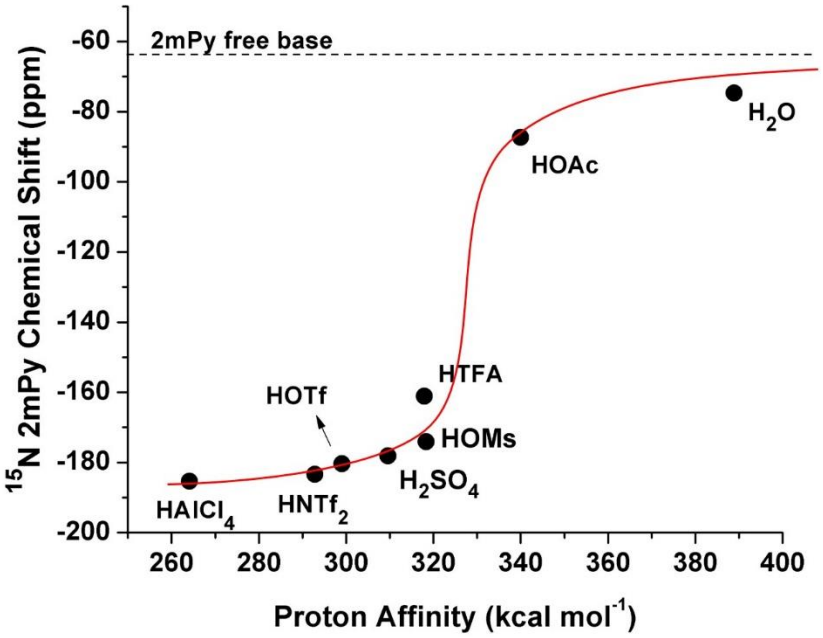

Figure 3-6- ^{15}N chemical shift of nitrogen nucleus of 2mPy in its PILs as a function of gas phase proton affinity of the acid used.

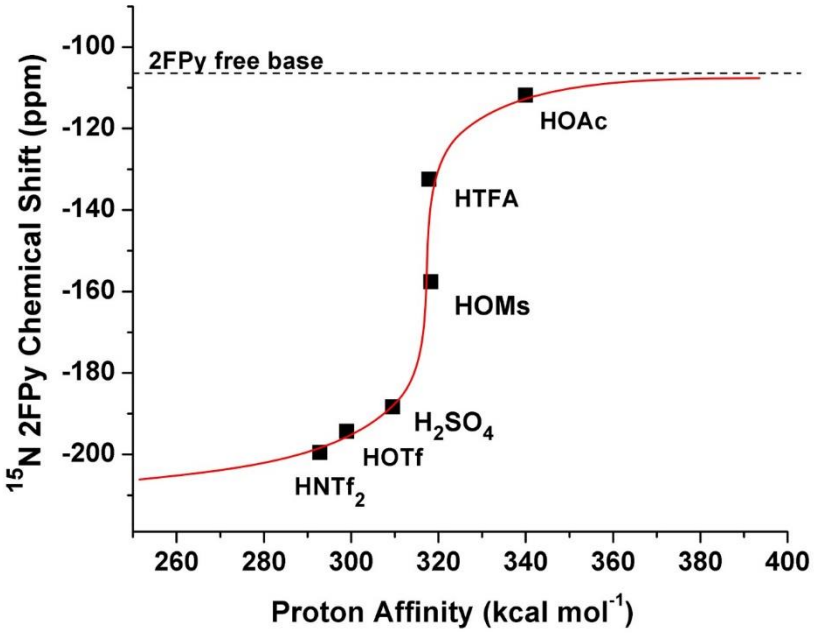

Figure 3-7- ^{15}N chemical shift of nitrogen nucleus of 2FPy in its PILs as a function of gas phase proton affinity of the acid used.

As expected, the equivalence point for the weaker base 2FPy occurs at a lower proton affinity (higher acidity). Considering the methanesulfonate (OMs) salts of the two bases helps clarifying the point. While, as suggested by the chemical shift, 2FPy is only halfway protonated by HOMs, 2mPy has the ^{15}N chemical shift of a fully protonated form. We believe the equivalence points of the titration-like curves, which matches the maximum in the proton chemical shift as mentioned above, corresponds to the start of a regime in which the base is protonated and going to lower proton affinities only changes the hydrogen bond interaction between the anion and the cation.

It is noteworthy that the equivalence points for the two cases are approximately 15 kcal mole^{-1} apart, which corresponds to the difference between the PA values of the two bases, a value also obtained from DTF calculations. To demonstrate this fact and the

similarity of the behaviors of the two cases, the normalized change in the 15N chemical shifts are plotted against the difference between the proton affinities of the acids and the bases (ΔPA). The result is shown in Figure 3-8.

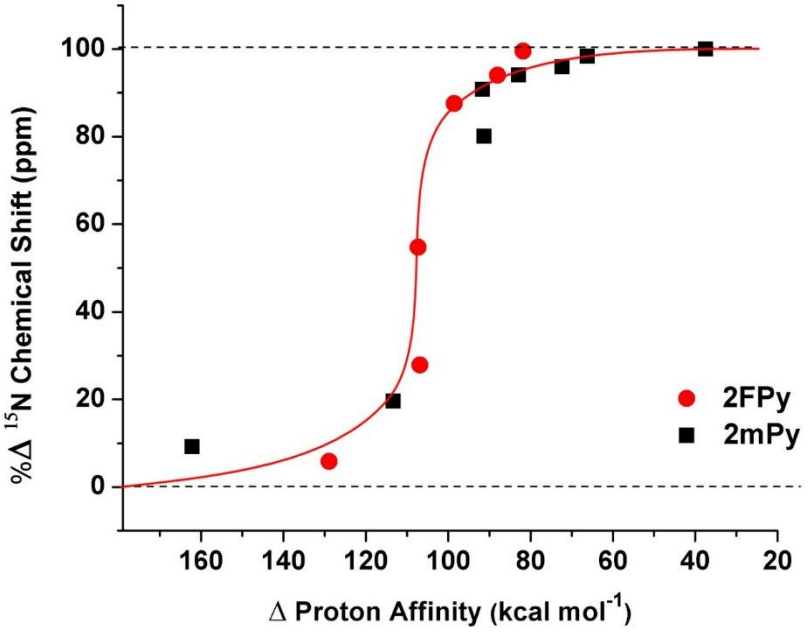

Figure 3-8- ^{15}N chemical shift of nitrogen nuclei of in its PILs as a function of gas phase proton affinity of the acid used.

The ^{15}N chemical shift change for DMI, discussed in more detail in the previous chapter, shows a completely different and a more interesting trend. Due to the specific electronic structure of this base and the fact that it is not the nitrogen atom that is directly protonated, the molecule shows a linear change of the ^{15}N chemical shift toward higher ppm values as it is protonated by stronger acids (Figure 3-9).

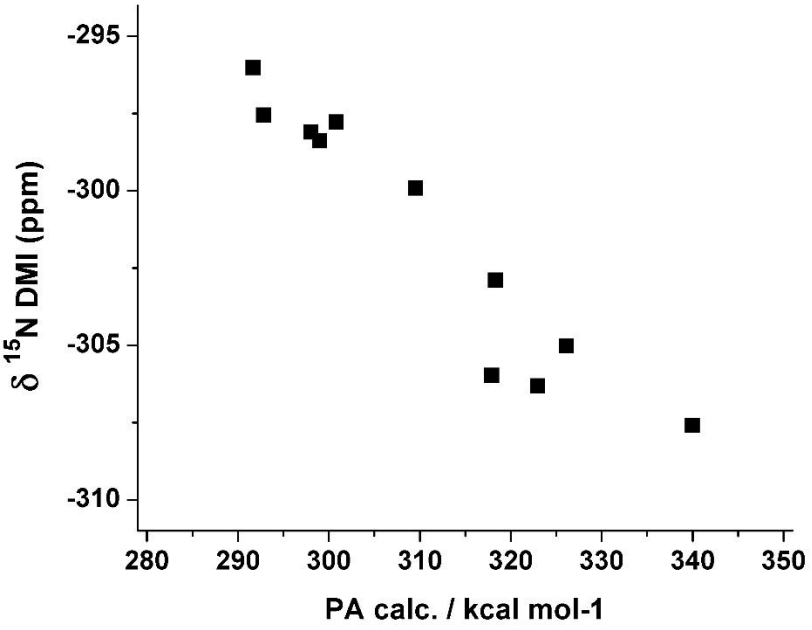

Figure 3-9- ^{15}N chemical shift of nitrogen nuclei of DMI in its PILs as a function of gas phase proton affinity of the acid used.

Pulsed field gradient stimulated echo (PFG-STE) NMR provides a useful tool for measuring the diffusion coefficients of ionic liquids ions.[30] The stimulated echo pulse sequence was used instead of the spin echo (SE) pulse sequence[31] because it has a better sensitivity. It is possible to determine the diffusion coefficients by measuring the decrease in the area under each peak when the gradient strength is changed and fitting it to the Stejskal-Tanner[32,33] equation below:

$$\ln\left(\frac{S(2\tau)}{S_0}\right) = -Dg^2\gamma^2\delta^2\left(\Delta - \frac{\delta}{3}\right) \qquad (2)$$

where S(2τ) is the attenuated signal, S(0) is the signal with zero gradient strength, g is the gradient strength, γ is the gyromagnetic ratio, δ is the gradient length, and Δ is the diffusion delay.

Figure 3-10 provides an example of a Stejskal-Tanner plot for the case of DEMA acetate.

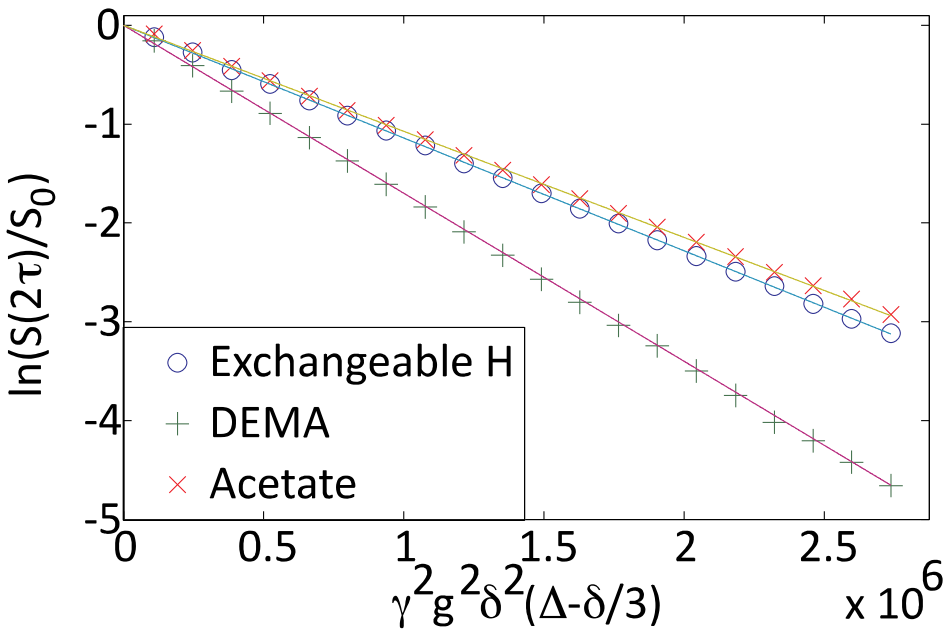

Figure 3-10- Example Stejskal-Tanner plot obtained from ^{1}H PFG-NMR experiments for DEMA-Ac protic ionic liquid using the stimulated echo sequence with bipolar gradients. (Reprinted with permission from Ref.[15])

It might seem reasonable to conclude from Figure 3-10 that the acidic proton spends its whole time on the anion and so there has been no proton transfer from the acid to the base. It should then be noted that the signal recorded by the NMR machine of DEMA's alkyl protons is an average of both the cation and the free base and hence the attenuation of it is not solely due to the diffusion of the cation but is a weighted average of those of both the cation and the free base. Similarly, the acetate's methyl signal loss is due to the diffusion of both the anion and the free acid. The diffusion coefficients obtained from the PFG experiments for acid (D_b^{PFG}), base (D_a^{PFG}) and the exchangeable proton (D_H^{PFG}) are better expressed as:

$$D_b^{PFG} = \alpha D_b^+ + \beta D_b^0 \quad (3)$$

$$D_a^{PFG} = \alpha D_a^- + \beta D_a^0 \quad (4)$$

$$D_H^{PFG} = \alpha D_b^+ + \beta D_a^0 \quad (5)$$

where α is the degree of dissociation and β is the fraction of the acid/base in the neutral from; we have:

$$\alpha + \beta = 1 \quad (6)$$

The contribution of each of the anion/cation and the free acid/base to the measured diffusion coefficient from the Stejskal-Tanner plot is dependent on both the mole ratios of each species and their diffusion coefficients. In a set of PILs made of a certain base and different acids, we are interested in the difference of the diffusion rates of the base/cation and the exchangeable proton which is given by:

$$D_b^{PFG} - D_H^{PFG} = \beta(D_b^0 - D_a^0) \quad (7)$$

The difference observed for the acetate case is a result of a non-zero β and a difference between the diffusion coefficients of the acid and the base. It is reasonable to assume that the neutral species diffuse faster than the charged ones and hence the terms including βD^0 become dominant over αD_a^- or αD_b^+ even when β is not close to 1. For the cases with a large proton transfer energy between the acid and the base, such as the triflate case mentioned below, as β approaches 0, no difference between the diffusion coefficients of the base and the exchangeable proton is observed.

It is desirable to have assessment of each of the parameters introduced above. It is proposed here to use analogues of the acid and the base without proton exchange ability to obtain, through PFG experiments, values for diffusion coefficients of charged and

neutral species. As an example, to obtain a diffusion coefficient of DEMA cation (D_b^+) in DEMA-OAc medium without any interference from the free base, diethyldimethylammonium (methylated DEMA) can be used. The diffusion coefficient of the free base (D_b^0) then can be easily worked out using the relations above. The diffusion coefficient of the anion (D_a^-) can be obtained in the same manner using this time the diffusion coefficient of the acid's methyl ester, methylacetate (MeOAc) here, as an approximation of D_a^0.

The author believes the above formulation can explain the behavior of the majority of the PILs. The equations below are the more general forms of the same ideas which take into account the possibility of ion-pair diffusion and proton hopping:

$$D_b^{PFG} = \alpha D_b^+ + \beta D_b^0 + \gamma D^{ip} \quad (8)$$

$$D_a^{PFG} = \alpha D_a^- + \beta D_a^0 + \gamma D^{ip} \quad (9)$$

$$D_H^{PFG} = \alpha D_b^+ + \beta D_a^0 + \gamma D^{ip} + D^{hop} \quad (10)$$

where:

$$\alpha + \beta + \gamma = 1 \quad (11)$$

A summary of the diffusion ^{1}H NMR results is shown below in Table 3-2.

Table 3-2- Results of diffusion NMR experiments and conductivity measurements. Diffusion coefficients are shown as D*10^9 (m^2/s) and conductivities are reported in mS/cm. (Reprinted with permission from Ref.[15])

PIL	D_a	D_H	D_b	Λ_{NE}	Λ_{exp}	$\Lambda_{exp}/\Lambda_{NE}$
DEMA-OAc	8.46	9.03	13.1	49.5	2.72	0.055
DEMA-TFA	3.90	3.93	3.97	16.0	3.69	0.231
DEMA-OMs	2.48	2.46	2.45	10.7	3.55	0.332
DEMA-OTf	1.91	4.40	4.35	12.5	7.69	0.615

Nernst Einstein equation (eq. 12) can be used to calculate an ideal conductivity using the self-diffusion coefficients resulted from the PFG-STE experiments.

$$\Lambda_{NE} = \frac{N_A e^2}{kT}(D^+ + D^-) \qquad (12)$$

where Λ_{NE} is the ionic conductivity predicted via PFG-NMR, N_A is the Avogadro number, e is the electronic charge, k is Boltzmann's constant, T is temperature, D^+ and D^- are the measured diffusion coefficients of the cation and anion respectively. The conductivity measured from electrochemical impedance spectroscopy is only a fraction of the value obtained from NE equation, this ratio can also be used as a measure of ionicity of the PIL. One reason for the discrepancy is using the diffusion coefficients measured by PFG-STE method (D_b^{PFG} and D_a^{PFG}) for the diffusion coefficients of the cation and the anion (D_b^+ and D_a^-). This is an overestimation which gives rise to $\Lambda_{exp}/\Lambda_{NE}$ ratios of 0.2 or lower. The ratio is smaller for the cases with bigger β values according to the equations 4-6.

Additionally, the deviation from the ideal viscosity limited Walden conductivity (ΔW) can be used as a measure of ionicity.[10,11,34,35] The ΔW is measured from the deviation of the equivalent conductivity from what expected from the fluidity of the medium according to Walden rule.[10,34] Figure 3-11 summarizes the ionicity characterization of a number of the DEMA PILs using the Walden and NE methods.

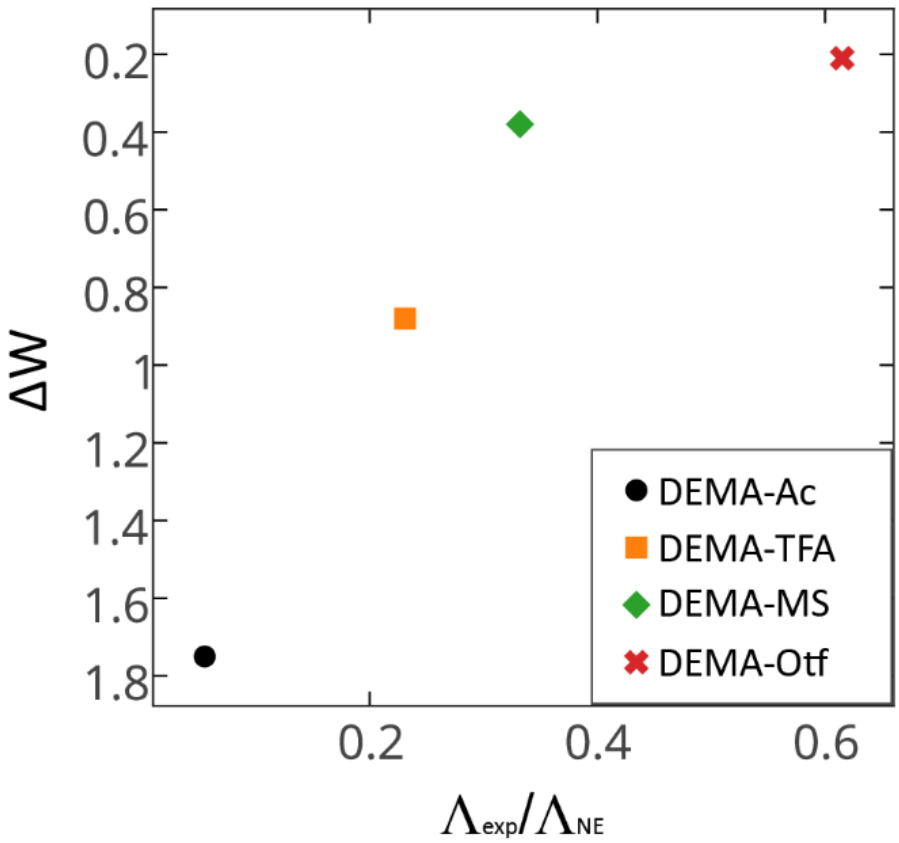

Figure 3-11- Summary of the characterization of the ionicity of a subset of the DEMA based ionic liquids studied via the deviation from Walden conductivity (ΔW) and the ratio of the measured conductivity through impedance measurements, and the predicted conductivity from NMR ($\Lambda_{exp}/\Lambda_{NE}$). (Reprinted with permission from Ref.[15])

The two different measures of ionicity are in good agreement, as was also found by Miran et al.[13] for the case of a series of acids protonating the super base 1,8-diazabicyclo-[5,4,0]-undec-7-ene (DBU). However, the data point for the most ionic IL analyzed (DEMA-OTf) deviates from linearity, which indicates a difference between these two methods for determining ionicity as the ionic liquid approaches higher ionicities. The inability of an ionic liquid's conductivity to approach the ideal Nernst-Einstein conductivity has previously been attributed to the effects from ion-pair diffusion.[11,36] PFG-NMR results for the PILs with intermediate proton transfer strengths

showed the cation and anion diffusing at approximately the same rate, which supports the presence of ion-pairing (see Table 3-2). However, for the strong proton transfer case (DEMA-OTf), different diffusion rates were observed for the anion and cation, suggesting that ion pairing is not prominent for this PIL. In cases where ion-pairing is not expected, the deviation from the Nernst-Einstein conductivity can be attributed to interionic friction as described previously for molten salts by Berne and Rice.[37] The effect should be a function of the magnitude of opposing ion fluxes and thus should diminish with decreasing conductivity, as seen in both aqueous solutions and molten salts where it approaches zero in the glassy state.[38]

3.4 Conclusions

The degrees of ionization and ionicities of several liquids in 3 sets of tertiary amine based PILs were characterized using ^{1}H and ^{15}N NMR spectroscopy, electronic structure calculations, and conductivity/viscosity measurements. The chemical shift of the nitrogen nucleus in the pyridine-based PILs was observed to show the degree of protonation. It is shown that even in the cases where the ^{15}N chemical shift suggests full ionization low ionicities are observed. Additionally, we have found proton affinity to better describe the spectroscopic changes than aqueous ΔpK_a values. The difference in the proton affinities of the acid and the base (ΔPA) can be used to predict the acid-base and charge transport properties of PILs.

3.5 Works Cited

(1) Walden, P. *Bull. Acad. Imp. Sci.* **1914**, *8*, 405–422.

(2) Wasserscheid, P.; Welton, T. *Ionic Liquids in Synthesis*, Second.; Wiley-VCH: Weinheim, 2008.

(3) *Ionic Liquids*; Kirchner, B., Ed.; Topics in Current Chemistry; Springer Berlin Heidelberg: Berlin, Heidelberg, 2010; Vol. 290.

(4) Endres, F.; MacFarlane, D.; Abbott, A. *Electrodeposition from Ionic Liquids*; 2008.

(5) Smiglak, M.; Pringle, J. M.; Lu, X.; Han, L.; Zhang, S.; Gao, H.; MacFarlane, D. R.; Rogers, R. D. *Chem. Commun.* **2014**, *50* (66), 9228–9250.

(6) MacFarlane, D. R.; Tachikawa, N.; Forsyth, M.; Pringle, J. M.; Howlett, P. C.; Elliott, G. D.; Davis, J. H.; Watanabe, M.; Simon, P.; Angell, C. A. *Energy Environ. Sci.* **2014**, *7* (1), 232–250.

(7) Yasuda, T.; Watanabe, M. *MRS Bull.* **2013**, *38* (July), 560–566.

(8) Ohno, H. *Electrochemical Aspects of Ionic Liquids*; Ohno, H., Ed.; Wiley and Sons: Hoboken, New Jersey, 2011.

(9) Xu, W.; Angell, C. A. *Science* **2003**, *302* (5644), 422–425.

(10) Yoshizawa, M.; Xu, W.; Angell, C. A. *J. Am. Chem. Soc.* **2003**, *125* (8), 15411–15419.

(11) MacFarlane, D. R.; Forsyth, M.; Izgorodina, E. I.; Abbott, A. P.; Annat, G.; Fraser, K. *Phys. Chem. Chem. Phys.* **2009**, *11* (25), 4962–4967.

(12) Tokuda, H.; Tsuzuki, S.; Susan, M. A. B. H.; Hayamizu, K.; Watanabe, M. *J. Phys. Chem. B* **2006**, *110*, 19593–19600.

(13) Miran, M. S.; Kinoshita, H.; Yasuda, T.; Susan, M. A. B. H.; Watanabe, M. *Phys. Chem. Chem. Phys.* **2012**, *14*, 5178.

(14) MacFarlane, D. R.; Pringle, J. M.; Johansson, K. M.; Forsyth, S. A.; Forsyth, M. *Chem. Commun. (Camb).* **2006**, 1905–1917.

(15) Davidowski, S. K.; Thompson, F.; Huang, W.; Hasani, M.; Amin, S. A.; Angell, C. A.; Yarger, J. L. *J. Phys. Chem. B* **2016**, *120* (18), 4279–4285.

(16) Izgorodina, E. I.; Forsyth, M.; Macfarlane, D. *Aust. J. Chem.* **2007**, *60*, 15–20.

(17) Denisov, G. S.; Gindin, V. A.; Golubev, N. S.; Ligay, S. S.; Shchepkin, D. N.; Smirnov, S. N. *J. Mol. Liq.* **1995**, *67*, 217–234.

(18) Gutowski, K. E.; Dixon, D. A. *J. Phys. Chem. A* **2006**, *110* (43), 12044–12054.

(19) Zhang, M.; Sonoda, T.; Mishima, M.; Honda, T.; Leito, I.; Koppel, I. A.; Bonrath, W.; Netscher, T. *J. Phys. Org. Chem.* **2014**, *27* (8), 676–679.

(20) Ross, B. D.; True, N. S. *J. Am. Chem. Soc.* **1984**, *106* (11), 2451–2452.

(21) Rollet, A.; Bessada, C. *NMR Studies of Molten Salt and Room Temperature Ionic Liquids*, 1st ed.; Elsevier Ltd., 2013; Vol. 78.

(22) Burrell, G. L.; Burgar, I. M.; Separovic, F.; Dunlop, N. F. *Phys. Chem. Chem. Phys.* **2010**, *12*, 1571–1577.

(23) Lyčka, A.; Doleček, R.; Šimůnek, P.; Macháček, V. *Magn. Reson. Chem.* **2006**, *44* (February), 521–523.

(24) Lethesh, K. C.; Van Hecke, K.; Van Meervelt, L.; Nockemann, P.; Kirchner, B.; Zahn, S.; Parac-Vogt, T. N.; Dehaen, W.; Binnemans, K. *J. Phys. Chem. B* **2011**, *115* (26), 8424–8438.

(25) Perinu, C.; Saramakoon, G.; Arstad, B.; Jens, K. J. *Energy Procedia* **2014**, *63* (1876), 1144–1150.

(26) Katsyuba, S. A.; Vener, M. V.; Zvereva, E. E.; Fei, Z.; Scopelliti, R.; Laurenczy, G.; Yan, N.; Paunescu, E.; Dyson, P. J. *J. Phys. Chem. B* **2013**, *117* (30), 9094–9105.

(27) Besnard, M.; Cabaço, M. I.; Vaca Chávez, F.; Pinaud, N.; Sebastião, P. J.; Coutinho, J. a P.; Mascetti, J.; Danten, Y. *J. Phys. Chem. A* **2012**, *116* (20), 4890–4901.

(28) Judeinstein, P.; Iojoiu, C.; Sanchez, J. Y.; Ancian, B. *J. Phys. Chem. B* **2008**, *112*, 3680–3683.

(29) Wu, D. H.; Chen, A. D.; Johnson, C. S. *J. Magn. Reson. Ser. A* **1995**, *115* (2), 260–264.

(30) Burrell, G. L.; Burgar, I. M.; Gong, Q.; Dunlop, N. F.; Separovic, F. *J. Phys. Chem. B* **2010**, *114*, 11436–11443.

(31) Tanner, J. E. *Rev. Sci. Instrum.* **1965**, *36* (8), 1086–1087.

(32) Stejskal, E. O.; Tanner, J. E. *J. Chem. Phys.* **1965**, *42* (1), 5.

(33) Tanner, J. E.; Stejskal, E. O. *J. Chem. Phys.* **1968**, *49* (4), 1768–1777.

(34) Xu, W.; Angell, C. A. *Science* **2003**, *302* (2003), 422–425.

(35) Belieres, J.-P.; Angell, C. A. *J. Phys. Chem. B* **2007**, *111*, 4926–4937.

(36) Ueno, K.; Tokuda, H.; Watanabe, M. *Phys. Chem. Chem. Phys.* **2010**, *12* (8), 1649.

(37) Berne, B.; Rice, S. A. *J. Chem. Phys.* **1964**, *40* (5), 1336–1346.

(38) Videa, M.; Xu, W.; Geil, B.; Marzke, R.; Angell, C. A. *J. Electrochem. Soc.* **2001**, *148*, A1352.

4 References

(1) MacFarlane, D. R.; Forsyth, M.; Howlett, P. C.; Kar, M.; Passerini, S.; Pringle, J. M.; Ohno, H.; Watanabe, M.; Yan, F.; Zheng, W.; Zhang, S.; Zhang, J. *Nat. Rev. Mater.* **2016**, 15005.

(2) Rupp, A. B. A.; Krossing, I. *Acc. Chem. Res.* **2015**, *48* (1), 2537–2546.

(3) Greaves, T. L.; Drummond, C. J. *Chem. Rev.* **2015**, *115*, 11379–11448.

(4) Greaves, T. L.; Drummond, C. J. *Chem. Rev.* **2008**, *108*, 206–237.

(5) Lei, Z.; Dai, C.; Chen, B. *Chem. Rev.* **2014**, *114* (2), 1289–1326.

(6) Estager, J.; Holbrey, J. D.; Swadźba-Kwaśny, M. *Chem. Soc. Rev.* **2014**, *43* (3), 847–886.

(7) Angell, C. A. *ECS Trans.* **2014**, *64* (4), 9–20.

(8) MacFarlane, D. R.; Tachikawa, N.; Forsyth, M.; Pringle, J. M.; Howlett, P. C.; Elliott, G. D.; Davis, J. H.; Watanabe, M.; Simon, P.; Angell, C. A. *Energy Environ. Sci.* **2014**, *7* (1), 232–250.

(9) Angell, C. A. *Molten Salts Ion. Liq. Never Twain?* **2012**, 1–24.

(10) Angell, C. A.; Ansari, Y.; Zhao, Z. *Faraday Discuss.* **2012**, *154* (1), 9.

(11) Angell, C. A.; Byrne, N.; Belieres, J. P. *Acc. Chem. Res.* **2007**, *40*, 1228–1236.

(12) Greaves, T. L.; Drummond, C. J. *Chem. Soc. Rev.* **2008**, *37* (8), 1709–1726.

(13) Endres, F. *Phys. Chem. Chem. Phys.* **2010**, *12*, 1648.

(14) Patel, D. D.; Lee, J. M. *Chem. Rec.* **2012**, *12* (3), 329–355.

(15) Earle, M. J.; Seddon, K. R. *Pure Appl. Chem.* **2000**, *72* (7), 1391–1398.

(16) Preiss, U.; Verevkin, S. P.; Koslowski, T.; Krossing, I. *Chem. - A Eur. J.* **2011**, *17* (23), 6508–6517.

(17) Slattery, J. M.; Daguenet, C.; Dyson, P. J.; Schubert, T. J. S.; Krossing, I. *Angew. Chemie - Int. Ed.* **2007**, *46* (28), 5384–5388.

(18) Xu, X.; Hussey, C. L. **1993**, *140* (3), 618–626.

(19) Wilkes, J. S. *Green Chem.* **2002**, *4*, 73–80.

(20) Mandai, T.; Yoshida, K.; Ueno, K.; Dokko, K.; Watanabe, M. *Phys. Chem. Chem. Phys.* **2014**, *16* (19), 8761–8772.

(21) Walden, P. *Bull. Acad. Imp. Sci.* **1914**, *8*, 405–422.

(22) Yoshizawa, M.; Xu, W.; Angell, C. A. *J. Am. Chem. Soc.* **2003**, *125* (8), 15411–15419.

(23) Xu, W.; Cooper, E. I.; Angell, C. A. *J. Phys. Chem. B* **2003**, *107*, 6170–6178.

(24) MacFarlene, D. R.; Seddon, K. R. *Aust. J. Chem.* **2007**, *60*, 3–5.

(25) MacFarlane, D. R.; Pringle, J. M.; Johansson, K. M.; Forsyth, S. A.; Forsyth, M. *Chem. Commun. (Camb).* **2006**, 1905–1917.

(26) Davidowski, S. K.; Thompson, F.; Huang, W.; Hasani, M.; Amin, S. A.; Angell, C. A.; Yarger, J. L. *J. Phys. Chem. B* **2016**, *120* (18), 4279–4285.

(27) Nuthakki, B.; Greaves, T. L.; Krodkiewska, I.; Weerawardena, A.; Burgar, M. I.; Mulder, R. J.; Drummond, C. J. *Aust. J. Chem.* **2007**, *60*, 21–28.

(28) Miran, M. S.; Kinoshita, H.; Yasud, T. *Phys. Chem. Chem. Phys.* **2012**, *14*, 5178.

(29) Tokuda, H.; Tsuzuki, S.; Susan, M. A. B. H.; Hayamizu, K.; Watanabe, M. *J. Phys. Chem. B* **2006**, *110*, 19593–19600.

(30) Angell, C. A.; Byrne, N.; Belieres, J. P. *Acc. Chem. Res.* **2007**, *40* (11), 1228–1236.

(31) Belieres, J.-P.; Angell, C. A. *J. Phys. Chem. B* **2007**, *111*, 4926–4937.

(32) Gillespie, R. J.; Peel, T. E. *J. Am. Chem. Soc.* **1973**, *95* (16), 5173–5178.

(33) Robert, T.; Magna, L.; Olivier-Bourbigou, H.; Gilbert, B. *J. Electrochem. Soc.* **2009**, *156*, F115.

(34) Johnson, K. E.; Pagni, R. M.; Bartmess, J. *Monatshefte fur Chemie* **2007**, *138*, 1077–1101.

(35) Kamlet, M. J.; Abboud, J. L.; Taft, R. W. *J. Am. Chem. Soc.* **1977**, *99* (18), 6027–6038.

(36) Kurnia, K. A.; Lima, F.; Claudio, A. F.; Coutinho, J. A. P.; Freire, M. G. *Phys. Chem. Chem. Phys.* **2015**, *17* (29), 18980–18990.

(37) Macfarlane, D. R.; Vijayaraghavan, R.; Ha, H. N.; Izgorodin, A.; Weaver, K. D.; Elliott, G. D. *Chem. Commun. (Camb).* **2010**, *46*, 7703–7705.

(38) Shukla, S. K.; Kumar, A. *J. Phys. Chem. B* **2013**, *117*, 2456–2465.

(39) Adam, C.; Bravo, M. V.; Mancini, P. M. E. *Tetrahedron Lett.* **2014**, *55* (1), 148–150.

(40) Thomazeau, C.; Olivier-Bourbigou, H.; Magna, L.; Luts, S.; Gilbert, B. *J. Am. Chem. Soc.* **2003**, *125* (18), 5264–5265.

(41) Bartosik, J.; Mudring, A. V. *Phys. Chem. Chem. Phys.* **2010**, *12*, 1648.

(42) Schmeisser, M.; Illner, P.; Puchta, R.; Zahl, A.; Van Eldik, R. *Chem. - A Eur. J.* **2012**, *18*, 10969–10982.

(43) McCune, J. A.; He, P.; Petkovic, M.; Coleman, F.; Estager, J.; Holbrey, J. D.; Seddon, K. R.; Swadźba-Kwaśny, M. *Phys. Chem. Chem. Phys.* **2014**, *16*, 23233–23243.

(44) Gräsvik, J.; Hallett, J. P.; To, T. Q.; Welton, T. *Chem. Commun. (Camb).* **2014**, *50*, 7258–7261.

(45) Tang, L.; Zeller, R.; Angell, C. A.; Friesen, C. *J. Phys. Chem. C* **2009**, *113*, 12586–12593.

(46) Miran, M. S.; Yasuda, T.; Susan, M. A. B. H.; Dokko, K.; Watanabe, M. *RSC Adv.* **2013**, *3* (13), 4141–4144.

(47) Kanzaki, R.; Doi, H.; Song, X.; Hara, S.; Ishiguro, S. I.; Umebayashi, Y. *J. Phys. Chem. B* **2012**, *116*, 14146–14152.

(48) Hashimoto, K.; Fujii, K.; Shibayama, M. *J. Mol. Liq.* **2013**, *188*, 143–147.

(49) Miran, M. S.; Kinoshita, H.; Yasuda, T.; Susan, M. A. B. H.; Watanabe, M. *Phys. Chem. Chem. Phys.* **2012**, *14*, 5178.

(50) Davidowski, S. K.; Thompson, F.; Huang, W.; Hasani, M.; Amin, S.; Yarger, J. L.; Angell, C. A. *J. Phys. Chem. B, Submitt.*

(51) Angell, C. A.; Shuppert, J. W. *J. Phys. Chem.* **1980**, *84*, 538–542.

(52) Johansson, K. M.; Izgorodina, E. I.; Forsyth, M.; MacFarlane, D. R.; Seddon, K. R. *Phys. Chem. Chem. Phys.* **2008**, *10*, 2972–2978.

(53) Laurence, C.; Graton, J.; Gal, J. F. *J. Chem. Educ.* **2011**, *88* (12), 1651–1657.

(54) Laurence, C.; Gal, J. F. *Lewis Basicity and Affinity Scales; Data and Measurement*; John Wiey & Sons: Chichester, U.K., 2010.

(55) Ahrland, S.; Chatt, J.; Davies, N. R. *Quart. Rev.* **1958**, *12*, 265–276.

(56) Ohno, H. *Electrochemical Aspects of Ionic Liquids*; Ohno, H., Ed.; Wiley and Sons: Hoboken, New Jersey, 2011.

(57) Wasserscheid, P.; Welton, T. *Ionic Liquids in Synthesis*, Second.; Wiley-VCH: Weinheim, 2008.

(58) Idris, A.; Vijayaraghavan, R.; Patti, A. F.; Macfarlane, D. R. *ACS Sustain. Chem. Eng.* **2014**, *2* (7), 1888–1894.

(59) Maase, M.; Massonne, K.; Halibritter, K. No Title. WO 2003062171, 2008.

(60) Wang, L.; Kefalidis, C. E.; Roisnel, T.; Sinbandhit, S.; Maron, L.; Sarazin, Y. **2015**, No. Ii.

(61) Fumino, K.; Fossog, V.; Stange, P.; Wittler, K.; Polet, W.; Hempelmann, R.; Ludwig, R. *ChemPhysChem* **2014**, *15*, 2604–2609.

(62) Engesser, T. A.; Lichtenthaler, M. R.; Schleep, M.; Krossing, I. *Chem. Soc. Rev.* **2016**.

(63) Dong, K.; Zhang, S.; Wang, J. *Chem. Commun.* **2016**.

(64) Weber, C. C.; Kunov-Kruse, A. J.; Rogers, R. D.; Myerson, A. S. *Chem. Commun. (Camb).* **2015**, *51* (20), 4294–4297.

(65) Kumar, A.; Rani, A.; Venkatesu, P. *New J. Chem.* **2015**, *39* (2), 938–952.

(66) Anslyn, E. V; Dougherty, D. A. *Modern Physical Organic Chemistry*; University Science Books: Sausalito, California, 2006.

(67) Mihichuk, L. M.; Driver, G. W.; Johnson, K. E. *ChemPhysChem* **2011**, *12*, 1622–1632.

(68) Cox, R. A. *Can. J. Chem.* **1983**, *61*, 2225–2243.

(69) Klumpp, D. A.; Yeung, K. Y.; Prakash, G. K. S.; Olah, G. A. *Superacid chemistry*; 1998.

(70) Kütt, A.; Rodima, T.; Saame, J.; Raamat, E.; Mäemets, V.; Kaljurand, I.; Koppel, I. A.; Garlyauskayte, R. Y.; Yagupolskii, Y. L.; Yagupolskii, L. M.; Bernhardt, E.; Willner, H.; Leito, I. *J. Org. Chem.* **2011**, *76* (2), 391–395.

(71) Himmel, D.; Goll, S. K.; Leito, I.; Krossing, I. *Angew. Chemie - Int. Ed.* **2010**, *49* (38), 6885–6888.

(72) Himmel, D.; Goll, S. K.; Scholz, F.; Radtke, V.; Leito, I.; Krossing, I. *ChemPhysChem* **2015**, *16* (7), 1428–1439.

(73) Suu, A.; Jalukse, L.; Liigand, J.; Kruve, A.; Himmel, D.; Krossing, I.; Rosés, M.; Leito, I. *Anal. Chem.* **2015**, *87* (5), 2623–2630.

(74) Koppel, I. A.; Burk, P.; Koppel, I.; Leito, I.; Sonoda, T.; Mishima, M. *J. Am. Chem. Soc.* **2000**, *122* (21), 5114–5124.

(75) Carlin, C.; Gordon, M. S. *J. Comput. Chem.* **2015**, *36* (9), 597–600.

(76) Olofsson, G.; Lindqvist, I.; Sunner, S. *Acta Chem. Scand.* **1963**, *17*, 259–265.

(77) Gutmann, V. *The Donor-Acceptor Approach to Molecular Interactions*; Plenum Press: New York, 1978.

(78) Driver, G. W. *ChemPhysChem* **2015**, *16* (11), 2432–2439.

(79) Cho, C.-W.; Stolte, S.; Ranke, J.; Preiss, U.; Krossing, I.; Thoeming, J. *ChemPhysChem* **2014**, *15* (11), 2351–2358.

(80) Muller, P. *Pure Appl. Chem.* **1994**, *66* (5), 1077–1184.

(81) Reichardt, C. *Angew. Chemie Int. Ed. …* **1965**, *4* (1), 29.

(82) Reichardt, C. *Green Chem.* **2005**, *7* (5), 339–351.

(83) Stark, A. *Top. Curr. Chem.* **2009**, *209*, 41–81.

(84) Kamlet, M. J.; Taft, R. W. *J. Am. Chem. Soc.* **1975**, *98*, 377–383.

(85) Cláudio, A. F. M.; Swift, L.; Hallett, J. P.; Welton, T.; Coutinho, J. a P.; Freire, M. G. *Phys. Chem. Chem. Phys.* **2014**, *16* (14), 6593–6601.

(86) Lungwitz, R.; Spange, S. *New J. Chem.* **2008**, *32* (3), 392.

(87) Holzweber, M.; Lungwitz, R.; Doerfler, D.; Spange, S.; Koel, M.; Hutter, H.; Linert, W. *Chem. - A Eur. J.* **2013**, *19*, 288–293.

(88) Schade, A.; Behme, N.; Spange, S. *Chem. - A Eur. J.* **2014**, *20* (8), 2232–2243.

(89) Robert, T.; Magna, L.; Olivier-Bourbigou, H.; Gilbert, B. *J. Electrochem. Soc.* **2009**, *156* (9), F115.

(90) Stoyanov, E. S.; Kim, K. C.; Reed, C. A. *J. Am. Chem. Soc.* **2006**, *128* (4), 8500–8508.

(91) Stoyanov, E. S.; Stoyanova, I. V.; Reed, C. A. *Chem. - A Eur. J.* **2008**, *14*, 7880–7891.

(92) Mayer, U.; Gutmann, V.; Gerger, W. *Monatshefte fur Chemie* **1975**, *106* (6), 1235–1257.

(93) Farcasiu, D.; Ghenciu, A. *J. Am. Chem. Soc.* **1993**, *115* (23), 10901–10908.

(94) Lungwitz, R.; Spange, S. *Chemphyschem* **2012**, *13*, 1910–1916.

(95) Scholz, F.; Himmel, D.; Eisele, L.; Unkrig, W.; Martens, A.; Schlüter, P.; Krossing, I. *Chem. - A Eur. J.* **2015**, *21* (20), 7489–7502.

(96) Bonhôte, P.; Dias, A.-P.; Armand, M.; Papageorgiou, N.; Kalyanasundaram, K.; Grätzel, M. *Inorg. Chem.* **1996**, *35* (5), 1168–1178.

(97) Ghandi, M.; Hasani, M.; Salahi, S. *Monatshefte fur Chemie* **2012**, *143* (3), 455–460.

(98) Gideon, B. Y. *J. Am. Chem. Soc.* **1960**, *82* (17), 4478–4483.

(99) Morgan, J.; Greenberg, A.; Liebman, J. F. *Struct. Chem.* **2012**, *23*, 197–199.

(100) Gillespie, R. J.; Birchall, T. *Can. J. Chem.* **1963**, *41* (6), 148–155.

(101) Polyakov, O. G.; Nolan, B. G.; Fauber, B. P.; Miller, S. M.; Anderson, O. P.; Strauss, S. H. *Inorg. Chem.* **2000**, *39* (8), 1735–1742.

(102) Foropoulos Jr, J.; DesMarteau, D. D. *Inorg. Chem.* **1984**, *12* (10), 3720–3723.

(103) Koppel, I. A.; Taft, R. W.; Zbu, A. S.; Hu, L.; Sung, K.; Desmarteau, D. D.; Yagupolskii, L. M.; Yagupolskii, Y. L.; Ignat, N. V; Kondratenko, V.; Volkonskii, Y.; Vlasov, V. M.; Notario, R.; Maria, P. *J. Am. Chem. Soc.* **1994**, *116* (2), 3047–3057.

(104) Raamat, E.; Kaupmees, K.; Ovsjannikov, G.; Trummal, A.; Kütt, A.; Saame, J.; Koppel, I.; Kaljurand, I.; Lipping, L.; Rodima, T.; Pihl, V.; Koppel, I. a.; Leito, I. *J. Phys. Org. Chem.* **2013**, *26*, 162–170.

(105) Stoyanov, E. S.; Kim, K. C.; Reed, C. A. *J. Phys. Chem. A* **2004**, *108* (42), 9310–9315.

(106) Gillespie, R. J.; Peel, T. E. *Adv. Phys. Org. Chem.* **1971**, *9*, 1–24.

(107) Gillespie, R. J.; Peel, T. E. *J. Am. Chem. Soc.* **1973**, *95* (2), 5173–5178.

(108) Olah, G. A.; Prakash, G. K. S.; Sommer, J. *Science (80-.).* **1979**, *206*, 13–20.

(109) Himmel, D.; Goll, S. K.; Scholz, F.; Radtke, V.; Leito, I.; Krossing, I. *ChemPhysChem* **2015**, *16* (7), 1428–1439.

(110) Lin, M.-C.; Gong, M.; Lu, B.; Wu, Y.; Wang, D.-Y.; Guan, M.; Angell, M.; Chen, C.; Yang, J.; Hwang, B.-J.; Dai, H. *Nature* **2015**, *520*, 324–328.

(111) Xue, L.; Tucker, T. G.; Angell, C. A. *Adv. Energy Mater.* **2015**, *5* (12), 1500271.

(112) Byrne, N.; Angell, C. A. *Chem. Today* **2009**, *27* (1), 51–53.

(113) Mantz, R. A.; Trulove, P. C.; Carlin, R. T.; Theim, T. L.; Osteryoung, R. A. *Inorg. Chem.* **1997**, *36* (10), 1227–1232.

(114) Brown, H. C.; Pearsall, H. W. *J. Am. Chem. Soc.* **1952**, *74*, 191–195.

(115) Nava, M.; Stoyanova, I. V; Cummings, S.; Stoyanov, E. S.; Reed, C. A. *Angew. Chem. Int. Ed. Engl.* **2014**, *53* (4), 1131–1134.

(116) Xu, W.; Angell, C. A. *Electrochem. Solid-State Lett.* **1999**, *3* (8), 366.

(117) Inoue, D.; Mitsushima, S.; Matsuzawa, K.; Lee, S.-Y.; Yasuda, T.; Watanabe, M.; Ota, K. I. *Electrochemistry* **2011**, *79*, 377−380.

(118) Lee, S. Y.; Yasuda, T.; Watanabe, M. *J. Power Sources* **2010**, *195* (18), 5909–5914.

(119) Mitsushima, S.; Shinohara, Y.; Matsuzawa, K.; Ota, K. I. *Electrochim. Acta* **2010**, *55* (22), 6639–6644.

(120) Li, H.; Jiang, F.; Di, Z.; Gu, J. *Electrochim. Acta* **2012**, *59*, 86–90.

(121) Li, Q.; He, R.; Jensen, J. O.; Bjerrum, N. J. *Chem. Mater.* **2003**, *15* (26), 4896–4915.

(122) Belieres, J.-P.; Gervasio, D.; Angell, C. A. *Chem. Commun. (Camb).* **2006**, 4799–4801.

(123) Miran, M. S.; Yasuda, T.; Susan, M. A. B. H.; Dokko, K.; Watanabe, M. *J. Phys. Chem. C* **2014**, *118* (48), 27631–27639.

(124) Xu, W.; Angell, C. A. *Science* **2003**, *302* (2003), 422–425.

(125) Menne, S.; Pires, J.; Anouti, M.; Balducci, A. *Electrochem. commun.* **2013**, *31*, 39–41.

(126) MacFarlane, D. R.; Forsyth, M.; Izgorodina, E. I.; Abbott, A. P.; Annat, G.; Fraser, K. *Phys. Chem. Chem. Phys.* **2009**, *11* (25), 4962–4967.

(127) Burrell, G. L.; Burgar, I. M.; Separovic, F.; Dunlop, N. F. *Phys. Chem. Chem. Phys.* **2010**, *12*, 1571–1577.

(128) Sarmini, K.; Kenndler, E. *J. Biochem. Biophys. Methods* **1999**, *38* (2), 123–137.

(129) Bordwell, G. *Acc. Chem. Res* **1988**, *21* (10), 456–463.

(130) Noda, A.; Hasan Susan, M. A. Bin; Kudo, K.; Mitsushima, S.; Hayamizu, K.; Watanabe, M. *J. Phys. Chem. B* **2003**, *107*, 4024–4033.

(131) Blanchard, J. W.; Beli, J.; Alam, T. M.; Yarger, J. L.; Holland, G. P. *J. Phys. Chem. Lett.* **2011**, *2*, 1077–1081.

(132) Judeinstein, P.; Iojoiu, C.; Sanchez, J. Y.; Ancian, B. *J. Phys. Chem. B* **2008**, *112*, 3680–3683.

(133) Iojoiu, C.; Judeinstein, P.; Sanchez, J. Y. *Electrochim. Acta* **2007**, *53* (4), 1395–1403.

(134) Iojoiu, C.; Martinez, M.; Maha, H.; Molmeret, Y.; Cointeaux, L.; Leprêtre, J. C.; El Kissi, N.; Guindet, J.; Judeinstein, P.; Sanchez. *Polym. Adv. Technol.* **2008**, *19*, 560–568.

(135) Mori, K.; Hashimoto, S.; Yuzuri, T.; Sakakibara, K. *Bull. Chem. Soc. Jap.* **2010**, *83*, 328–334.

(136) Mori, K.; Kobayashi, T.; Sakakibara, K.; Ueda, K. *Chem. Phys. Lett.* **2012**, *552*, 58–63.

(137) Römich, C.; Merkel, N. C.; Valbonesi, A.; Schaber, K.; Sauer, S.; Schubert, T. J. S. *J. Chem. Eng. Data* **2012**, *57* (8), 2258–2264.

(138) Wu, D. H.; Chen, A. D.; Johnson, C. S. *J. Magn. Reson. Ser. A* **1995**, *115* (2), 260–264.

(139) Frisch, M. J.; Trucks, G. W.; Schlegel, H. B.; Scuseria, G. E.; Robb, M. A.; Cheeseman, J. R.; Scalmani, G.; Barone, V.; Mennucci, B.; Petersson, G. A. *Gaussian 09*; Guassian, Inc.: Wallingford, CT.

(140) Miran, M. S.; Kinoshita, H.; Yasuda, T.; Susan, M. A.; Watanabe, M. *Chem Commun* **2011**, *47* (47), 12676–12678.

(141) Denisov, G. S.; Gindin, V. A.; Golubev, N. S.; Ligay, S. S.; Shchepkin, D. N.; Smirnov, S. N. *J. Mol. Liq.* **1995**, *67*, 217–234.

(142) Gutowski, K. E.; Dixon, D. A. *J. Phys. Chem. A* **2006**, *110* (43), 12044–12054.

(143) Zhang, M.; Sonoda, T.; Mishima, M.; Honda, T.; Leito, I.; Koppel, I. A.; Bonrath, W.; Netscher, T. *J. Phys. Org. Chem.* **2014**, *27* (8), 676–679.

(144) Zheng, A.; Liu, S. Bin; Deng, F. *Solid State Nucl. Magn. Reson.* **2013**, *55-56*, 12–27.

(145) Yi, D.; Zhang, H.; Deng, Z. *J. Mol. Catal. A Chem.* **2010**, *326* (1-2), 88–93.

(146) Chen, T.; Wouters, B. H.; Grobet, P. J. *J. Phys. Chem. B* **1999**, *103*, 6179–6184.

(147) Ross, B. D.; True, N. S. *J. Am. Chem. Soc.* **1984**, *106* (11), 2451–2452.

(148) Burrell, G. L.; Burgar, I. M.; Gong, Q.; Dunlop, N. F.; Separovic, F. *J. Phys. Chem. B* **2010**, *114*, 11436–11443.

(149) Tanner, J. E. *Rev. Sci. Instrum.* **1965**, *36* (8), 1086–1087.

(150) Stejskal, E. O.; Tanner, J. E. *J. Chem. Phys.* **1965**, *42* (1), 5.

(151) Tanner, J. E.; Stejskal, E. O. *J. Chem. Phys.* **1968**, *49* (4), 1768–1777.

(152) Ueno, K.; Tokuda, H.; Watanabe, M. *Phys. Chem. Chem. Phys.* **2010**, *12* (8), 1649.

(153) Berne, B.; Rice, S. A. *J. Chem. Phys.* **1964**, *40* (5), 1336–1346.

(154) Videa, M.; Xu, W.; Geil, B.; Marzke, R.; Angell, C. A. *J. Electrochem. Soc.* **2001**, *148*, A1352.

APPENDIX A

RESPECTIVE COORDINATES OF OPTIMIZED STRUCTURES

The structure of the neutral Brønsted acids, their conjugate anions, the neutral base and its conjugate cation were optimized. The respective coordinates are listed in the tables below.

Table A-1- DMI

Atom	x	y	z
N	1.096312	0.118807	-0.2288
C	0.000014	-0.70048	-9.9E-05
O	0.000031	-1.91706	0.000043
C	2.439589	-0.3827	-0.03615
H	2.799749	-0.19877	0.983432
H	2.432349	-1.45457	-0.21684
H	3.125052	0.093464	-0.7382
C	-2.43957	-0.38276	0.03593
H	-2.79973	-0.19908	-0.9837
H	-2.43232	-1.45458	0.216882
H	-3.12503	0.093578	0.737858
N	-1.0963	0.118824	0.22846
C	-0.76388	1.501267	-0.07765
H	-1.25427	2.194535	0.605697
H	-1.05801	1.760138	-1.10344
C	0.763854	1.501304	0.077028
H	1.254225	2.194446	-0.60646
H	1.05798	1.76039	1.102761

Table A-2-DMIH$^+$

Atom	x	y	z
N	1.106464	-0.13329	0.105162
C	0.009441	0.594687	-0.01104
O	0.084934	1.903987	-0.00573
C	2.478752	0.363678	0.057516
H	2.924672	0.148024	-0.91416
H	2.482629	1.435588	0.227404
H	3.060545	-0.12333	0.837403
C	-2.47002	0.370285	-0.03175
H	-2.81323	0.381234	1.004295
H	-2.55216	1.370835	-0.45573
H	-3.12035	-0.2753	-0.61739
N	-1.1034	-0.12588	-0.13866
C	-0.77189	-1.55286	0.057609
H	-1.25483	-2.16144	-0.70251
H	-1.1132	-1.8755	1.04266
C	0.766933	-1.55845	-0.05766
H	1.24501	-2.15407	0.715977
H	1.10803	-1.90569	-1.03428
H	-0.77924	2.334453	-0.04262

Table A-3- H2O

Atom	x	y	z
O	0	0	0.116038
H	0	0.762712	-0.46892
H	0	-0.76271	-0.46892

Table A-4- OH

Atom	x	y	z
O	0	0.002857	0.119618
H	0	-0.75906	-0.47182

Table A-5- HOAc

Atom	x	y	z
C	1.373554	0.02528	0.000021
H	1.696792	0.580096	-0.88271
H	1.841954	-0.95355	-0.00028
H	1.696831	0.579559	0.883078
C	-0.13149	-0.13829	0.000037
O	-0.84435	1.023906	0.000119
H	-0.25406	1.785535	0.000203
O	-0.70633	-1.18734	-0.00017

Table A-6- OAc

Atom	x	y	z
C	1.348208	-0.05806	-7.5E-05
H	1.734052	0.466206	-0.87884
H	1.71281	-1.08643	-0.0005
H	1.73384	0.465345	0.879303
C	-0.21266	0.00298	-0.0002
O	-0.69616	1.160428	0.000211
O	-0.81108	-1.09887	0.000001

Table A-7- HOAcCl2

Atom	x	y	z
C	0.194819	0.000007	0.545747
C	-1.265	-0.00025	0.072798
O	-1.47406	-0.00099	-1.24986
H	-0.63979	-0.00171	-1.73864
O	-2.16002	0.000519	0.864637
Cl	1.03837	-1.47811	-0.01668
Cl	1.037568	1.478604	-0.01654
H	0.211917	-0.00004	1.626193

Table A-8- OAcCl2

Atom	x	y	z
C	-0.12815	-0.00015	0.484977
C	1.360243	0.001101	-0.0553
O	1.511188	0.001352	-1.28083
O	2.17177	0.002174	0.893132
Cl	-1.04973	1.482446	-0.0266
Cl	-1.04713	-1.48443	-0.02629
H	-0.15532	-4.3E-05	1.564813

Table A-9- HTFA

Atom	x	y	z
C	0.582432	-0.01257	0.000008
C	-0.96901	-0.1564	0.000018
O	-1.64915	0.994542	-0.00009
H	-1.04753	1.752017	-0.00023
O	-1.47519	-1.23234	0.000163
F	1.103813	-0.58522	1.08444
F	1.10387	-0.58581	-1.08408
F	0.957965	1.294081	-0.00033

Table A-10- TFA

Atom	x	y	z
C	0.517413	0.01449	-5E-06
C	-1.07042	0.008948	-8.9E-05
O	-1.53482	-1.14099	0.000211
O	-1.59456	1.131381	-0.00028
F	1.034724	-0.62633	-1.08744
F	1.085917	1.245463	-0.00062
F	1.034544	-0.62516	1.088218

Table A-11- H3PO4

Atom	x	y	z
P	0.042112	0.041195	-0.0905
O	-0.97804	0.943333	0.729608
H	-1.65976	0.447084	1.19638
O	-0.95868	-0.79587	-1.01258
H	-0.50531	-1.29945	-1.69765
O	0.5518	-1.08797	0.936143
H	1.434732	-0.8814	1.26343
O	1.107075	0.799022	-0.73742

Table A-12- H2PO4

Atom	x	y	z
P	0.113348	-0.00665	-0.08563
O	1.335745	-0.66831	-0.59626
O	-0.9207	-1.2034	0.435435
H	-1.40378	-0.82345	1.17447
O	-0.71527	0.591744	-1.40017
H	-1.15324	1.388704	-1.08878
O	0.069839	1.067899	0.96077

Table A-13- HOMs

Atom	x	y	z
C	-1.63366	-0.37457	0.000022
H	-2.06241	0.059049	0.898271
H	-2.06245	0.059108	-0.89818
H	-1.7506	-1.45508	-1.2E-05
S	0.11416	-0.06886	-8E-06
O	0.691369	-0.49818	-1.24253
O	0.691406	-0.49812	1.242514
O	0.025646	1.555071	-4.4E-05
H	0.925218	1.913454	-2E-06

Table A-14- OMs

Atom	x	y	z
C	-1.64783	0.132727	0.000027
H	-1.95049	0.675226	0.893609
H	-1.95052	0.675248	-0.89353
H	-2.0767	-0.86746	0.000019
S	0.159033	-0.01501	0
O	0.466376	-0.75324	-1.23216
O	0.466405	-0.75324	1.232156
O	0.639425	1.373254	-1.7E-05

Table A-15- HCl

Atom	x	y	z
Cl	0	0	0.053446
H	0	0	-1.22728

Table A-16- H2SO4

Atom	x	y	z
O	0.32744	-0.73346	1.2539
O	-1.16989	-0.63946	-0.70482
S	-0.01967	0.087221	0.132643
O	-0.42179	1.440615	0.237687
O	1.20706	0.029265	-0.90244
H	1.885261	-0.55426	-0.53477
H	-1.10761	-1.59582	-0.5698

Table A-17- HSO4

Atom	x	y	z
O	0.487281	-0.70915	1.223754
O	0.485482	1.42857	0
S	0.154333	0.01533	0
O	0.487281	-0.70915	-1.22375
O	-1.53369	0.066842	0
H	-1.80199	-0.85874	0

Table A-18- HOTf

Atom	x	y	z
C	-1.00089	-0.00036	-0.00205
O	1.242548	0.230744	1.407924
O	1.247979	1.046262	-0.92553
H	1.386739	1.862143	-0.42096
F	-1.37602	1.222121	0.381658
F	-1.42544	-0.21956	-1.24031
F	-1.53106	-0.9016	0.817712
S	0.857416	-0.13518	0.081577
O	1.218921	-1.35737	-0.54672

Table A-19- OTf

Atom	x	y	z
C	-0.425	0.837695	0
O	-0.07146	-1.4304	1.2313
O	1.830367	-0.46514	0
F	-0.09568	1.573015	1.084815
F	-0.09568	1.573015	-1.08482
F	-1.77155	0.723297	0
S	0.421466	-0.83078	0
O	-0.07146	-1.4304	-1.2313

Table A-20- FSO3H

Atom	x	y	z
O	-0.44188	-0.70028	1.244794
S	-0.099	-0.11195	0
O	-0.44188	-0.70028	-1.24479
O	-0.44676	1.444626	0
H	-1.40901	1.556822	0
F	1.454032	0.135316	0

Table A-21- FSO3

Atom	x	y	z
O	0.462212	0.709561	1.228607
S	0.163446	-1.8E-05	0
O	0.462212	0.709561	-1.22861
O	0.462583	-1.41883	0
F	-1.51197	-0.00033	0

Table A-22- HClO4

Atom	x	y	z
O	1.454445	0.016377	0
O	-0.51671	-1.44653	0
H	0.295065	-1.97884	0
O	-0.51796	0.687072	1.192808
Cl	0.029519	0.145544	0
O	-0.51796	0.687072	-1.19281

Table A-23- ClO4

Atom	x	y	z
O	0.84572	0.84572	0.84572
O	-0.84572	-0.84572	0.84572
O	-0.84572	0.84572	-0.84572
Cl	0	0	0
O	0.84572	-0.84572	-0.84572

Table A-24- HNTf2

Atom	x	y	z
C	2.578436	-0.41535	-0.09549
O	1.694351	1.76863	1.113631
F	2.834294	-0.96027	1.09354
F	2.199707	-1.3601	-0.94233
F	3.669286	0.189119	-0.55178
S	1.240807	0.882335	0.090331
O	0.853906	1.282515	-1.21808
N	-0.00001	0.000055	0.796994
S	-1.24079	-0.88229	0.090333
O	-0.8539	-1.28243	-1.2181
O	-1.69426	-1.76863	1.113627
C	-2.57847	0.415346	-0.09544
F	-2.19976	1.360152	-0.94224
F	-3.66928	-0.18915	-0.55177
F	-2.83436	0.960205	1.093607
H	0.000049	-3.8E-05	1.810782

Table A-25- NTf2

Atom	x	y	z
C	-0.00061	2.585257	-0.00877
O	-2.06157	1.32909	0.976413
F	0.356522	2.993501	1.218057
F	1.11224	2.44132	-0.73804
F	-0.73687	3.564616	-0.56687
S	-1.00092	1.00561	0.05521
O	-1.32649	0.738887	-1.32261
N	0	0	0.77212
S	1.000921	-1.00561	0.05521
O	1.326494	-0.73889	-1.32261
O	2.061567	-1.32909	0.976413
C	0.000613	-2.58526	-0.00877
F	-1.11224	-2.44132	-0.73804
F	0.736867	-3.56462	-0.56687
F	-0.35652	-2.9935	1.218057

Table A-26- HBF4

Atom	x	y	z
H	-2.15279	1.034757	0
F	0.620503	1.246243	0
F	-1.94769	0.133483	0
F	0.615143	-0.72449	1.138674
F	0.615143	-0.72449	-1.13867
B	0.582786	-0.0729	0

Table A-27- BF4

Atom	x	y	z
F	-0.47006	-1.32948	0
F	1.410023	-0.00018	0
F	-0.47008	0.664809	1.151099
F	-0.47008	0.664809	-1.1511
B	0.000306	0.000238	0

Table A-28- HAlCl4

Atom	x	y	z
Al	-0.3065	-0.00066	0.282061
Cl	1.481501	0.002483	-1.63931
Cl	-1.27515	1.801183	-0.16348
Cl	-1.27935	-1.79774	-0.17338
Cl	1.136074	-0.00654	1.819579
H	2.458317	-0.00023	-0.79846

Table A-29- AlCl4

Atom	x	y	z
Al	-0.00002	0.000056	-1E-06
Cl	-0.18476	1.775046	1.232703
Cl	-1.76609	-0.20459	-1.24225
Cl	1.755268	0.175664	-1.26185
Cl	0.195603	-1.74618	1.271392

Table A-30- HAlBr4

Atom	x	y	z
Al	-0.38278	0.000215	0.269591
H	2.757389	-0.00046	-0.56988
Br	-1.36212	1.940042	-0.35202
Br	-1.36165	-1.94028	-0.35069
Br	0.941828	0.001001	2.115165
Br	1.777076	-0.00013	-1.61093

Table A-31- AlBr4

Atom	x	y	z
Al	-0.00011	0.000035	-3.8E-05
Br	0.264074	1.991669	1.200877
Br	2.104622	-0.86576	-0.54742
Br	-1.16543	-1.55159	1.308809
Br	-1.20325	0.425648	-1.96223

Table A-32- HAsF6

Atom	x	y	z
As	-0.18138	0.001661	-0.00146
F	0.084913	-1.69573	0.02271
F	-0.0604	-0.0427	-1.70965
F	0.391591	0.044386	1.632413
F	-1.85602	0.007021	0.239635
F	0.083173	1.698244	-0.06559
F	2.270083	-0.00448	-0.21954
H	2.579338	0.008488	0.656681

Table A-33- AsF6

Atom	x	y	z
As	0.114345	0.051975	0
F	0.114345	1.813329	0
F	-1.64701	0.051975	0
F	0.114345	0.051975	1.761354
F	0.114345	-1.70938	0
F	1.875699	0.051975	0
F	0.114345	0.051975	-1.76135

Table A-34- HPF6

Atom	x	y	z
F	-0.53592	1.59375	0.0228
F	0.099903	-0.04745	1.380804
F	0.288136	0.061328	-1.35709
F	-2.09101	-0.00352	-0.14344
F	-0.51286	-1.58632	-0.10193
F	2.845349	-0.00302	0.194806
H	3.32782	0.012253	-0.59162
P	-0.53782	0.003481	-0.03543

Table A-35- PF6

Atom	x	y	z
P	0.363825	0.093555	0
F	0.363825	1.725386	0
F	-1.26801	0.093555	0
F	0.363825	0.093555	1.631831
F	0.363825	-1.53828	0
F	1.995657	0.093555	0
F	0.363825	0.093555	-1.63183

Table A-36- DMI-HAlBr4

Atom	x	y	z
Al	-2.00963	-0.12681	-0.16064
N	2.881734	-0.81026	-0.06898
C	2.125411	-0.00927	0.679685
O	1.710821	-0.3804	1.858328
C	3.044238	-2.23935	0.146848
H	4.086854	-2.51151	-0.01362
H	2.764557	-2.4789	1.167563
H	2.40771	-2.80007	-0.53879
C	1.42517	2.379511	0.784804
H	0.54423	2.755862	0.268497
H	1.157238	2.153027	1.811354
H	2.214248	3.13446	0.776799
N	1.908434	1.175738	0.122379
C	2.532823	1.230529	-1.20585
H	3.319373	1.98721	-1.20451
H	1.789913	1.490521	-1.95731
C	3.091432	-0.19945	-1.38881
H	2.527679	-0.75938	-2.13566
H	4.147036	-0.21102	-1.6557
H	0.762763	-0.10245	2.02653
Br	-1.68034	1.848389	-1.35069
Br	-1.37529	0.273249	2.12113
Br	-0.53547	-1.74852	-0.9904
Br	-4.18473	-0.83611	-0.18737

Table A-37 DMI-HAlCl4

Atom	x	y	z
Al	-1.80911	-0.13667	-0.10277
Cl	-3.81147	-0.82874	-0.11797
Cl	-1.52596	1.686991	-1.2195
Cl	-1.20933	0.265632	2.003072
Cl	-0.40551	-1.61567	-0.85017
N	2.868282	-0.81136	-0.09172
C	2.124424	-0.00914	0.668915
O	1.721903	-0.3766	1.852775
C	3.014291	-2.24373	0.117803
H	4.047707	-2.53142	-0.07162
H	2.759495	-2.47989	1.145766
H	2.350325	-2.79405	-0.55006
C	1.43309	2.380227	0.78642
H	0.553577	2.768774	0.277917
H	1.168975	2.15039	1.813111
H	2.230574	3.126422	0.777995
N	1.897538	1.17488	0.113907
C	2.494285	1.226396	-1.22642
H	3.288449	1.975209	-1.24085
H	1.73712	1.493848	-1.96083
C	3.034083	-0.20885	-1.42195
H	2.43504	-0.76768	-2.14172
H	4.078167	-0.23136	-1.72957
H	0.765505	-0.11594	2.006885

Table A-38-DMI-HBF4

Atom	x	y	z
N	1.964402	-0.69655	0.021181
C	1.070631	0.064954	0.666701
O	0.487422	-0.3294	1.752636
C	2.027613	-2.14221	0.180903
H	3.055888	-2.47466	0.04785
H	1.694572	-2.40167	1.180577
H	1.381358	-2.63507	-0.54833
C	0.118304	2.360696	0.612424
H	-0.74768	2.524632	-0.02634
H	-0.22911	2.122499	1.612831
H	0.737661	3.25803	0.652896
N	0.909916	1.25437	0.10129
C	1.698188	1.351348	-1.12772
H	2.468643	2.116599	-1.01333
H	1.059184	1.618273	-1.96803
C	2.293856	-0.06873	-1.26483
H	1.815112	-0.62847	-2.07033
H	3.369745	-0.06033	-1.43058
H	-0.53226	-0.22392	1.663363
F	-1.9157	-0.11025	1.302602
F	-2.25492	0.827763	-0.78108
F	-1.04501	-1.10605	-0.58774
F	-3.31898	-1.13441	-0.22466
B	-2.1774	-0.39858	-0.13904

Table A-39-DMI-HClO4

Atom	x	y	z
N	1.836558	-0.99669	0.102463
C	1.299187	0.179869	0.543662
O	0.41038	0.307186	1.39884
C	1.193124	-2.28078	0.300928
H	1.952739	-3.0573	0.389404
H	0.618435	-2.24922	1.222241
H	0.520363	-2.5273	-0.52478
C	1.83294	2.58294	0.382287
H	1.772532	3.268938	-0.46269
H	0.934512	2.682777	0.984779
H	2.702691	2.849793	0.992015
N	1.91731	1.218193	-0.09222
C	3.045894	0.736946	-0.87769
H	3.985821	0.873863	-0.33006
H	3.12013	1.261058	-1.82951
C	2.70217	-0.75188	-1.0466
H	2.160898	-0.93419	-1.98135
H	3.582682	-1.39236	-1.02276
H	-0.97872	-0.28325	1.347625
O	-1.9248	-0.68878	1.322836
O	-2.81808	1.076929	-0.11474
O	-3.73125	-1.13423	-0.15499
O	-1.5654	-0.70431	-1.08802
Cl	-2.55871	-0.3289	-0.1186

Table A-40- DMI-FSO3H

Atom	x	y	z
N	-1.82263	1.203904	0.25818
C	-1.37817	-0.03242	0.626119
O	-0.53677	-0.25375	1.515068
C	-1.06878	2.406749	0.558914
H	-1.75329	3.244368	0.690241
H	-0.52018	2.249466	1.483214
H	-0.35884	2.640513	-0.23928
C	-2.04954	-2.38062	0.25182
H	-1.91977	-3.00637	-0.63143
H	-1.2388	-2.57914	0.947043
H	-2.99884	-2.64059	0.731534
N	-2.01401	-0.98147	-0.11658
C	-3.05067	-0.37498	-0.94301
H	-4.03594	-0.5079	-0.48158
H	-3.07283	-0.81463	-1.9392
C	-2.62464	1.102446	-0.95779
H	-2.01201	1.332526	-1.8356
H	-3.47286	1.784925	-0.93331
H	0.827034	-0.69459	1.164761
O	1.780932	-1.0002	0.900024
S	2.334883	-0.19333	-0.28847
O	3.455363	-0.86546	-0.84014
O	1.285686	0.336551	-1.10162
F	2.925137	1.07329	0.494094

Table A-41- DMI-HOTf

Atom	x	y	z
N	2.336284	1.36209	-0.15051
C	1.999464	0.128969	-0.62889
O	1.134339	-0.08853	-1.4952
C	1.442724	2.498497	-0.27698
H	2.025785	3.416458	-0.34638
H	0.857376	2.380408	-1.18421
H	0.762647	2.565395	0.576796
C	2.930407	-2.159	-0.54202
H	2.908444	-2.88366	0.272114
H	2.111652	-2.37069	-1.22372
H	3.876917	-2.26385	-1.08235
N	2.770149	-0.81744	-0.02263
C	3.78424	-0.19135	0.816994
H	4.750679	-0.17129	0.300326
H	3.90619	-0.72535	1.758347
C	3.212961	1.22312	1.008919
H	2.631661	1.296728	1.933947
H	3.985102	1.990981	1.018438
H	-0.10585	-0.80197	-1.12745
O	-0.96433	-1.31532	-0.85712
S	-1.57454	-0.79906	0.472574
O	-2.33129	-1.84517	1.079579
O	-0.61547	-0.02985	1.216313
C	-2.81535	0.427829	-0.17454
F	-3.71044	-0.17284	-0.95549
F	-3.44646	0.997276	0.854058
F	-2.19707	1.381152	-0.88123

Table A-42-DMI-H2SO4

Atom	x	y	z
N	2.196474	-0.95089	0.073181
C	1.366419	-0.04371	0.677688
O	0.650072	-0.28194	1.663085
C	1.993872	-2.37712	0.241395
H	2.949565	-2.89627	0.170371
H	1.567203	-2.55175	1.225041
H	1.311793	-2.7749	-0.51659
C	0.970156	2.400702	0.570246
H	0.357926	2.919501	-0.16731
H	0.358303	2.189469	1.442459
H	1.800961	3.047696	0.86835
N	1.460498	1.149925	0.031334
C	2.472857	1.099666	-1.01387
H	3.393442	1.591991	-0.68034
H	2.128234	1.590356	-1.92336
C	2.670372	-0.41436	-1.19981
H	2.057488	-0.79672	-2.0229
H	3.709908	-0.68265	-1.38346
H	-0.87031	-0.14722	1.482896
O	-1.87434	-0.05165	1.317574
S	-2.18201	-0.01981	-0.21739
O	-2.30612	1.320162	-0.68953
O	-1.32147	-0.95109	-0.89621
O	-3.6747	-0.59684	-0.20256
H	-3.64279	-1.54033	0.008636

Table A-43-DMI-HCl

Atom	x	y	z
N	-1.62159	-0.76816	0.245076
C	-0.40802	-0.23385	-0.12942
O	0.620394	-0.88244	-0.30405
C	-1.90674	-2.17706	0.072401
H	-2.38622	-2.37749	-0.89261
H	-0.96997	-2.72556	0.11918
H	-2.56479	-2.52579	0.868505
C	0.565286	2.036017	-0.26775
H	0.809994	2.367667	0.747099
H	1.433733	1.538181	-0.68826
H	0.334186	2.910687	-0.87579
N	-0.56068	1.124472	-0.27994
C	-1.86683	1.541127	0.213958
H	-2.28945	2.335703	-0.39982
H	-1.79682	1.900366	1.247977
C	-2.67014	0.235575	0.129827
H	-3.40495	0.141322	0.928617
H	-3.18978	0.148728	-0.83259
H	2.314362	-0.6207	-0.09258
Cl	3.607138	-0.43802	0.08429

Table A-44- DMI-HOMs

Atom	x	y	z
N	2.163306	-0.98611	0.076754
C	1.403328	-0.02687	0.697381
O	0.705625	-0.21105	1.705847
C	1.878391	-2.39553	0.26736
H	2.794316	-2.97484	0.150738
H	1.494834	-2.53716	1.273889
H	1.131796	-2.75154	-0.44926
C	1.110054	2.429209	0.552026
H	0.497396	2.951701	-0.18313
H	0.512071	2.255941	1.442352
H	1.967994	3.055339	0.816436
N	1.544211	1.15154	0.032708
C	2.501562	1.031475	-1.05593
H	3.462948	1.477348	-0.77576
H	2.140644	1.526112	-1.9572
C	2.605946	-0.49414	-1.22533
H	1.932892	-0.85118	-2.01174
H	3.619239	-0.823	-1.45252
H	-0.85004	-0.10374	1.489089
O	-1.8435	-0.01925	1.302041
S	-2.13172	0.002547	-0.251
O	-2.23954	1.361969	-0.71444
O	-1.20828	-0.88246	-0.92544
C	-3.75394	-0.72452	-0.24951
H	-4.09591	-0.72716	-1.28118
H	-3.68347	-1.73597	0.138698
H	-4.40513	-0.11121	0.366621

Table A-45- DMI-HTFA

Atom	x	y	z
N	2.456846	-0.84602	0.009345
C	1.570053	0.057632	-0.51702
O	0.627737	-0.2315	-1.25789
C	2.60494	-2.17894	-0.53629
H	2.816914	-2.88844	0.263611
H	1.673292	-2.45764	-1.02062
H	3.415694	-2.22458	-1.27162
C	1.011644	2.44067	-0.15091
H	1.579172	3.361585	-0.28364
H	0.344802	2.319491	-0.99985
H	0.411837	2.524503	0.761034
N	1.921368	1.31438	-0.09547
C	2.957406	1.22997	0.927453
H	2.517371	1.280377	1.930174
H	3.682052	2.036689	0.825776
C	3.565851	-0.15339	0.651447
H	4.42598	-0.08474	-0.02543
H	3.881381	-0.66261	1.561128
H	-0.91137	0.230559	-1.33583
O	-1.83692	0.569433	-1.51233
C	-2.75545	0.254211	-0.62226
C	-2.25086	-0.60978	0.573922
O	-3.90359	0.586434	-0.68132
F	-1.76813	-1.79208	0.148357
F	-1.24846	0.024549	1.231218
F	-3.22102	-0.84826	1.449132

Table A-46- DMI-HOAcCl2

Atom	x	y	z
N	-2.63335	0.954357	-0.35543
C	-1.71887	-0.05765	-0.52081
O	-0.62996	0.067179	-1.08063
C	-2.24387	2.34708	-0.44356
H	-2.01039	2.761761	0.542958
H	-1.36021	2.41767	-1.0717
H	-3.04798	2.933186	-0.88902
C	-1.75202	-2.52479	-0.33829
H	-2.3178	-2.9309	-1.18409
H	-0.70319	-2.46768	-0.61207
H	-1.85339	-3.20388	0.508
N	-2.22842	-1.20656	0.034374
C	-3.62406	-1.00523	0.406706
H	-3.86507	-1.51515	1.338539
H	-4.29115	-1.38158	-0.37819
C	-3.7094	0.522979	0.526512
H	-4.67316	0.916411	0.20531
H	-3.52449	0.854988	1.555245
H	0.82041	-0.69144	-0.89668
O	1.589148	-1.32527	-0.89311
C	2.67079	-0.94475	-0.24121
C	2.675862	0.436588	0.437818
H	3.640253	0.577659	0.903133
O	3.657288	-1.62694	-0.1487
Cl	1.451021	0.515734	1.752465
Cl	2.459994	1.759823	-0.74828

Table A-47- DMI-HOAc

Atom	x	y	z
N	2.220713	-0.89024	-0.14105
C	1.095496	-0.111	0.014633
O	-0.05795	-0.53587	-0.00564
C	2.181464	-2.32045	0.082137
H	2.432861	-2.57518	1.118062
H	1.177498	-2.67567	-0.13305
H	2.886388	-2.82155	-0.5814
C	0.602522	2.317408	-0.03704
H	0.632381	2.645615	-1.08194
H	-0.41642	2.040747	0.214348
H	0.900877	3.151022	0.59834
N	1.489984	1.193184	0.193802
C	2.920992	1.322534	-0.05393
H	3.380126	2.033688	0.631549
H	3.107659	1.659481	-1.08082
C	3.415885	-0.11419	0.161217
H	4.242189	-0.37817	-0.49776
H	3.733322	-0.27605	1.19869
H	-1.62914	0.144887	0.270708
O	-2.45619	0.650353	0.437591
C	-3.56238	-0.10427	0.303731
C	-3.32118	-1.5583	-0.05007
H	-2.75054	-1.63528	-0.97622
H	-2.73419	-2.0421	0.731828
H	-4.27463	-2.0653	-0.15943
O	-4.65521	0.373643	0.464171

Table A-48- DMI-H2O

Atom	x	y	z
N	-1.394	-0.57486	0.21994
C	-0.05629	-0.28925	0.020918
O	0.849097	-1.11337	0.039714
C	-1.90319	-1.91698	0.03551
H	-2.25714	-2.07956	-0.98954
H	-1.10132	-2.61984	0.245121
H	-2.72923	-2.10284	0.722553
C	1.320854	1.766945	-0.01374
H	1.441625	2.107528	1.020962
H	2.147888	1.108622	-0.26347
H	1.354144	2.635712	-0.6716
N	0.065112	1.065724	-0.20159
C	-1.20094	1.733023	0.069301
H	-1.37573	2.55393	-0.62548
H	-1.22093	2.133007	1.090915
C	-2.20882	0.588079	-0.09922
H	-3.06274	0.6769	0.571855
H	-2.58177	0.534206	-1.1301
H	2.703667	-1.0218	-0.01817
O	3.659322	-0.84093	-0.06364
H	4.026172	-1.54954	-0.59715

APPENDIX B

^{1}H-^{1}H AND ^{1}H-^{14}N J-COUPLING OF DEMAALCL4 PROTON

Exchangeable protons in general and those of ammonium salts in particular usually result in relatively broad peaks in ^{1}H NMR because of their fast intermolecular exchange. For this reason, neither splitting by vicinal CHs ($^{3}J_{HNCH}$ = 5-6 Hz) nor coupling to ^{14}N ($^{1}J_{NH}$ = 52.8 Hz in the case of NH_4^+) are normally observed. In the case of $DEMAAlCl_4$, the high acidity of the medium (very low basicity of the anion) reduces the rate of exchange/eliminates it so that the latter can be seen.

A triplet at δ=5.69 ppm (J=52.8 Hz) with an integral of 1 is the acidic proton, split into a triplet by ^{14}N (*I*=1). When recorded on a 500 MHz spectrometer, the spectrum shows the signal at the same position with the same splitting (in Hz) indicating that it indeed is a J-splitting (Figure B-1).

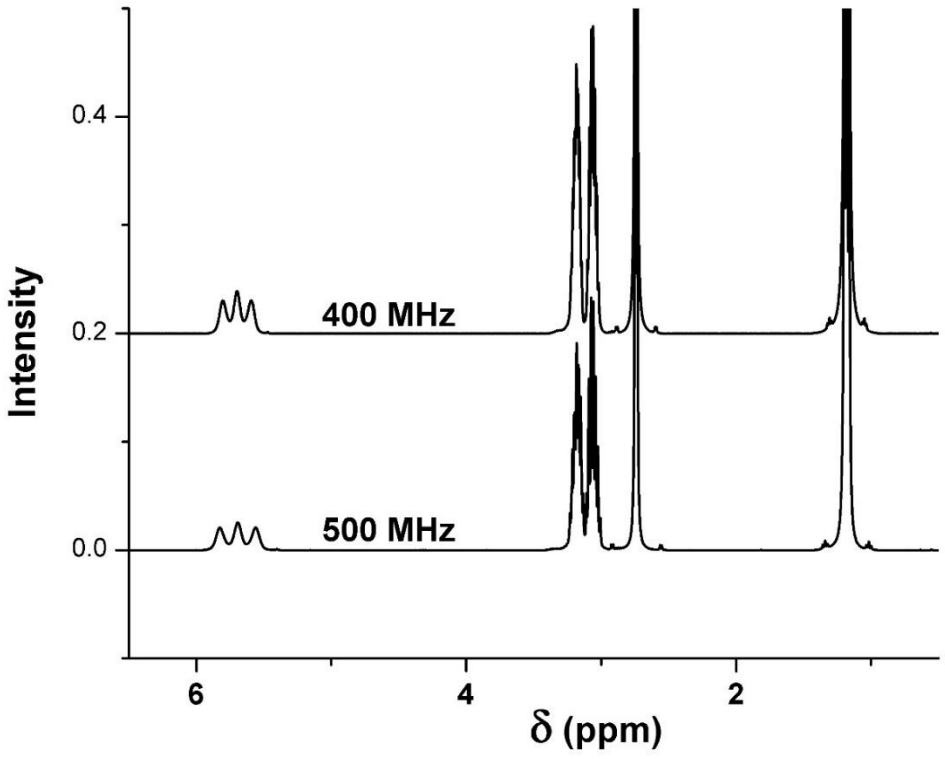

Figure B-1- ^{1}H NMR spectrum of $DEMAAlCl_4$. The triplet at 5.69 ppm is resolved more in the bottom spectrum with the same coupling constant of 52.8 Hz.

Figure B-2 shows the change in the spectrum collected at 500 MHz with increasing the temperature. There is a very small change in the chemical shifts, the acidic proton's chemical shift at 25 ^{o}C is 5.62 ppm. As it is seen in the spectra, raising the temperature results in better resolution as it reduces the viscosity of the sample but does not change the splitting patterns of any of the peaks, indicating that none of the patterns are caused by any dynamic exchange phenomena.

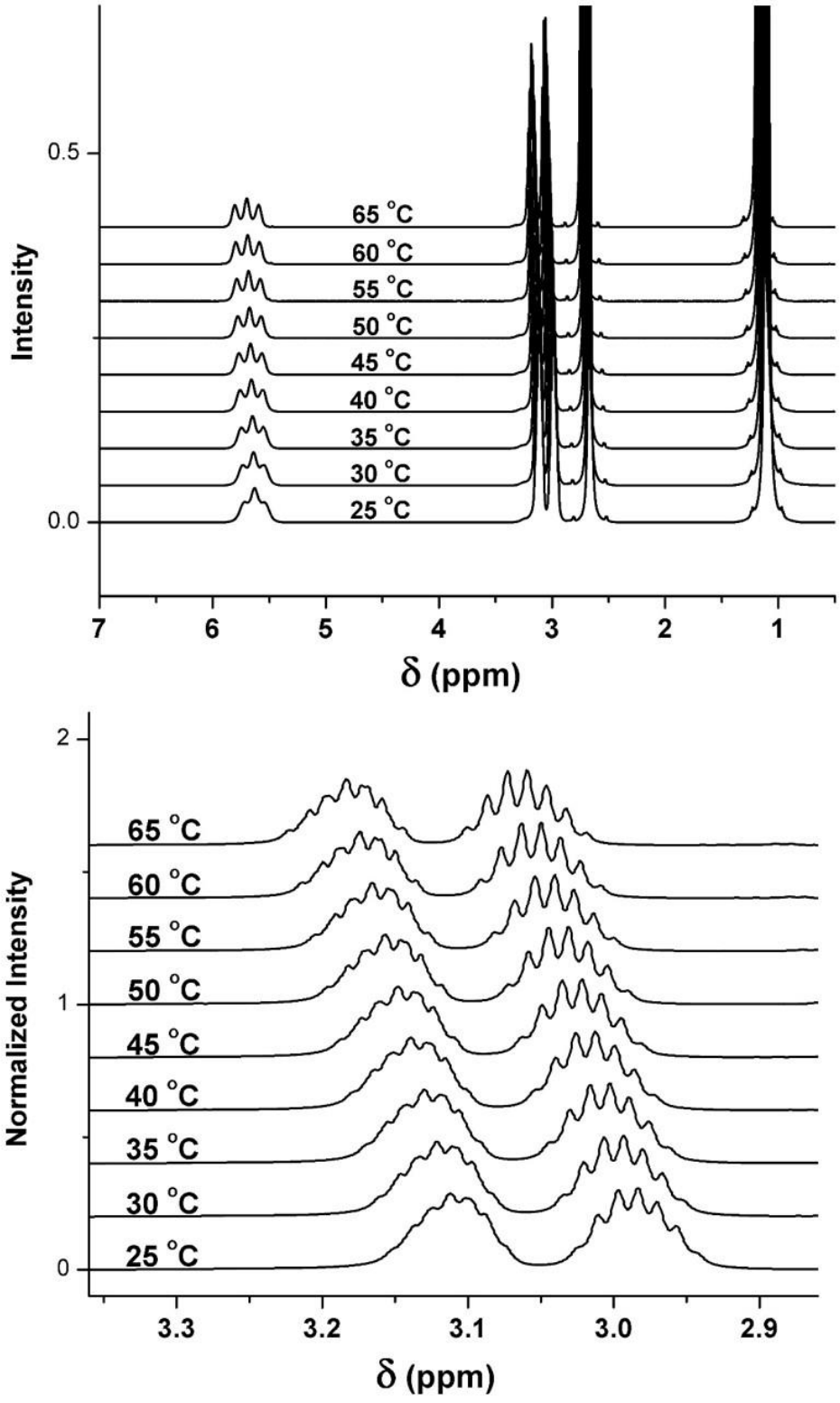

Figure B-2- ^{1}H NMR spectra of $DEMAAlCl_4$ at different temperatures

The peaks at 3.06 and 3.18 ppm are the methylene peaks of the ethyl groups. It is noteworthy that they are not the result of a J splitting, neither are they of different conformers but rather magnetically non-equivalent protons. The two protons on each of the methylene groups are called diastereotopic protons and are known to have different chemical shifts at all conditions. The fact that their chemical shifts do not change with changing the temperature (Figure B-2) or the spectrometer's frequency (Figure B-3) is an evidence. The splitting pattern is what is expected from an $ABMX_3$ system. The proton at higher field has a simpler pattern possibly because of a small coupling constant with the NH proton due to the dihedral angle between them.

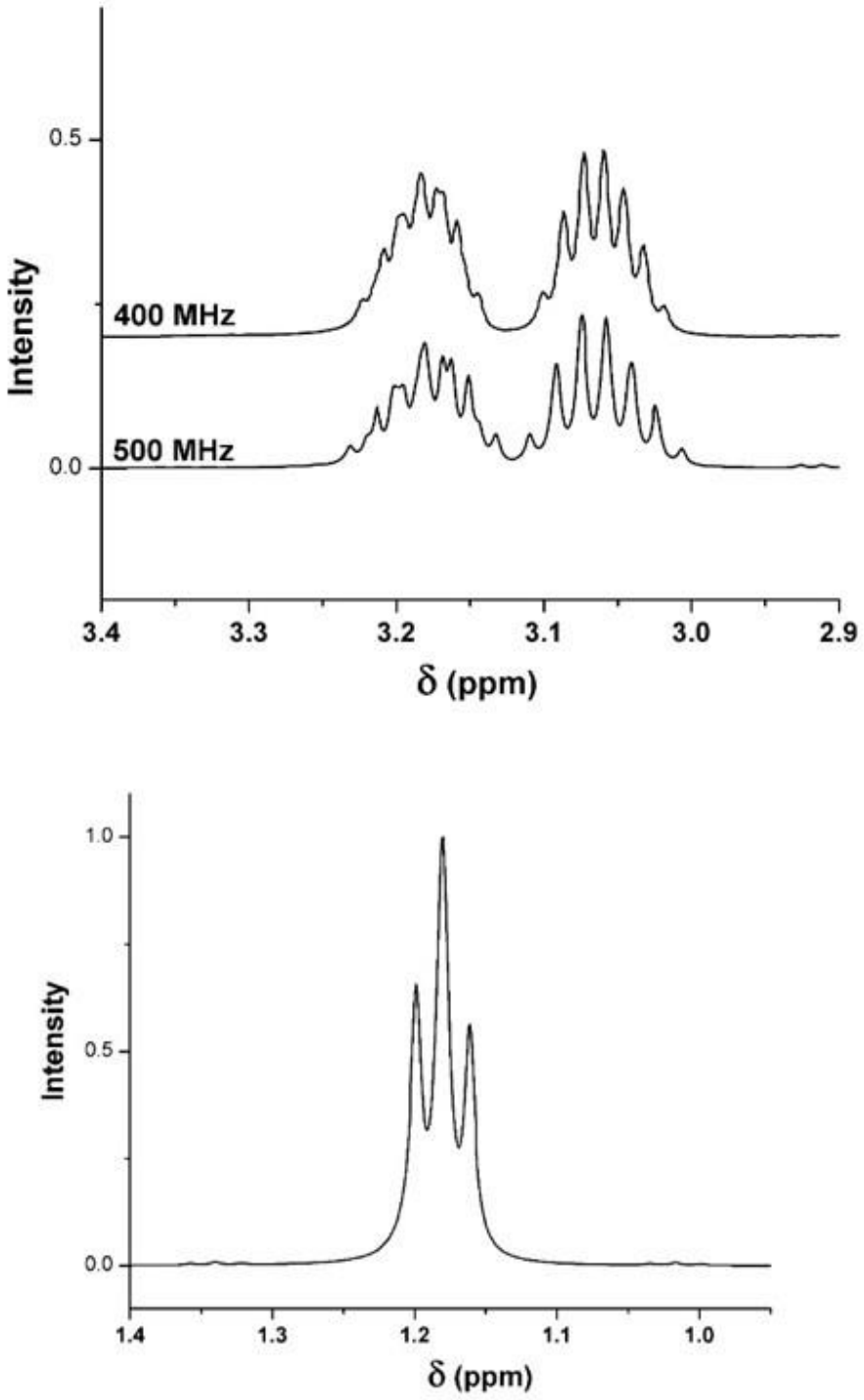

Figure B-3- $ABMX_3$ pattern seen for CH_2 (AB) and CH_3 (X_3) of ethyl groups.

The methyl group directly attached to the nitrogen atom is split by the NH proton into a doublet (Figure B-4).

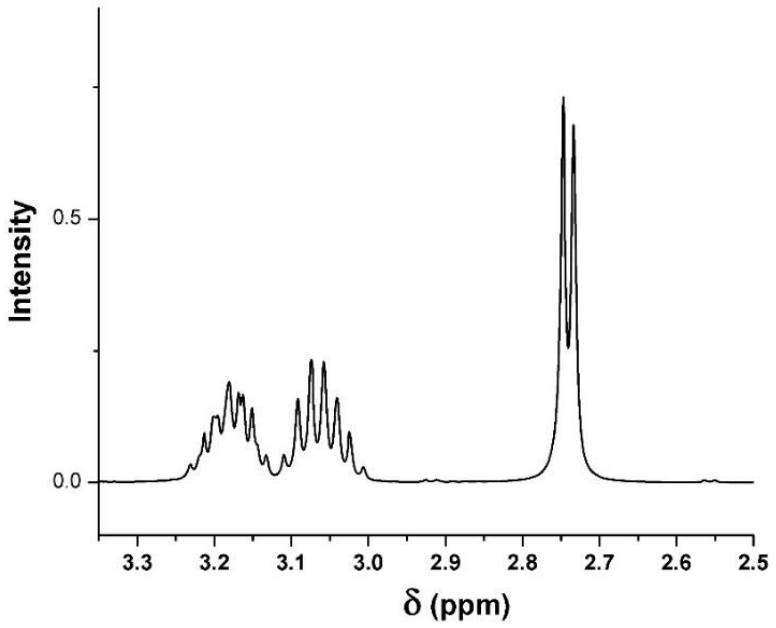

Figure B-4- Protons on the NMe group split into a doublet visible at 2.74 ppm

2D COSY NMR of the sample shows the expected couplings. It shows that the NH proton is mostly coupled to the NMe group and to a lesser extent to the methylene protons (Figure B-5).

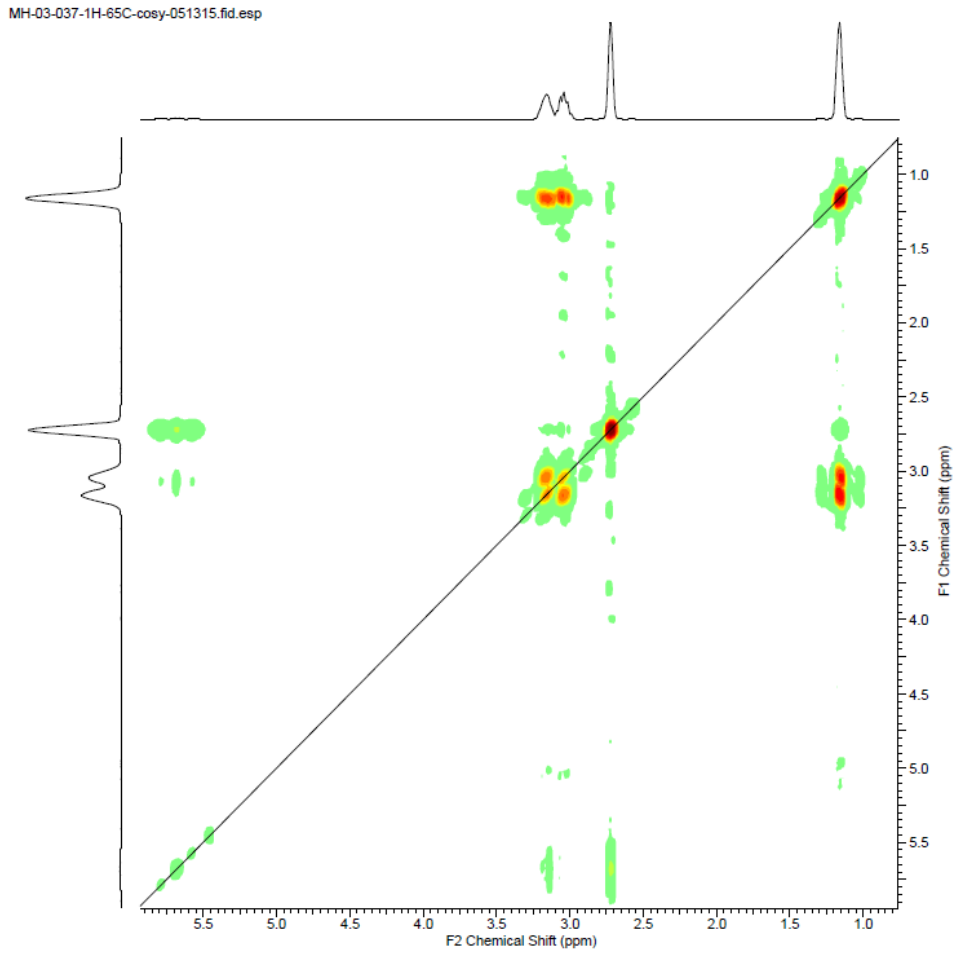

Figure B-5- COSY spectrum of DEMA$AlCl_4$ at 500MHz and 65 ^oC

In conclusion, the ionic liquid made by proton transfer from transient superacidic $HAlCl_4$ to DEMA is characterized by ^1H NMR. The rarely seen $^3J_{HNCH}$ and $^1J_{NH}$ couplings can be observed because of the heavily reduced/eliminated exchange of the acidic proton. 2D spectrum supports the interpretations.